Max-Planck-Institut
für Meteorologie

MAX-PLANCK-GESELLSCHAFT

International Max Planck Research School
on Earth System Modelling

Drivers of Precipitation Biases in the Tropical Atlantic Sector

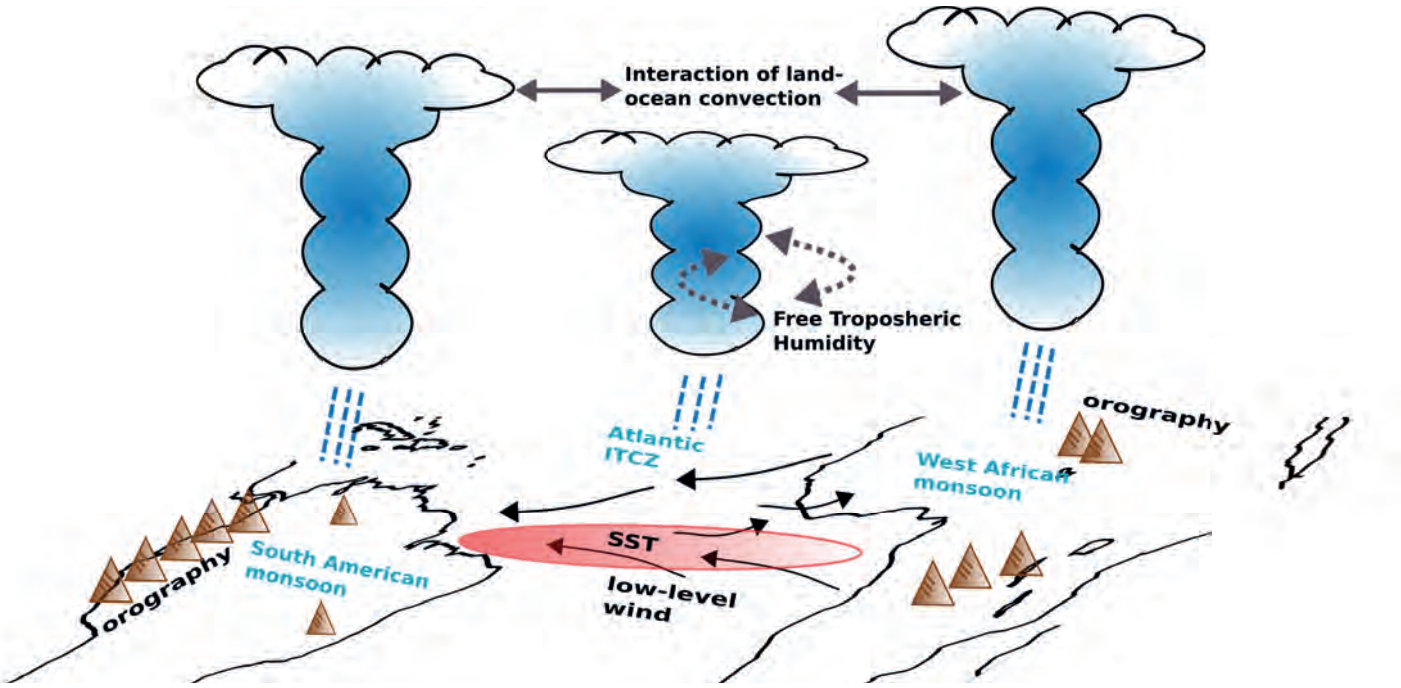

Angela Cheska Siongco

Hamburg 2016

Berichte zur Erdsystemforschung
Reports on Earth System Science

181
2016

Hinweis

Die Berichte zur Erdsystemforschung werden vom Max-Planck-Institut für Meteorologie in Hamburg in unregelmäßiger Abfolge herausgegeben.

Sie enthalten wissenschaftliche und technische Beiträge, inklusive Dissertationen.

Die Beiträge geben nicht notwendigerweise die Auffassung des Instituts wieder.

Die "Berichte zur Erdsystemforschung" führen die vorherigen Reihen "Reports" und "Examensarbeiten" weiter.

Notice

The Reports on Earth System Science are published by the Max Planck Institute for Meteorology in Hamburg. They appear in irregular intervals.

They contain scientific and technical contributions, including Ph. D. theses.

The Reports do not necessarily reflect the opinion of the Institute.

The "Reports on Earth System Science" continue the former "Reports" and "Examensarbeiten" of the Max Planck Institute.

Anschrift / Address

Max-Planck-Institut für Meteorologie
Bundesstrasse 53
20146 Hamburg
Deutschland

Tel./Phone: +49 (0)40 4 11 73 - 0
Fax: +49 (0)40 4 11 73 - 298

name.surname@mpimet.mpg.de
www.mpimet.mpg.de

Layout

Bettina Diallo and Norbert P. Noreiks
Communication

Copyright

Drivers of Precipitation Biases in the Tropical Atlantic Sector

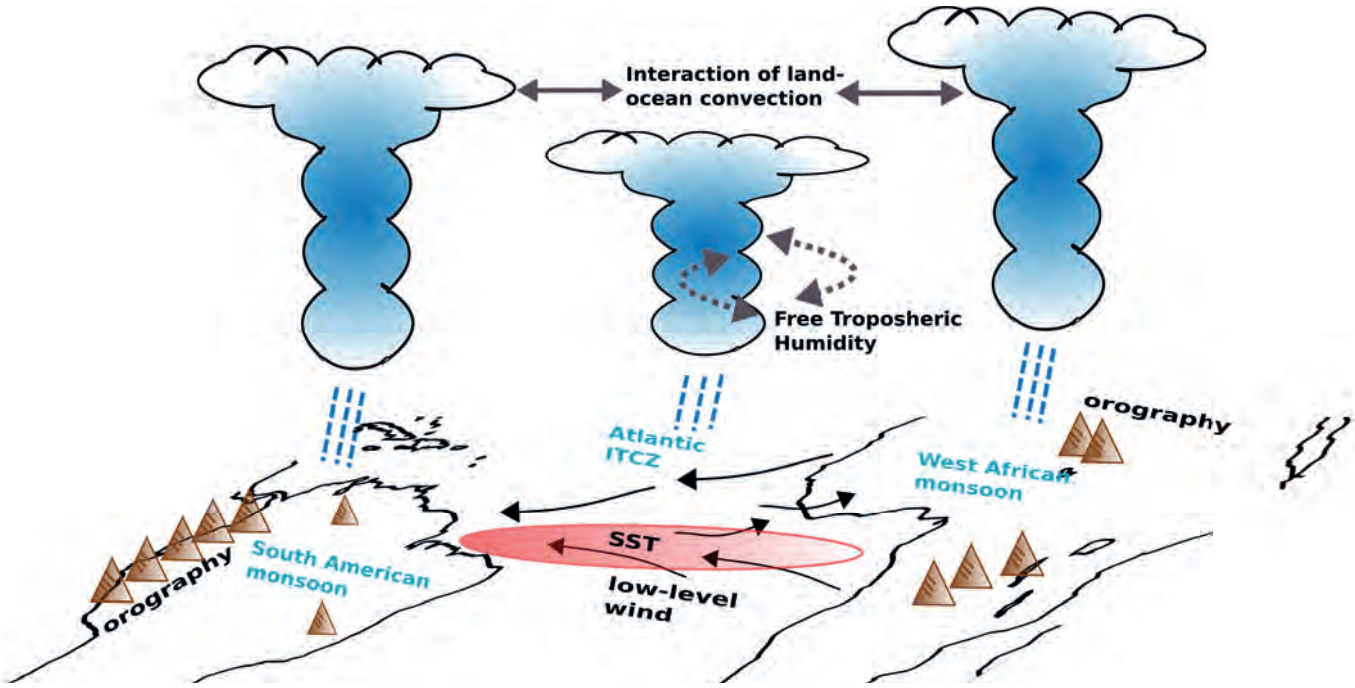

Angela Cheska Siongco

Hamburg 2016

Angela Cheska Siongco

Max-Planck-Institut für Meteorologie
Bundesstrasse 53
20146 Hamburg

Tag der Disputation: 13.4.2016

Folgende Gutachter empfehlen die Annahme der Dissertation:

Prof. Dr. Martin Claussen
Dr. Cathy Hohenegger

Berichte zur Erdsystemforschung / Max-Planck-Institut für Meteorologie 181
Reports on Earth System Science / Max Planck Institute for Meteorology 2016

ISSN 1614-1199

Abstract

A realistic simulation of the tropical precipitation distribution remains a challenge for our climate models, owing to their too coarse resolution that makes it necessary to parameterize convection. In this thesis, we identify and analyze drivers of precipitation biases over the tropical Atlantic sector using general circulation models (GCMs), in order to gain a better understanding of factors controlling the precipitation distribution over land and over ocean. This study is divided into three main parts.

First, we employ an object-based analysis to quantify the structure, amplitude, and location of precipitation biases in 24 atmospheric GCMs. We find that over land, all models show a dry bias, especially over South America. Over ocean, even when forced with observed sea surface temperatures (SSTs), models fail to simulate the Atlantic ITCZ position. While observations show a central Atlantic ITCZ maximum in the annual mean state, models misplace the precipitation maximum over the West Atlantic coast or East Atlantic coast. The Atlantic ITCZ bias in the annual mean is traced to the erroneous east-west partitioning of precipitation in boreal spring and summer. The two distinct representations of the ITCZ suggest that the model biases are driven by factors other than oversensitivity to SSTs. In particular, it is found that one factor which affects these two distinct model behaviors is the horizontal resolution, with models of higher resolution raining more over the East Atlantic during spring and summer.

The effect of horizontal resolution on the Atlantic ITCZ position is thus investigated in more detail using the ECHAM6 model. Sensitivity experiments are performed to isolate the relative contributions of a high-resolution atmosphere, orography, and land surface. During spring and summer, the default low-resolution version of ECHAM6 has a West Atlantic bias, whereas the high-resolution version rains more over the East Atlantic. We find that in both seasons, with a high-resolution atmosphere, convection occurs more easily. This expresses itself as an enhancement of precipitation upstream on the east coast and consequent reduction downstream on the west coast. The effect of a high-resolution orography is only evident in summer, when it can strengthen the existing monsoon circulation, thus enhancing precipitation on the east coast. A high resolution surface has a minimal effect. The atmospheric effect in high resolution can be achieved in low resolution by changing the convection scheme such that it is easier to rain, showing that another factor which affects the longitudinal position of the ITCZ is the convective parameterization.

In the last part of this study, we explore the role of the convection scheme on the precipitation distribution over land and over ocean. Modifications are applied to the convection scheme in order to test the relative roles of the trigger, entrainment, and closure formulations. It is found that over ocean, a weakened entrainment makes it easier to produce deep convection, enhancing rain east and decreasing rain west, similar to the high-resolution atmospheric effect in spring and summer. In summer, a closure based on local thermal instability (CAPE) places

the precipitation maximum over the SST maximum in the West Atlantic, whereas a closure based on moisture convergence places it near the monsoon circulation in the East Atlantic. In spring, without a monsoon circulation, the precipitation follows the warmest SSTs over the coasts and its structure is insensitive to changes in the convection scheme. Over land, in both spring and summer, we find that the entrainment parameter is the cause for the dry bias. The relatively infrequent triggering of convection over land than ocean makes the entrainment parameter a decisive factor on the success rate of convection over land.

Zusammenfassung

Eine realistische Simulation der tropischen Niederschlagsverteilung stellt nach wie vor eine Herausforderung für unsere Klimamodelle, in denen Konvektion durch die zu grobe Auflösung parametrisiert werden muss, dar. In der vorliegenden Arbeit identifizieren und analysieren wir die Einflussfaktoren für Fehler in der Niederschlagssimulation über dem tropischen Atlantik in Allgemeinen Zirkulationsmodellen (general circulation models, GCMs) zum besseren Verständnis der Faktoren, die die Niederschlagsverteilung über Land und Ozean bestimmen. Diese Arbeit ist in drei Teile gegliedert.

Im ersten Teil wenden wir eine objektbasierte Analyse zur Quantifizierung der Struktur, Amplitude und der Position der Niederschlagsfehler in 24 atmosphärischen GCMs an. Unsere Ergebnisse zeigen, dass alle Modelle einen Trockenheitsfehler, vor allem über Südamerika, zeigen. über dem Ozean scheitern die Modelle darin die Position der atlantischen ITCZ korrekt zu simulieren, sogar wenn sie durch beobachtete Meeresoberflächentemperaturen (sea surface temperatures, SSTs) angetrieben werden. Während die Beobachtungen im Mittel ein ITCZ Maximum über dem zentralen Atlantik zeigen, platzieren die Modelle das Niederschlagsmaximum falsch über der atlantischen West- oder der Ostküste. Der jahresmittlere atlantische ITCZ Fehler kann auf die falsche Darstellung der Ost-West Aufteilung des Niederschlags im borealen Frühling und Sommer zurückverfolgt werden. Diese zwei merklich verschiedenen Darstellungen der ITCZ deuten an, dass die Fehler in den Modellen von anderen Faktoren als der Übersensitivität auf SSTs hervorgerufen werden. Wir finden insbesondere, dass die horizontale Auflösung bestimmend für die zwei unterschiedlichen Modellverhalten ist, wobei Modelle mit höherer Auflösung bevorzugt über dem Ostlatlantik während des Frühlings und Sommers regnen.

Der Effekt der horizontalen Auflösung auf die Position der atlantischen ITCZ wird daher ausführlich mit dem ECHAM6 Modell untersucht. Sensitivitätsexperimente werden durchgeführt um die relativen Beiträge einer hochaufgelösten Atmosphäre, der Orographie und der Landoberfläche zu isolieren. Im Frühling und Sommer hat die standardmäßig niedrige Auflösung von ECHAM6 einen westatlantischen Fehler, während die hochaufgelöste Version mehr über dem Ostatlantik regnet. Wir finden, dass Konvektion in beiden Jahreszeiten durch die höhere Auflösung leichter auftreten kann. Dies äußert sich durch erhöhten Niederschlag stromaufwärts an der Ostküste und dadurch bedingte Verringerung stromabwärts an der Westküste. Der Effekt der höher aufgelösten Orographie ist nur im Sommer bemerkbar, wenn sie die vorhandene Monsunzirkulation verstärkt und damit den Niederschlag an der Westküste erhöht. Eine höher aufgelöste Oberfläche hat nur einen minimalen Effekt. Der atmosphärische Effekt der höheren Auflösung kann in der geringeren Auflösung erreicht werden indem das Konvektionsschema so verändert wird, dass Regen leichter entsteht. Dies zeigt, dass das Konvektionsschema ein weiterer Faktor ist, der die longitudinale Position der ITCZ beeinflusst.

Im letzten Teil dieser Studie untersuchen wir die Rolle des Konvektionsschemas für die Verteilung des Niederschlags über Land und Ozean. Das Konvektionsschema wird verändert um die relativen Einflüsse des Triggers, der Einmischung und der Schließungsformulierung zu testen. Über dem Ozean begünstigt eine verringerte Einmischung die Entstehung von hochreichender Konvektion, was den Regen im Osten steigert und im Westen verringert, und dem Effekt der hochaufgelösten Atmosphäre im Frühling und Sommer ähnelt. Im Sommer sorgt eine Schließung basierend auf lokaler thermischer Instabilität (CAPE) für die Platzierung des Niederschlagsmaximums über dem SST Maximum im Westatlantik, wohingegen eine Schließung basierend auf Feuchtigkeitskonvergenz das Niederschlagsmaximum in der Nähe der Monsunzirkulation im Ostatlantik platziert. Im Frühling in Abwesenheit einer Monsunzirkulation folgt der Niederschlag den wärmsten SSTs über den Küsten und reagiert nicht empfindlich auf Änderungen in der Schließung. über dem Land sowohl im Frühling als auch im Sommer finden wir, dass der Einmischungsparameter die Ursache für den Trockenheitsfehler ist. Das relativ seltene Auslösen von Konvektion über Land im Vergleich zum Ozean weist dem Einmischungsparameter seine entscheidende Rolle für die Erfolgsrate der Konvektion über Land zu.

Contents

Chapter 1

Introduction

1.1 Background

1.1.1 The tropical precipitation distribution

In the tropics, much of the rainfall is concentrated in a region commonly referred to as the Intertropical Convergence Zone (ITCZ). Understanding what controls the spatial pattern, location, and intensity of the ITCZ in past, present, and future climates is one of the most important challenges for climate science today (Bony et al., 2015). Even in the present-day context, a comprehensive theory which can explain the observed precipitation distribution (figure 1.1) remains elusive, mainly because the underlying dynamics and interactions between moist convection and tropical circulation are thoroughly complex. In addition, progress on this topic has also been hampered by the differing definitions and a widening gap of perspectives on the ITCZ over the last decades.

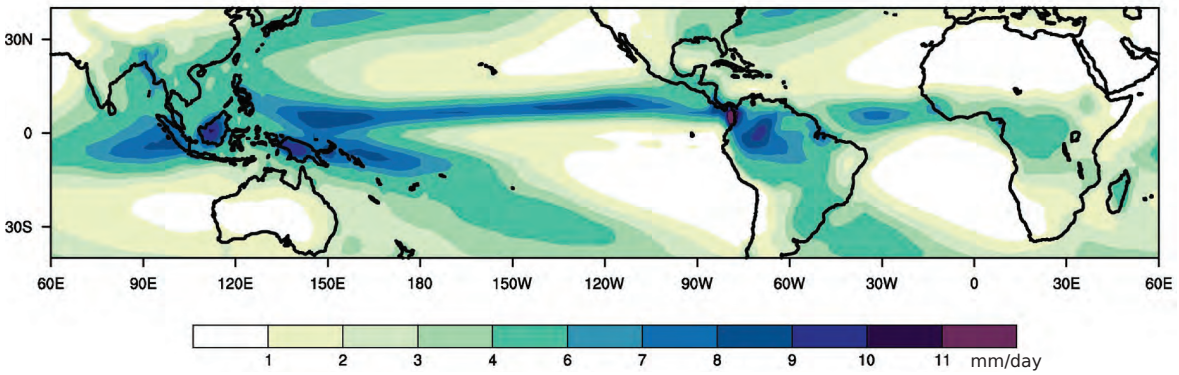

Figure 1.1: Mean (1979-2008) precipitation from the Global Precipitation Climatology Project (GPCP) version 2 (Adler et al., 2003).

Early observations of the ITCZ came from aircraft measurements during World War II (Alpert, 1945; Simpson, 1947). The ITCZ was initially defined as the line where trade winds from the North and South hemispheres meet, and was sometimes referred to as the intertropical front or equatorial front (Fletcher, 1945). This convergence zone was typically found

near the equatorial trough and over the maximum of sea surface temperature (Riehl, 1954). The first set of satellite observations of clouds indicated that areas of maximum cloud cover do not actually lie along the ITCZ, which was instead marked by clear skies (Godshall, 1968; Sadler, 1964; Ramage, 1974). However, the coarse-resolution of these measurements led to conflicting analyses (Hastenrath, 1991). A contrary definition for the ITCZ was provided by Balogun (1973) who found that: "*the ITCZ marks the boundary between the N.E. trades and the low level cross equatorial flow. It is a narrow band about 2-3° latitude wide extending east and west and comprising lines of active meso-scale cumulus convection.*" It is this definition which was eventually adopted by numerical modellers at that time (Ramage, 1974). For instance, in the first simulation of the seasonal cycle using a global model by Manabe et al. (1974), the terms "ITCZ" and "tropical rainbelt" were used interchangeably. Most of the studies which followed have adhered to this view, and today's definition of the ITCZ is one based on maximum cloudiness and rainfall (Schneider et al., 2015).

The ITCZ marks the ascending branch of the Hadley cell, where warm and moist air converge, leading to deep convective clouds and increased rainfall. Its mean location is found north of the equator and spans 4-12° north during its seasonal migration. The off-equatorial position of the ITCZ puzzled many researchers. If on average, solar radiation is maximum at the equator, why is the ITCZ located away from it? Some authors suggested the cold SST at the eastern equatorial Pacific as an explanation (Bjerknes et al., 1969; Pike, 1971), but even in areas where SSTs are warm, the ITCZ remains north of the equator (Waliser and Gautier, 1993). Various theories have been proposed as to why convection is suppressed at the equator and enhanced north of it. There have been two schools of thought regarding this issue, one based on dynamical constraints, and the other which takes a thermodynamical perspective.

Dynamical constraints for the off-equatorial ITCZ latitude are founded on momentum balance in the planetary boundary layer (PBL) (Sobel, 2007). Under this framework, the ITCZ latitude is primarily governed by a positive feedback between PBL convergence and latent heating from deep convection, a mechanism also known as conditional instability of the second kind (CISK) (Charney, 1971). The only point of contention is what controls the PBL convergence. In Charney (1971), it is related to the growth rate of stability that results from a balance between the Ekman layer convergence that increases away from the equator, and the boundary layer potential temperature lapse rate that increases towards the equator. This growth rate maximizes off the equator, marking the ITCZ position. Several other theories have been proposed as to why convergence is preferred away from the equator, among which are SST gradients (Lindzen and Nigam, 1987), the frequency distribution of equatorial waves (Holton et al., 1971), and Earth's rotation (Sumi, 1992; Chao and Chen, 2004).

Another way to interpret the ITCZ position is to look at convection in terms of moist static energy (MSE), a thermodynamic variable conserved in adiabatic motion. In a tropical atmosphere, simplifications applied to the MSE budget results in a relation which says that: a positive energy input (radiation, surface fluxes) into a column is balanced by upward motion and MSE export (Neelin and Held, 1987). Extending this to a global, zonally averaged perspective, the ITCZ location would then depend on the atmospheric MSE flux between North

and South hemispheres and the net energy input near the equator (Bischoff and Schneider, 2014). The ITCZ is located approximately at the latitude where the atmospheric energy flux changes sign. With a warmer Northern Hemisphere, this latitude is found northwards.

Studies which focused on the ITCZ latitude de-emphasized the importance of continents on the ITCZ position, and with that, the concept of monsoons. Monsoons were considered as part of the ITCZ, with the monsoon onset analogous to the off-equatorial position of the ITCZ (Chao and Chen, 2001; Bordoni and Schneider, 2008). However, the different structures of precipitation between land and ocean is apparent in figure 1.1. Over ocean, a concept of a well-defined ITCZ may apply, but over land, monsoon flows wash out the narrow-banded structure (Waliser and Gautier, 1993).

While there is no doubt that monsoons and the well-defined oceanic ITCZ are linked, they are still not exactly the same. We have yet to arrive at a framework which can consistently account for actual spatial structure of the ITCZ, with its latitudinal and longitudinal positions, and with its continental and oceanic aspects. If such a framework were to exist, it would have to be translated to yet another perspective– of convection as it is parameterized in a model gridbox.

1.1.2 Parameterization of moist convection

As early as 1960s, the need to parameterize convection was realized by meteorologists and numerical modellers (Manabe and Strickler, 1964). A typical model grid box is on the order of hundreds of kilometers, whereas convection occurs at the scale of a few kilometers. To parameterize convection, one must be able to express the subgrid effects of convection in terms of grid-scale variables. Moist convection is a small-scale process, whereas the background circulation occurs in larger scales. It is precisely because of this that we can hope to simplify the problem– by considering convection to be in statistical equilibrium with the large-scale circulation. This idea was first proposed by Arakawa and Schubert (1974) as the quasi-equilibrium hypothesis and they considered this the main foundation of parameterizability: "*unless a cumulus ensemble is in quasi-equilibrium with the large-scale processes, we cannot uniquely relate the statistical properties of the ensemble to the large-scale variables.*" For typical climate model grids with resolution coarser than 50-100 km, the quasi-equilibrium assumption is considered valid (Xu et al., 1992).

The convective parameterization has two classical objectives: 1) to calculate the vertically integrated convective heating, proportional to surface precipitation, and 2) to determine the vertical distribution of heat and moisture (Arakawa, 2004). The former is called the closure and the latter is performed through a cloud model. Different approaches to the closure and cloud model have resulted in a number of parameterization schemes. Since the mid-1980s, most models have used the mass-flux approach for parameterization (Gregory, 1995).

The mass-flux approach, first formulated by Ooyama (1971), represents the cumulus ensemble within a gridbox as updrafts which transport heat, moisture, and momentum vertically. The

strength of these updrafts, set by the mass flux at cloud base, is based on the amount of convective instability, measured by the convective available potential energy (CAPE). This constitutes the closure. Most schemes have a CAPE-closure, although some others use a moisture convergence closure (Tiedtke, 1989). The mass-flux is then combined with a cloud model, which determines how the updrafts are modified by the lateral inflow of environmental air into the cloud (entrainment) and outflow of cloudy air into the environment (detrainment). Entrainment and detrainment rates are calculated for large-scale (dynamic) and small-scale (turbulent) mixing.

To activate the convection scheme, the model must determine whether convection is indeed possible. This is done through the trigger function. The trigger is typically based on convective instability. In some convection schemes, a buoyancy perturbation is addded to the updraft at the lifting condensation level to account for subgrid variability. The added buoyancy can be computed in different ways, through the grid-scale vertical velocity (Kain and Fritsch, 1990; Bechtold et al., 2001) or through a temperature perturbation (Tiedtke, 1989).

The trigger, the cloud model, and the closure make up the main components of a convection scheme. As a basic test of a convection scheme, we must look at how well the model captures the tropical precipitation distribution.

1.1.3 Tropical precipitation biases in general circulation models

Biases in the diurnal cycle, frequency and intensity of rainfall, intraseasonal variability, and mean patterns of precipitation have existed and persisted in general circulation models (GCMs) over the years (Trenberth et al., 2003; Dai, 2006). Among these, the double ITCZ bias over the Pacific has perhaps received the most attention. Decades since it was first documented by Mechoso et al. (1995), the anomalous double band of precipitation straddling the equator is still a prominent feature of current GCMs (figure 1.2). The double ITCZ is accompanied by several other biases such as the westward extension of cold SSTs along the equatorial Pacific, a warm SST bias in the southeastern coast, and underestimation of stratus cloud along the west coast of South America (Mechoso et al., 1995; Davey et al., 2002; Lin, 2007; Song and Zhang, 2009). This problem has been approached from a theoretical perspective, by revisiting arguments for an off-equatorial ITCZ, and also from a modelling perspective, by testing its sensitivity to model parameters in simplified set-ups such as a water-covered earth (Hess et al., 1993; Chao and Chen, 2004; Moebis and Stevens, 2012). Studies find that the ITCZ position is maintained by a positive feedback between convection and the large-scale circulation, akin to a CISK mechanism. Whether this feedback is initiated at or away from the equator depends on the model's sensitivity to humidity. Decreased sensitivity to humidity through entrainment (Moebis and Stevens, 2012) or resolution (Landu et al., 2014), can initiate a double ITCZ.

Compared to the number of studies on the Pacific ITCZ, there has been less attention on ITCZs in other sectors such as the Atlantic. Over the tropical Atlantic, model biases are actually quite similar to that of the Pacific. GCMs show a southward ITCZ shift (see figure

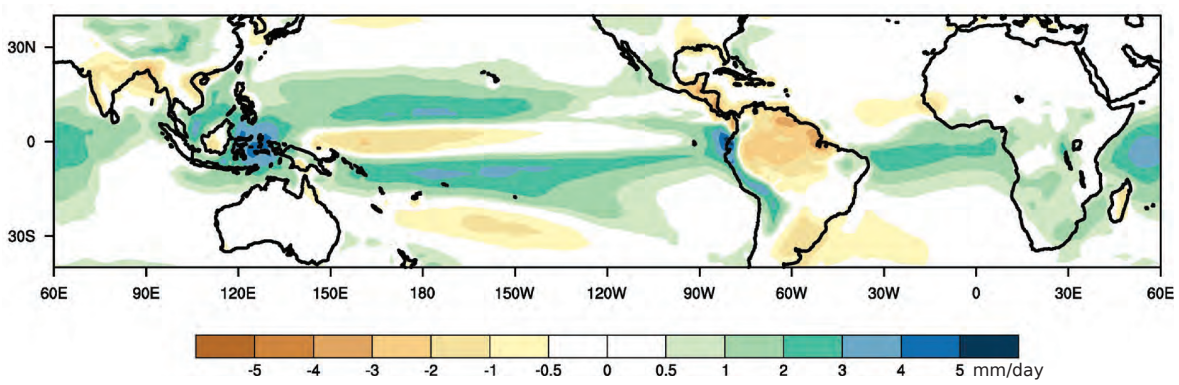

Figure 1.2: CMIP5 multimodel ensemble mean minus GPCP precipitation (1979-2008).

1.2), accompanied by a warm SST bias on the east equatorial Atlantic and underestimated stratus cloud cover along the southeast African coast (Richter and Xie, 2008). Several authors identify the erroneous representation of the Atlantic ITCZ in the atmospheric component of the models as the root cause of biases in winds and SST. Reasons for the Atlantic ITCZ bias are unknown, and there are few studies (Biasutti et al., 2006; Davey et al., 2002; Richter et al., 2013) on this issue. Unlike the Pacific which can be idealized as a water-covered earth, the Atlantic ITCZ is strongly influenced by the presence of the South American and African continents. It is unclear whether proposed solutions for model biases in the tropical Pacific also apply for the tropical Atlantic.

1.1.4 The tropical Atlantic sector

In the mean state, the ITCZ over the Atlantic ocean is observed to lie north of the equator, similar to the Pacific (figure 1.1). Whereas various theories are proposed for an off-equatorial Pacific ITCZ, the northward position of the Atlantic ITCZ is understood to be an obvious consequence of the West African bulge and the associated meridional land-sea contrast (Philander et al., 1996). In continental areas such as the Amazon and Sahel, the mean precipitation structure and intensity are strongly modulated by the seasonal cycle (Hastenrath, 1984).

In boreal winter, the South American monsoon circulation drives moist inflow and enhances convection over most of the continent. The northwesterly monsoon flow converges with the South Atlantic High in a region called South Atlantic Convergence Zone (SACZ), forming part of the northwest-southeast band of continental precipitation. The Atlantic ITCZ is found at the western equatorial Atlantic (figure 1.3a). In boreal spring, a continuous rainband forms, extending across the equator from the Amazon towards central Africa (figure 1.3b). It is during this season that equatorially trapped waves occur most frequently (Dunkerton and Crum, 1995). Convection over Amazon forces Kelvin waves which traverse the tropical Atlantic and reach Africa, linking convection in the three regions (Wang and Fu, 2006). Near the end of boreal spring, the eastern equatorial Atlantic starts cooling and the equatorial cold tongue develops. The equatorial cold tongue enhances the cross-equatorial flow associated with the

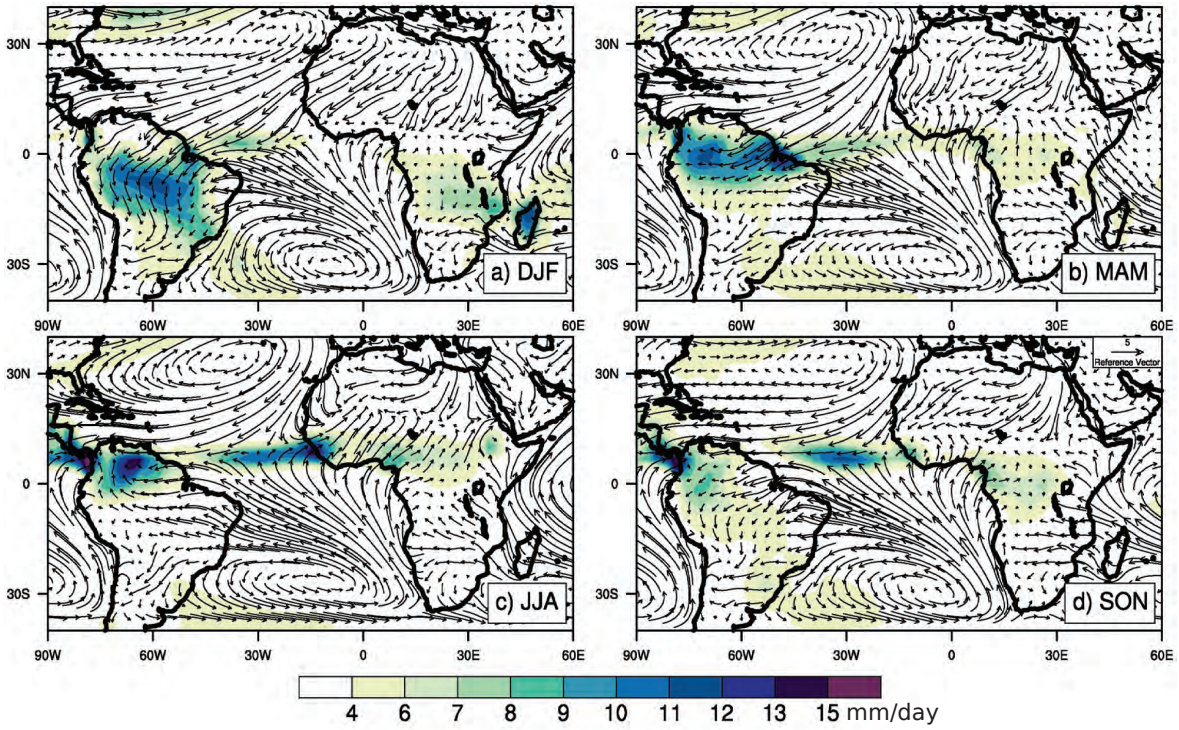

Figure 1.3: Seasonal mean precipitation (shaded contours) and 950hPa winds (vectors) during boreal winter (DJF), spring (MAM), summer (JJA), and fall (SON). Precipitation data is obtained from GPCP and wind data from ERA-Interim.

onset of the West African monsoon (Okumura and Xie, 2004; Mitchell and Wallace, 1992). The West African monsoon brings moisture inland and the rainband extends northwards into the Sahel. The Atlantic ITCZ shifts northwards and eastwards, towards the monsoon region (figure 1.3c). By then end of boreal summer and beginning of autumn, the eastern equatorial Atlantic warms and the West African monsoon enters its withdrawal phase. The Atlantic ITCZ moves to the central Atlantic (figure 1.3d).

Nicholson (2013) cautions against viewing the monsoon as an ITCZ because in West Africa, the rainbelt does *not* coincide with the line of wind convergence. The Saharan heat low drives the confluence of the southwesterly monsoon flow and the northeasterly Harmattan winds, forming a shallow meridional overturning circulation. The rainbelt develops as part of a deep meridional overturning circulation which does not extend as far north as its shallow counterpart (figure 1.3c).

The South American and West African monsoons are both primarily driven by land-sea contrast (Lenters and Cook, 1995; Nicholson, 2013). These two monsoon systems are responsible for much of the zonal asymmetry in the tropical Atlantic.

1.2 Research objectives

The goal of this thesis is to gain a better understanding of factors controlling the tropical Atlantic precipitation distribution. We approach this from a modelling perspective, with the

idea that precipitation biases in our climate models are expressions of and benchmark for how well we understand the coupling of convection and circulation. The simulated precipitation distribution in a model is a product of (1) the interaction of convection with other physical processes such as wind circulation and SST patterns, (2) the horizontal resolution which sets the scale at which physical processes are parameterized, and (3) the parameterization scheme which decides how convection occurs in each gridbox (figure 1.4). With this in mind, we pose three main research questions. They target points 2 and 3, which will implicitly allow us to shed some light on point 1. The three main research questions are:

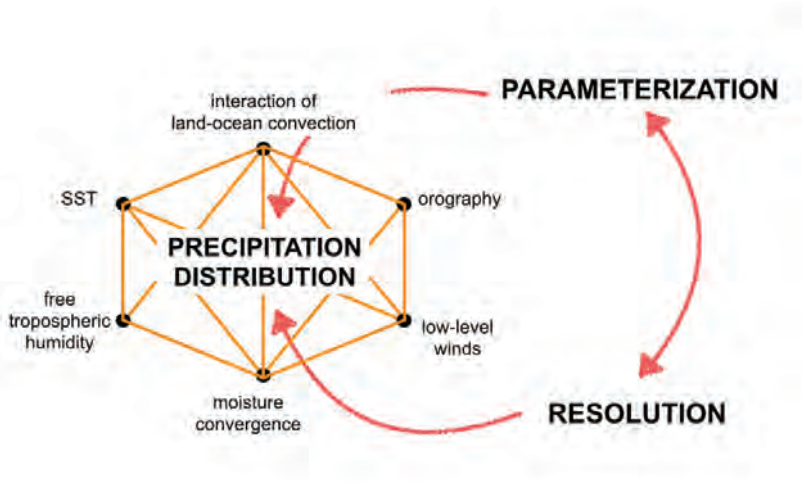

Figure 1.4: Sketch of factors influencing the simulated precipitation distribution.

- **How well do state-of-the-art atmospheric models represent the tropical Atlantic distribution?**

  Most coupled GCMs suffer from biases in SST, surface winds, and precipitation over the tropical Atlantic (Richter and Xie, 2008). Diagnosing the root cause of such biases is difficult because of the strong coupling among the processes involved. To reduce the complexity of the problem, a common strategy is to focus on atmosphere-only simulations which are forced with observed SSTs. The study by Biasutti et al. (2006) was one of the first intercomparisons of the tropical Atlantic precipitation distribution in six atmospheric models. They find that models tend to collocate precipitation and SST too strongly, leading to biases in precipitation. To test the validity and robustness of these findings in current generation climate models, we evaluate the precipitation in twenty two atmospheric models used in the Coupled Model Intercomparison Project Phase 5 (CMIP5) and in two high-resolution versions of the MPI-ESM model. Recognizing that precipitation has a complex structure and cannot be evaluated based on rainfall intensity alone, we employ an object-based approach that has been originally developed to assess weather forecasts (Wernli et al., 2008). With this approach, rainy areas in the

models are clustered as precipitation objects with properties such as size, amplitude, and location, allowing for a three-dimensional quality measure of model performance. The large ensemble of models combined with a detailed analysis of the precipitation distribution in each ensemble member allow us to identify biases which are robust across models and thus allow us to formulate hypotheses as to the origin of such biases. The biases are presented and analyzed in Chapter 2.

- **How does horizontal resolution impact the Atlantic ITCZ position?**

  On one hand, increasing horizontal resolution would tend to improve certain aspects of the large-scale circulation, through smaller grid-spacing and better resolved boundary conditions like orography (Pope and Stratton, 2002; Schiemann et al., 2013). On the other hand, small-scale processes like convection remain parameterized, and a higher resolution would not necessarily translate to a better parameterization performance (Duffy et al., 2003). For instance, in the Pacific, switching to a higher resolution leads to an even higher tendency of the model to have a double ITCZ (Landu et al., 2014). In Chapter 3 of this thesis, we investigate how horizontal resolution impacts the tropical Atlantic precipitation biases described in the previous chapter. We focus on the boreal summer season, when a monsoon circulation is active over West Africa. The relative roles of a high-resolution atmosphere, land surface, and orography on controlling the ITCZ position are identified through a series of sensitivity experiments with the ECHAM model.

- **How does the convection scheme influence the simulated precipitation over land and over ocean in the tropical Atlantic?**

  The occurence of convection in a model gridbox is determined by the convection scheme through a set of criteria that evaluates whether conditions are prone to convection. This set of criteria is designed to be applicable in all situations, for both land and ocean gridpoints, and through seasonally varying large-scale conditions, although derived from a small set of case studies. In Chapters 4 and 5, we are interested in how different parts of the convection scheme– the trigger, the cloud model, and the closure– affect the precipitation distribution over the tropical Atlantic. We study the impact of the convection scheme in two different scenarios, one with a monsoon, and the other without. In Chapter 4, we investigate how the convection scheme influences the precipitation distribution during boreal summer, when the West African monsoon is active. In Chapter 5, we look at the case of boreal spring, a season when there is no monsoon circulation. Modifying specific aspects of the precipitation distribution, such as rainfall amount over land and rainfall amount over ocean, through the performed sensitivity experiments also allow us to understand how different aspects of the precipitation distribution couple with each other.

In Chapter 6, the main findings of this thesis are summarized by revisiting the three main research questions, followed by concluding remarks.

Chapter 2

The Atlantic ITCZ bias in CMIP5 models[1]

2.1 Introduction

The tropical Atlantic circulation is largely controlled by land-ocean interactions involving the continents, Africa and South America, and the Atlantic basin in between. Sea surface temperature (SST) modulates the seasonal cycle of rainfall and its interannual variability in key areas such as the Amazonia and West Africa (Mitchell and Wallace, 1992; Zebiak, 1993; Okumura and Xie, 2004; Yin et al., 2012). Orographic features like the Atlas-Ahaggar mountains in north Africa induce changes in the large-scale circulation and influence the location of the intertropical convergence zone (ITCZ) (Sultan and Janicot, 2003; Cook et al., 2004; Hagos and Cook, 2005). Because the circulation depends on such coupled processes, simulating the tropical Atlantic climate remains a challenge for climate models. For instance, most coupled general circulation models (GCMs) show a reversed SST gradient along the equator, with an anomalously warm SST in the east and cold SST in the west (Richter et al., 2013). This reversed SST gradient is a result of the westerly wind bias originating from the atmospheric component of the models, and persists even in high-resolution models (Chang et al., 2007; Richter and Xie, 2008; Richter et al., 2012; Patricola et al., 2012; Richter et al., 2013; Zermeno-Diaz and Zhang, 2013). Using the diagnostic framework developed by Stevens et al. (2002), Zermeno-Diaz and Zhang (2013) deduced that the westerly wind bias over the equatorial Atlantic ocean was a result of insufficient mixing of momentum into the boundary layer and erroneous sea level pressure (SLP) gradient. The latter is linked to precipitation biases in the atmospheric component which are exacerbated in coupled simulations (Richter and Xie, 2008; Chang et al., 2008; Richter et al., 2013).

Despite continued model improvement, precipitation biases over the tropical Atlantic persist in current GCMs in their coupled as well as uncoupled mode. Previous studies have shown

[1]Siongco, A.C., Hohenegger C., and B. Stevens (2014): The Atlantic ITCZ bias in CMIP5 models. Climate Dynamics, **45**, 1169-1180

that some models exhibit common biases in this area such as the overestimation of precipitation in the Southern hemisphere, the rainfall excess in the Caribbean, and the Amazonian dry bias during boreal summer (Davey et al., 2002; Biasutti et al., 2006; Stockdale et al., 2006; Yin et al., 2012). An explanation for the tropical Atlantic precipitation bias has been provided by Biasutti et al. (2006). Using a set of 6 atmospheric GCMs, they showed that in contrast to observations, models collocate precipitation and SST. This leads to excessive precipitation south of the equator during boreal spring and in the Caribbean sector during summer. The models' apparent oversensitivity to SST is amplified by their lack of sensitivity to atmospheric humidity. The robustness of this result has not been tested with a larger ensemble of models and it remains unclear whether oversensitivity to SST is indeed the root cause of most model biases. In fact, there is a shortage of studies which try to identify atmospheric controls on tropical Atlantic precipitation.

In this chapter, our aim is to fill this gap by considering a larger ensemble of atmosphere-only models and by investigating controls on the precipitation distribution in each ensemble member. Focus is set on identifying and explaining robust precipitation biases across the models which are less likely to be influenced by the particular design of a model. Detailed consideration of the structure of precipitation simulated by each model is performed through an object-based method. The role of model sensitivity to SST and other factors which control the structure of the Atlantic ITCZ are explored in order to explain the results of the object-based analysis.

The chapter is organized as follows: Section 2.2 describes the datasets and the object-based method for precipitation analysis. Section 2.3 presents the results of the object-based analysis in terms of the mean state and seasonal cycle of precipitation. Section 2.4 discusses possible controls on the Atlantic ITCZ structure, explaining the results of Section 2.3. Conclusions are given in Section 2.5.

2.2 Methods

2.2.1 Description of the dataset

Precipitation is analyzed from 22 atmosphere-only models under the Coupled Model Intercomparison Project Phase 5 (CMIP5). The models are run with prescribed SSTs from observations following an Atmospheric Model Intercomparison Project (AMIP) style of integration (Gates, 1992). Monthly output of model precipitation covering the period 1979-2008 is used. In addition to the CMIP5 models, two high resolution versions of the MPI model under the German consortium project STORM/AMIP are examined (Stevens et al., 2013). Table 2.1 lists the models included in this study together with their respective resolution (indicated by nLon, the number of gridpoints along the equator) and reference for their deep convection scheme. All models employ a mass-flux type of parameterization except for INMCM4, which uses a convective adjustment scheme. All data are interpolated to a fixed lat-lon grid with 96 gridpoints in latitude and 192 in longitude, equivalent to a grid of 1.875°. The study covers

Table 2.1: Description of models used in this study with information on resolution and deep convection scheme. The model classification in the last column is discussed in Section 3.

Model Name	**nLon**	**Deep Convection Scheme**	**Class**
ACCESS1.0	192	Gregory and Rowntree (1990)	West Atl
BCC-CSM1	128	Zhang and Mu (2005)	East Atl
BNU-ESM	128	Zhang and McFarlane (1995)	West Atl
CanAM4	128	Zhang and McFarlane (1995)	East Atl
CESM(CAM5)	288	Zhang and McFarlane (1995)	East Atl
CCSM4	288	Zhang and McFarlane (1995)	East Atl
CMCC-CM	480	Tiedtke (1989)/Nordeng (1994)	East Atl
CNRM-CM5	256	Bougeault (1985)	East Atl
CSIRO-Mk3.6.0	192	Gregory and Rowntree (1990)	East Atl
EC-EARTH	320	Fritsch and Chappell (1980)/Nordeng (1994)	West Atl
FGOALS-s2	128	Tiedtke (1989)/Nordeng (1994)	East Atl
GISS-E2-R	144	Gregory (2001)/Del Genio et al. (2007)	West Atl
GFDL-HIRAM-C180	576	Bretherton et al. (2004)	East Atl
GFDL-CM3	144	Donner (1993)/Wilcox and Donner (2007)	West Atl
HADGEM2-A	192	Gregory and Rowntree (1990)	West Atl
INMCM4	180	Betts and Miller (1986)	West Atl
IPSL-CM5A-LR	96	Emanuel (1991)	West Atl
IPSL-CM5B-LR	96	Bony and Emanuel (2001)	West Atl
MIROC5	256	Chikira and Sugiyama (2010)	East Atl
MPI-ESM-LR	192	Tiedtke (1989)/Nordeng (1994)	West Atl
MPI-ESM-HR	384	Tiedtke (1989)/Nordeng (1994)	West Atl
MPI-ESM-XR	768	Tiedtke (1989)/Nordeng (1994)	West Atl
MRI-AGCM32H	640	Yukimoto et al. (2011)	East Atl
NorESM1-M	144	Zhang and McFarlane (1995)	West Atl

the tropical Atlantic sector, which is defined here as the domain encompassing 90°W-45°E, 30°S-30°N. This includes the continents South America, Africa and the tropical Atlantic basin.

Precipitation from the AMIP models is compared with three observational data sets: the Global Precipitation Climatology Project (GPCP) version 2 (Adler et al., 2003), the Tropical Rainfall Measuring Mission (TRMM) product 3B-42 (Huffman et al., 2007), and the Hamburg Ocean Atmosphere Parameters and Fluxes from Satellite Data (HOAPS) version 3 (Andersson et al., 2010). The GPCP dataset is a combination of satellite and rain gauge data and covers the period 1979-2010 with a 2.5° spatial resolution. Precipitation data from TRMM is a merged product of high quality microwave and infrared precipitation and root-mean-square precipitation error estimates. It covers the period 1998-2010 with a 0.25° spatial resolution. HOAPS only gives data for ocean points and is used as a supplementary dataset to GPCP and TRMM over the tropical Atlantic ocean. It covers the period 1987-2005 with a 0.5° spatial resolution. All observational data are interpolated to the same model grid as is used to analyze the model results.

2.2.2 Object-based approach for analyzing precipitation distribution

Comparing precipitation between models and observations is usually performed through gridpoint-based measures such as root-mean-square error (RMSE) analysis. This gives information on where the model overestimates or underestimates the amplitude of precipitation with respect to observed values. However, precipitation is not only characterized by amplitude but it takes on a complex structure as well. A gridpoint-based evaluation of precipitation is susceptible to the double penalty problem, where a model with correct amplitude and structure of precipitation but with a slight displacement in its position is rated as a low-score model. Such a model would be rated as poorly as another model which did not get the precipitation event at all (Wernli et al., 2008). To circumvent the double penalty problem and to extract more meaningful information from the model, object-based measures in evaluating precipitation distribution have been proposed (Ebert and McBride, 2000; Davis et al., 2006; Wernli et al., 2008). Instead of comparing precipitation values gridpoint by gridpoint, the original precipitation field is condensed into precipitation objects. The object identification procedure is illustrated in figure 2.1. A threshold P_f is set and only gridpoints with precipitation values $P > P_f$ are considered. These remaining gridpoints are then clustered into objects described by their structure, amplitude, and location, also known as SAL (Wernli et al., 2008). This allows for a three-dimensional quality measure of model performance. The SAL method has been originally developed for high-resolution weather forecasts (Gilleland et al., 2009; Ebert and Gallus, 2009) but has recently been proven useful for assessing low-resolution climate simulations (Hohenegger and Stevens, 2013).

In this study, the threshold is set as: $P_f = f \cdot P_{\max}$ where $P_{\max}$ is the maximum precipitation value of a model over a certain area and f is a fraction of this value. Note that $P_{\max}$ is not an absolute reference value but instead depends on the model. The objects essentially represent

regions where the model prefers to rain. Since precipitation differs between land and ocean, with stronger and more peaked precipitation over land, different thresholds are chosen for land and oceanic sectors. Hereafter, land and ocean terms will be denoted by the subscripts l and o, respectively. For the mean state precipitation over land, $P_{fl} = 0.35 \cdot P_{\text{maxl}}$ while for oceanic precipitation $P_{fo} = 0.60 \cdot P_{\text{maxo}}$. To capture the seasonal cycle of the multimodel mean, the fraction f_o is increased to 0.70 when considering seasonal averages. As pointed out by Wernli et al. (2008), there is no objective criteria for the choice of f_l and f_o but a general rule is that if the fractions are well-chosen, the resulting precipitation objects should be consistent with features which can be seen by eye. This is the case with the chosen thresholds. Note that if the threshold is too high, robust precipitation features cannot be captured because the objects will be too sensitive to sharp peaks (one or two pixels of very intense rainfall). On the other hand, if the threshold is too low, the objects will not be sensitive enough to capture distinct features of precipitation. The model classification described in the next sections are found to be robust even if other thresholds are used, ranging from 50-70%.

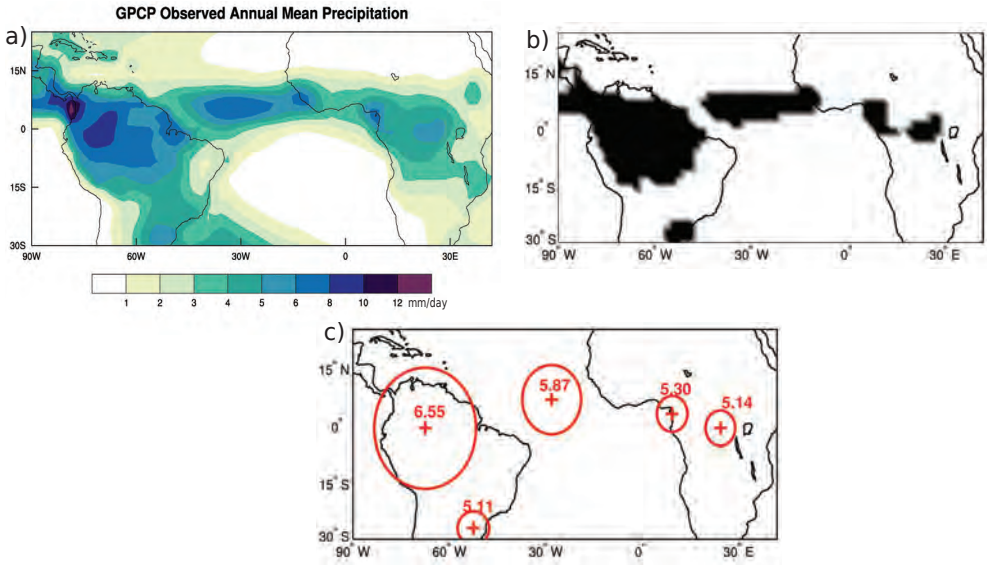

Figure 2.1: From the a) original precipitation field, a threshold P_f is set and only b) gridpoints with precipitation values $P > P_f$ are considered to get c) precipitation objects with properties such as size (circle), amplitude (numbers), and location (cross).

After setting the thresholds P_{fl} and P_{fo}, land and ocean precipitation objects are identified. For each object, a set of three properties is calculated: 1) Size, the number of pixels comprising the object, 2) Amplitude, the mean intensity of the pixels of the object, and 3) Location, the coordinates of the weighted centroid of the object. To capture the observed precipitation structure in the central Atlantic as seen in figure 2.1a, it is practical to identify the main ocean object as the largest object. Precipitation features near the coasts are found to be insensitive to the land-ocean separation implemented here. The results discussed in the succeeding sections are robust even when taking a larger area for the ocean to include the equatorial coastal regions.

2.3 Representing tropical Atlantic precipitation

2.3.1 The mean state

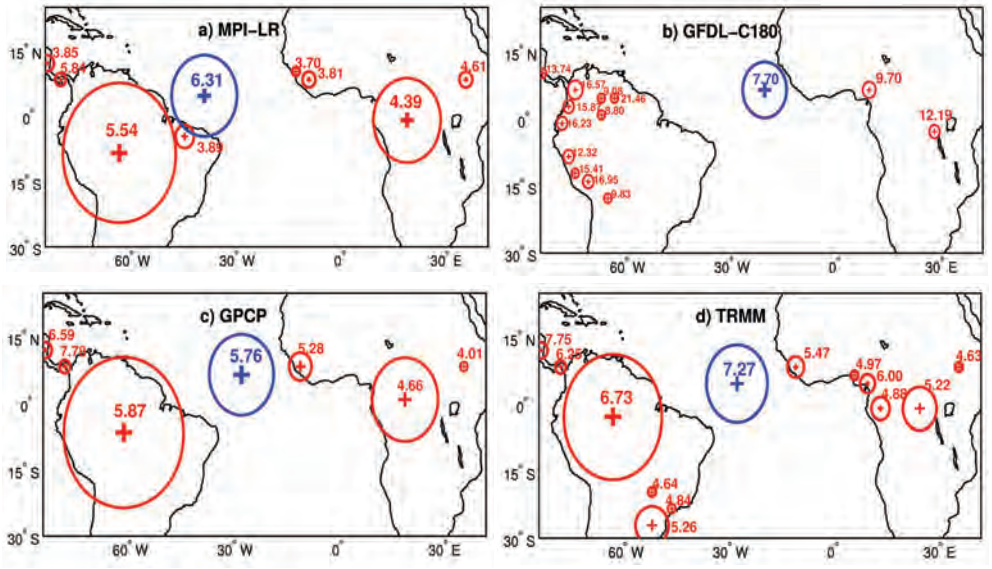

Figure 2.2: Land and ocean precipitation objects from two models, a) MPI-LR and b) GFDL-C180, and observations c) GPCP and d) TRMM. Land objects are marked in red and ocean objects in blue. The cross marks the weighted centroid, the circle shows the equivalent area, and the numbers indicate the mean intensity of the precipitation object.

The ability of models to represent the mean state of precipitation over the Atlantic sector is assessed using the previously described object-based approach. By doing so, two classes of models emerge. Figure 2.2 illustrates the two classes of model behavior using MPI-LR and GFDL-C180 as examples. The MPI-LR has a reasonable representation of the distribution of objects over land, with comparable properties to objects in the observed precipitation field. The ocean object, however, is misplaced too far west, near the coast of Brazil. The GFDL-C180 model shows small-sized land objects with very high precipitation values. These land objects are located in regions with pronounced relief in the terrain, especially over the Andes in South America. For GFDL-C180, the oceanic precipitation structure is more longitudinally distributed, with the ocean object located near West Africa, hence too far east. It is noteworthy that over ocean, neither MPI-LR nor GFDL-C180 matches the observed precipitation distribution. GPCP and TRMM place the main object in the central Atlantic (28.125°W). HOAPS also has a central ocean object located at 30°W (not shown). The models place the ocean object either too far west (MPI-LR) or too far east (GFDL-C180). Further examination of the two models indicate that this behavior is evident in the individual years of the simulation. The MPI-LR ocean object has a mean location of 41.25°W with an interquartile range of ±1.875° across the years while the GFDL-C180 ocean object at 20.62°E varies by ±3.75° across the years. Over land, GFDL-C180 does not reproduce the observed land objects and instead shows peaked precipitation objects. This is because GFDL-C180 has a very strong P_{maxl}, and thus a high threshold P_{fl}, preventing the object identification algorithm

to pick out the land objects seen in observations and in MPI-LR. The object identification algorithm emphasizes the fact that GFDL-C180 has a very different representation of land precipitation over Africa and South America as compared to observations or MPI-LR due to excessive production of orographic precipitation. Because of its higher spatial resolution, TRMM has four objects over equatorial Africa while GPCP clusters these features as one big object. Even so, the amplitude of the TRMM objects over Africa is not nearly as high as the two peaked objects in GFDL-C180.

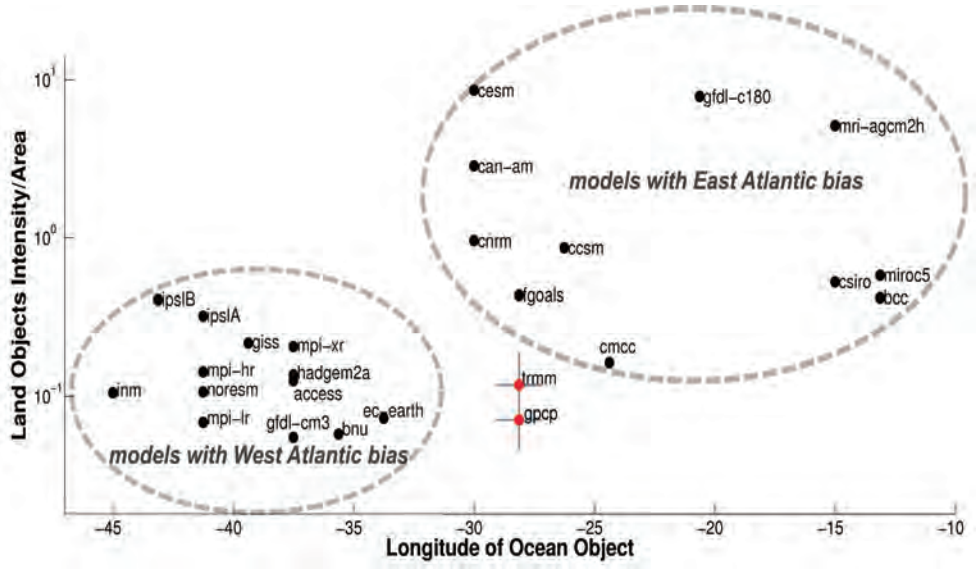

Figure 2.3: Longitude of the ocean object plotted against the intensity-area ratio (measure of peakedness) averaged over the three most rainy objects over land. The gray lines in GPCP and TRMM show the interquartile range of the interannual variability of their object properties.

Given the MPI-LR and GFDL-C180 object distribution, figure 2.3 summarizes the behavior of all models in terms of the longitude of the ocean object plotted against the intensity-area ratio of the land objects. This ratio is high when intense precipitation is concentrated over small areas. Models with land objects like GFDL-C180 have high intensity-area ratios. The low-ratio models, on the other hand, systematically place the ocean object westward, as seen in MPI-LR. The lower left and upper right circles in figure 2.3 indicate the model separation to West Atlantic class (low ratio, westward ocean object) and East Atlantic class (high ratio, eastward ocean object). None of the models can reproduce the observations and the biases appear larger than the observed yearly variability in the object properties as given by the interquartile range.

Figure 2.4 shows the mean state behavior of the ensemble of these two groups. The models have a similar precipitation structure over land, except that East Atlantic models (GFDL-C180) have intense precipitation values over orographic regions. Over ocean, even though SST is prescribed, the models show two different oceanic precipitation structures. The West Atlantic class (MPI-LR) has an ITCZ structure which appears as a dense blob of precipitation in the western part of the Atlantic basin. The East Atlantic class (GFDL-C180) has a much more longitudinal structure but rains more in the eastern than in the central part of the basin. Both model types miss the central Atlantic placement of the observed ITCZ

maximum in the mean state. Some East Atlantic models have ocean objects near the central Atlantic (FGOALS, CESM, CAN-AM, CNRM, CCSM). This is a consequence of their more longitudinally distributed ITCZ structure being clustered as one contiguous region. While these models still rain more in the eastern than in the central Atlantic, they have a weaker bias compared to other models like GFDL-C180.

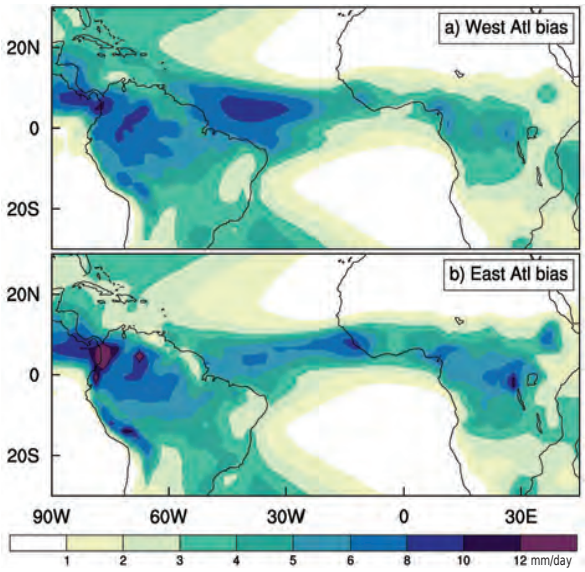

Figure 2.4: Mean state of precipitation over the tropical Atlantic for models with a) West Atlantic bias and b) East Atlantic bias.

2.3.2 The seasonal cycle

The mean state of precipitation in the models is influenced by how well they simulate the seasonal cycle. The relationship of mean state biases with the seasonal cycle of precipitation is explored by again performing an object-based analysis.

Figure 2.5 shows the seasonal evolution of the Atlantic marine ITCZ, as represented by the migration of the main ocean object per season. Observations (GPCP and TRMM averaged) show a central Atlantic placement of the precipitation object through all seasons, most markedly so in March-April-May (MAM). The West Atlantic bias is apparent with figure 2.5b showing a consistent westward placement of the ocean object for all four seasons. Figure 2.5c, representing models with the East Atlantic bias, shows a more longitudinally extended progression of the precipitation object following the seasonal cycle. During boreal fall and winter, the models and observations all show objects located in the western part of the basin. It is during spring that the two model groups begin to deviate from each other and from the observations. The models place the objects on opposite sides of the Atlantic with respect to the observations. Models with the East Atlantic bias place the main spring object at the Gulf of Guinea in West Africa. They have a secondary object located near the coast of Brazil (not shown), indicative of a tilted ITCZ structure in MAM (Richter and Xie, 2008).

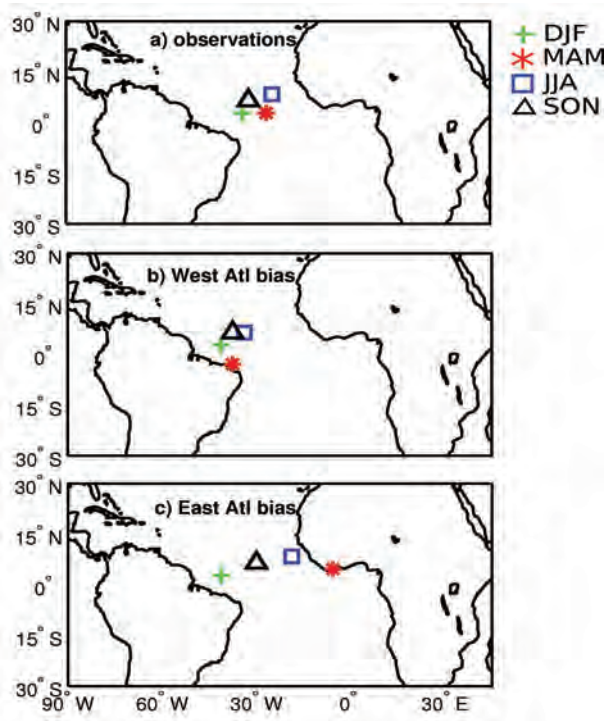

Figure 2.5: Seasonal progression of the main ocean precipitation object for the ensemble mean of a) observations (GPCP and TRMM, averaged), b) West Atlantic bias class, and c) East Atlantic bias class.

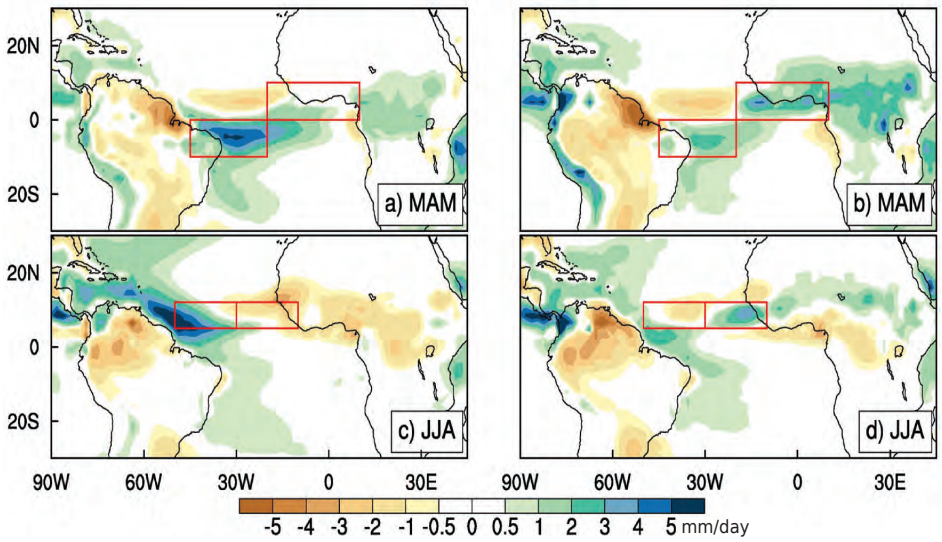

Figure 2.6: Precipitation anomaly (model minus GPCP observation) in MAM (a,b) and JJA (c,d) for models with the West Atlantic bias (a,c) and with the East Atlantic bias (b,d). Red boxes are used for the conceptual diagram in figure 2.9.

Previous studies have shown that the precipitation structure in MAM is a determining factor for the evolution of SST and surface winds during the next seasons in coupled simulations (DeWitt, 2005; Richter and Xie, 2008; Richter et al., 2013; Zermeno-Diaz and Zhang, 2013). Such studies often used an ensemble mean of models to highlight differences between observed and modeled precipitation distributions, which can give a distorted view in the presence of two

model clusters. Figure 2.6 shows the structure of precipitation anomaly when the ensembling takes into account the two classifications of models. During MAM, a southward shift of the ITCZ with a maximum over the coast of Brazil is apparent for models with the West Atlantic bias. This southward shift is also present in models with the East Atlantic bias, though it is less pronounced and is further accompanied by excessive precipitation over the Gulf of Guinea. Excessive precipitation over the Gulf of Guinea and deficient precipitation west of this region, akin to figure 2.6b, has already been noted by Richter and Xie (2008). They argued that it is this east-west precipitation bias in AMIP models which drives an anomalous westerly flow, causing a reversed SST gradient in coupled simulations. In a later paper, Richter et al. (2013) however proposed that it is the southward shift of the ITCZ in the models, a situation more akin to figure 2.6a, which leads to the westerly wind error by inhibiting southeasterlies from crossing the equator. While both the southward shift of the ITCZ and the excessive precipitation over the Gulf of Guinea during MAM will induce wind anomalies, it is unclear which one is actually responsible for the westerly wind error. But whether models rain more over the eastern or western coast in boreal spring is largely dependent on the models included in the ensemble. By distinguishing models with West Atlantic bias from those with East Atlantic bias and performing an ensemble mean for each group, one could see a clearer separation of the precipitation bias from one coast to the other.

During MAM, the East Atlantic models also have, in general, a wetter Sahel and Congo region than West Atlantic models. Over the Amazonia, both model classes have deficient precipitation, especially over the northeastern border (Amapa and Guiana regions). In JJA, both models have a dry Amazonia but East Atlantic models have a wetter Sahel (figure 2.6c and d). Noteworthy are especially the differences over the Atlantic ocean, in agreement with figure 2.5. Models with the West Atlantic bias show excessive precipitation along the coast of Brazil and deficient precipitation in the eastern basin. Models with the East Atlantic bias show excessive precipitation in a localized region along the coast of West Africa (Guinea Bissau and Senegal), accompanied by deficient precipitation west of this region. The anomaly structure in JJA is maintained in boreal fall. During boreal winter, the two classes both have excessive rain in the west and deficient rain in the east, but West Atlantic models rain more in the western basin than East Atlantic models (not shown).

2.4 Controls on the Atlantic ITCZ structure

With a wide range of parameters which could change from one model to another, it is not obvious why the set of models considered in this study separate into two clusters. Looking at table 2.1, the model classification seems to follow a trend based on horizontal resolution. There is a tendency for the East Atlantic class to have more gridpoints along the longitude while most models with the West Atlantic bias have less gridpoints. A detailed consideration of the model MPI indeed indicates a dependence of the ITCZ structure on horizontal resolution as illustrated in figure 2.7. A reduction in the West Atlantic bias is apparent as the resolution is increased from T63 to T255 and a structure closer to observations is attained.

Specifically, the precipitation maximum over ocean shifts towards the central Atlantic with higher resolution. The decrease in precipitation near the coast of Brazil is accompanied by an increase in precipitation near the coastal regions of West Africa. The improvement is not as apparent in the African continent, where the precipitation distribution does not change significantly when the resolution is increased. Over South America, the structure does not change except that the high resolution runs tend to show intense precipitation values over the Andes and Guiana highland regions. That MPI-HR and XR remain under the West Atlantic class is a consequence of the object-identification algorithm which still places the ocean object a little to the west of the observed object.

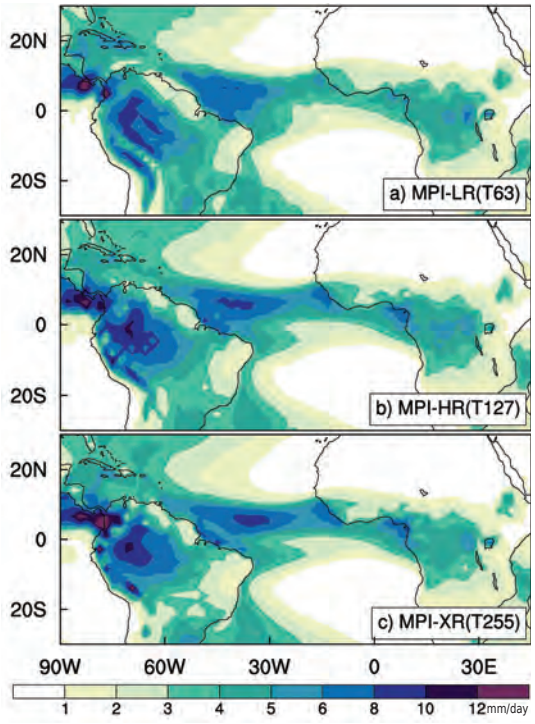

Figure 2.7: Mean state ITCZ structure in different resolutions of the MPI model: a) LR-T63, b) HR-T127, and c) XR-T255.

Figure 2.8 shows the circulation in MAM (the season when the two classes start to diverge) using the MPI and GFDL models with their low and high resolution versions. Although their low resolution versions exhibit a distinct pattern, especially in vertical velocity, increasing the resolution yields similar effects. Both models show that an increase in horizontal resolution leads to increased rainfall over the Gulf of Guinea, accompanied by stronger upward motion over this region. The enhanced convergence is associated with stronger low-level (850 hPa) westerlies which, on one hand, can reinforce the anomalous deep convection along the coast. On the other hand, it also suppresses some of the precipitation that would otherwise have fallen over the Brazil coast. This results in a more eastward placement of the ocean precipitation object.

Precipitation over the Gulf of Guinea in spring is crucial in determining the ITCZ structure during summer. The full loop is schematically illustrated in figure 2.9. The boxes in MAM indicate the location of the west and east coastal bias of the models. The boxes in JJA mark

the observed location of the ITCZ, split into an eastern and western part at 30°W (central Atlantic). Similar boxes are shown in figure 2.6 for reference. In MAM, the two model groups differ in the strength of convection from one coast to the other, as shown by the prominence of the symbols. The East Atlantic class rains more over the Gulf of Guinea and as the ITCZ moves northwards in JJA, these models continue to rain in the east. The West Atlantic class rains more over the coast of Brazil in MAM and continues to rain in the western basin during JJA. Note that in both model classes, the boreal summer season replicates the location of the precipitation maximum during spring. The east-west partitioning of precipitation in spring is carried over to the summer, and explains the two different Atlantic ITCZ structures in the mean state.

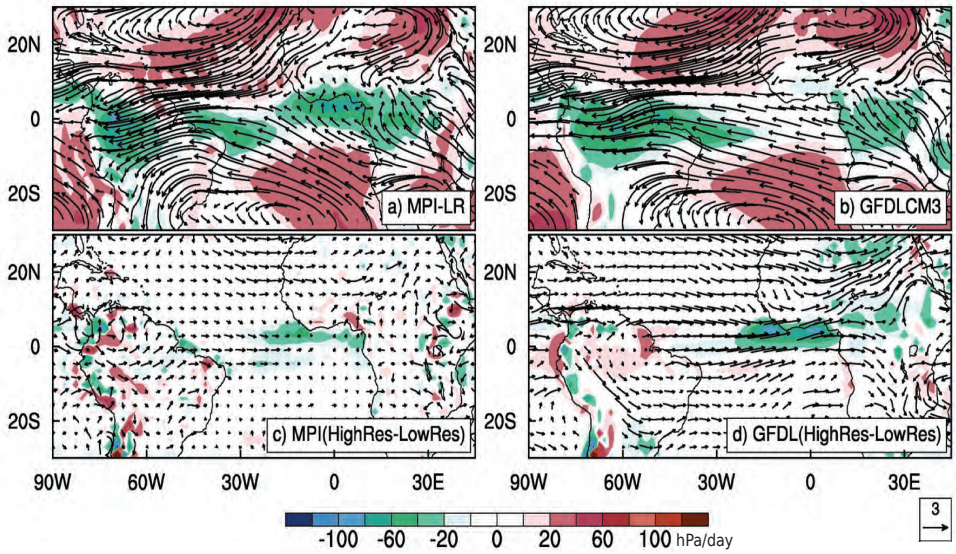

Figure 2.8: Mean large-scale circulation during boreal spring for low-resolution (top panel) versions of two models, a) MPI and b) GFDL. The vectors show the horizontal wind at 850hPa and the shadings represent the vertical velocity at 500hPa, green is for upward motion and red for subsidence. The bottom panel shows the horizontal wind difference (vectors) and vertical velocity difference (shading) between the high and low resolution versions of c) MPI and d) GFDL.

The previous explanation stresses the importance of the east-west partitioning of precipitation over the ocean and relates it to the effect of resolution. However, other factors may play a role. As Richter and Xie (2008) suggested, a small ocean basin like the Atlantic is strongly influenced by convection from the adjacent continents. Richter et al. (2012) emphasized the role of the precipitation deficit over Amazon and excess over Congo in controlling the circulation over the Atlantic. In particular, they suggested that increased convection over Amazon leads to stronger easterlies. If so, West Atlantic models with stronger easterlies than East Atlantic models (see figure 2.8) should have more Amazonian precipitation. However, this seems not to be the case with models investigated in this study as both model classes show a dry bias over Amazon in spring and summer (see figure 2.6). This is also supported by the study of Wahl et al. (2011) with one version of the Kiel Climate Model, where they demonstrated that stronger easterlies and a reduced SST bias emerge when there is more precipitation over the coast of Brazil, even though a dry bias persists over the Amazonia.

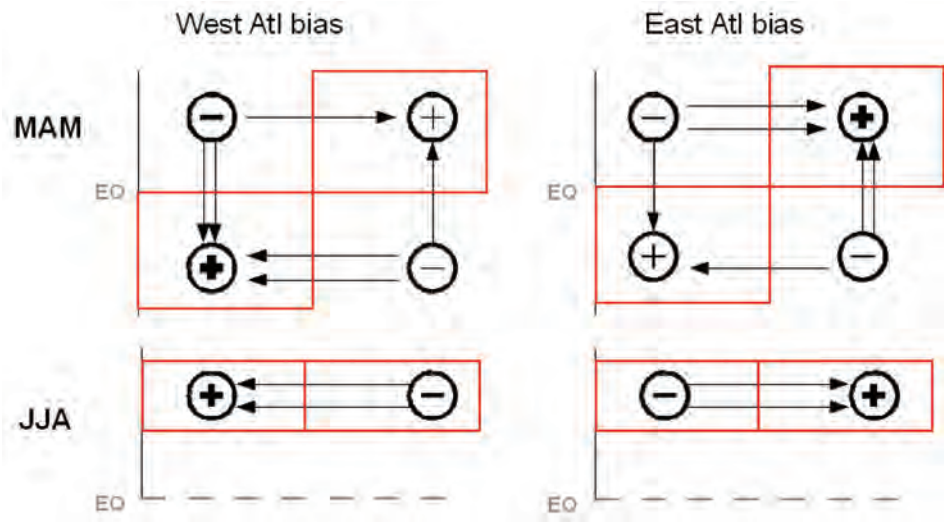

Figure 2.9: Simplified sketch of the circulation during MAM and JJA for the two types of models. A plus indicates overestimation of precipitation with respect to GPCP observations while a minus indicates underestimation. The thickness of the signs is proportional to the magnitude of the bias. The arrows illustrate the low-level zonal wind associated with the precipitation biases. The mean flow along the equator is easterly. The location of the red boxes is the same as in figure 2.6.

With a tercile difference ensemble approach, Zermeno-Diaz and Zhang (2013) also found no relation with Amazon rainfall deficit and wind errors during MAM. They noted instead a rainfall excess over the coast of Brazil. The atmospheric origin of the westerly wind problem may not be an issue of continent-to-continent precipitation biases alone but of how models represent the ITCZ structure from one coast to the other as well.

An alternative hypothesis for the West Atlantic bias would be the effect of the adjacent South American orography on the large-scale circulation. It is plausible that models with the East Atlantic bias capture the South American circulation better, do not rain excessively over the coast of Brazil, and can still rain over the Gulf of Guinea. However, a regime-sorting analysis on deep convection over northern regions of South America versus deep convection over the coast of Brazil does not show a clear connection between the two. The peaked precipitation behavior of the East Atlantic class, mostly occurring in the Andes, is likely a consequence of high resolution rather than a cause for the suppression of the West Atlantic bias. This further strengthens our hypothesis that it is horizontal resolution which appears to have the largest influence on the marine ITCZ structure through its influence on coastal precipitation along the equatorial Atlantic.

Biasutti et al. (2006) proposed that models collocate SST and precipitation too strongly, thus causing the southward shift of the ITCZ (near the coast of Brazil) during boreal spring. The present analysis does not support this SST-precipitation maxima hypothesis (see figure 2.10). In spring, the West Atlantic class rains excessively over the western basin even though the SST maximum is located on the eastern coast, at the Gulf of Guinea. While the precipitation maximum in the East Atlantic class is indeed at the Gulf of Guinea during spring, it remains in the eastern basin during summer, even though the SST maximum has shifted to the west.

Neither the West nor East Atlantic model classes show a clear connection between the seasonal evolution of the SST maximum and precipitation maximum over the tropical Atlantic ocean.

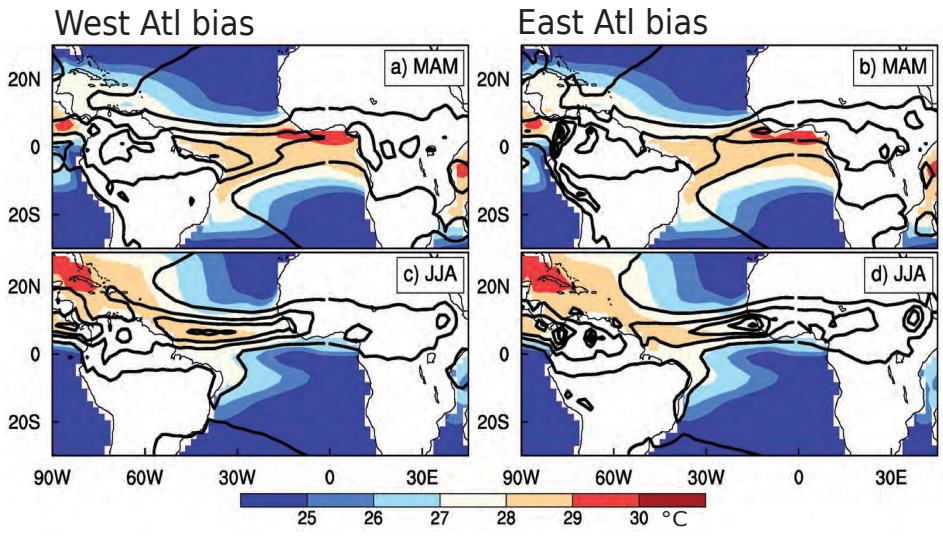

Figure 2.10: Boreal spring (a,b) and summer (c,d) SST (shaded) and precipitation (contours, interval is 4 mm/day starting at 2 mm/day) of West Atlantic (a,c) and East Atlantic class (b,d).

Another player could be the convection scheme. Table 2.1 indicates no obvious relationship between the model classification and the convective parameterization. It is difficult to see a systematic behavior, given that models with the same convection scheme fall into separate model clusters. The three versions of the MPI model, with different resolutions but same convective parameterization, indicate a reduction of the West Atlantic bias with increasing resolution. Even if convection is turned off, the low resolution MPI-LR still exhibits the West Atlantic bias. Furthermore, if the call to the deep convection scheme is inhibited and most of the convection is explicit, as in the case with GFDL-C180 (Zhao et al., 2009), the East Atlantic bias persists. However, the convection scheme may influence the resolution limit at which a particular model transitions from a West Atlantic bias to an East Atlantic bias. For instance, the GFDL model shows a transition from West to East Atlantic bias when the resolution is increased four times (see table 2.1). On the other hand, with the same increase in resolution, the MPI model does not show a full transition to the East Atlantic bias.

It should be noted that the tropical Atlantic basin is flanked by two land masses less than 3000km apart, with more African land mass north of the equator and more South American land mass south of the equator. Perhaps it is this relatively small distance between the two continents, combined with their asymmetric distribution near the equator, which makes the representation of the marine ITCZ structure particularly sensitive to coastal precipitation and to how well these coastlines are captured by a model. In fact, Schiemann et al. (2013) attributed the reduction in dry precipitation bias over the Maritime continent at higher horizontal resolution to better resolved land fraction and increased latent heat flux over coastal areas. The geometry of the tropical Atlantic is such that biases in coastal precipitation can significantly affect the overall marine ITCZ structure in the seasonal cycle and consequently, the mean state. The topography might also play a role, especially in north Africa whose

orographic features influence the circulation and precipitation patterns in Sahel. Indeed figure 2.8 shows stronger westerlies over north Africa for high resolution. These ideas must be explored further through sensitivity analyses.

Coupling with the ocean introduces more complexities. For instance, Patricola et al. (2012) found that the relationship between wind, SST, and precipitation is dependent on the spatial resolution of the ocean model used. It would be very interesting to investigate whether the relationships uncovered in this study remain apparent in coupled simulation, a topic for future studies.

2.5 Summary

In this chapter, we investigated the tropical Atlantic precipitation distribution in 24 atmosphere-only models under CMIP5. An object-based analysis patterned after Wernli et al. (2008) was employed in order to condense the original precipitation field to areas of interest called precipitation objects. By performing such an analysis for the mean precipitation state, two classes of model behavior were found. Class 1 models place the ocean precipitation object in the west basin, whereas it is in the central Atlantic in observations. These are the models with the West Atlantic bias. Class 2 models rain excessively over orographic regions, showing peaked land objects. The oceanic precipitation in class 2 models is more longitudinally distributed like in the observations, but these models rain more in the eastern basin than in the central Atlantic, showing the East Atlantic bias. The emergence of the two model classes are difficult to explain on the basis of the hypothesis of Biasutti et al. (2006), which says that model biases reflect a too strong coupling of convection to underlying SSTs.

Focusing on the marine ITCZ, the model classification in the mean state of precipitation is traced to a separation already present in the seasonal cycle. In boreal spring, the two classes of models place the ocean object on opposite coasts: south Brazil coast and Gulf of Guinea. In the succeeding boreal summer season, as the ITCZ moves northwards, the two classes maintain this west-east partitioning of precipitation. West Atlantic models continue to have their peak in precipitation over the coast of Brazil while East Atlantic models rain north of the Gulf of Guinea. The higher boreal spring precipitation over the Gulf of Guinea in East Atlantic models is found to be sensitive to horizontal resolution in the two models studied here. Models with high horizontal resolution show stronger deep convection over the Gulf of Guinea and stronger westerlies, suppressing precipitation in Brazil. Hence, the difference by which East and West Atlantic bias models represent coastal precipitation in the seasonal cycle results in the two different marine ITCZ structures.

The present study concludes that (1) the Atlantic ITCZ structure in the models is strongly influenced by the seasonal cycle of precipitation along the coasts of Brazil and Gulf of Guinea, (2) the coast-to-coast precipitation in boreal spring influences the east-west partitioning of precipitation in summer, and (3) horizontal resolution influences the weight of precipitation bias from one coast to the other.

Chapter 3

Impact of horizontal resolution on the longitudinal position of the Atlantic ITCZ

3.1 Introduction

The presence of continents has two main consequences for the ITCZ position. First, the introduction of boundaries changes the dynamics of atmosphere-ocean coupling. Philander et al. (1996) show that the slant of South America orients the trade winds parallel to the coastal boundary such that an upwelling region arises. This keeps the SST cold south of the equator and warm north of the equator, an asymmetry which they propose to be the main reason why the ITCZ position is northwards. Second, differential heating is established between land and ocean, generating a monsoon which influences the precipitation distribution. Over the tropical Atlantic, for instance, the presence of Africa and South America gives a preferred longitudinal position for the Atlantic ITCZ (Chao and Chen, 2001).

The Atlantic ITCZ is controlled by the seasonal variation of insolation and SST and by interactions with its adjacent continents (Cook et al., 2004; Wang and Fu, 2006). Simulating its position and structure remains a challenge for current climate models (Biasutti et al., 2006; Richter and Xie, 2008). In the previous chapter, we have shown that even when SSTs are prescribed, models cannot represent the observed east-west structure of the Atlantic ITCZ. We have found that during boreal spring and summer, the East and West Atlantic ITCZ biases are influenced, in part, by the horizontal resolution of the models.

Studies have shown that increasing the horizontal resolution in climate models lead to improvements in certain aspects of the global and regional climate such as precipitation distribution (Manabe et al., 1970; Pope and Stratton, 2002; Duffy et al., 2003). For certain regions like the Maritime Continent, the resolution of surface fields such as the land-sea mask strongly impacts the intensity of precipitation and surface latent heat flux in the model (Schiemann et al., 2013). Demory et al. (2014) note that with a finer grid, more weight is

given towards resolved processes than to those which are unresolved/parameterized. For precipitation over land, this means more contribution from moisture transport from the ocean and less contribution from local evaporation.

Although increased horizontal resolution may lead to general improvements, small-scale processes remain parameterized in climate models. How parameterizations respond to finer resolutions is not clear and may differ from model to model (Duffy et al., 2003). Long-standing issues such as the ability of models to simulate the diurnal cycle of precipitation cannot be solved by merely increasing the horizontal resolution (Dirmeyer et al., 2012). A deeper understanding of physical processes, together with improved ways of translating this knowledge to parameterizations in our models, is necessary to address current model biases.

In this chapter, we investigate how horizontal resolution impacts the structure of the Atlantic ITCZ in the model ECHAM6, with a focus on the boreal summer season. Our goal is twofold: to identify which aspects of the model determine the east-west partitioning of precipitation over the Atlantic, and to gain insights on mechanisms behind the precipitation responses. Sensitivity experiments are performed and analyzed using the factor separation framework in order to identify the relative contributions of a high-resolution atmosphere, orography, and surface. Mechanisms behind the factor-separated contributions are explored using additional experiments designed to test the effects of orography and convection scheme on the precipitation distribution.

The outline of the chapter is as follows: Section 3.2 describes the model, the factor separation framework, and the experimental set-up. Factor-separated contributions of the atmosphere, orography, and surface are presented in Section 3.3. In Sections 3.4 and 3.5, possible mechanisms behind the results of Section 3.3 are analyzed. A summary is given in Section 3.6.

3.2 Methods

3.2.1 Model

Simulations are performed using ECHAM6, the atmospheric component of MPI-ESM, described in Stevens et al. (2013). ECHAM6 uses a dry spectral-transform dynamical core. It supports triangular truncations at T31, T63, T127, and T255, corresponding to grid-point resolutions of 3.75°, 1.875°, 0.93°, 0.47° at the equator, respectively. ECHAM employs a hybrid sigma-pressure coordinate system, with either 47 or 95 levels in the vertical. The model includes a suite of physical parameterizations for the representation of diabatic processes. Convection is parameterized based on a mass-flux scheme developed by Tiedtke (1989), with modifications for deep convection by Nordeng (1994). In the Nordeng scheme, deep convection closure is based on a quasi-equilibrium assumption (CAPE relaxation) and organized entrainment is based on updraft buoyancy. The trigger of convection is related to the temperature variance in the boundary layer. Large-scale precipitation is treated diagnostically and is computed by integrating the conversion terms of cloud liquid and ice over the atmospheric column (Lohmann and Roeckner, 1996). ECHAM6 includes JSBACH, a land surface

model based on a tiling approach (Reick et al., 2013). A five-layer model is used to model soil moisture and temperature.

3.2.2 Factor separation

To investigate the effect of high resolution on the east-west partitioning of precipitation along the Atlantic, we consider three factors: a high-resolution atmosphere (A), orography (O), and surface (S). Following the factor separation analysis in Stein and Alpert (1993), we isolate the relative contribution of each factor on the precipitation distribution. Hereafter, precipitation fields from simulations are denoted by $\mathrm{F}_{A/O/S}$, with the subscript denoting the operating factor in each simulation. For example, F_A is a simulation with only the atmosphere in high resolution, whereas the surface and orography are in low-resolution. $\hat{F}_{A/O/S}$ denotes the relative contribution to the precipitation field by the operating factor.

The precipitation field from a simulation with all factors active, F_{AOS}, can be decomposed as in equation 3.1. It is equal to the sum of the precipitation field when all the factors are turned off (F_{off}), plus the contributions due to each factor ($\hat{F}_A$, $\hat{F}_O$, $\hat{F}_S$), and the contributions due to the interaction of the factors (e.g. $\hat{F}_{AS}$).

$$F_{AOS} = F_{off} + \hat{F}_A + \hat{F}_O + \hat{F}_S + \hat{F}_{AS} + \hat{F}_{OS} + \hat{F}_{AO} + \hat{F}_{AOS} \tag{3.1}$$

To isolate the relative contribution terms ($\hat{F}$'s), we would need eight simulations: F_A, F_O, F_S, F_{AS}, F_{OS}, F_{AO}, F_{AOS}, and F_{off}. We then get the individual contribution of each factor, say, orography as:

$$\hat{F}_O = F_O - F_{off} \tag{3.2}$$

The contribution due to the interaction terms, say, that of a high-resolution atmosphere and surface is given by:

$$\hat{F}_{AS} = F_{AS} - (F_A + F_S) + F_{off} \tag{3.3}$$

We can then apply equations 3.2 and 3.3 to the other factors and combinations thereof in order to complete the set of eight equations needed to resolve all the terms with $\hat{F}$.

As a caveat, note that the factor-separated effect $\hat{F}$ represents the separation from the two other tested factors and not from the rest of untested but possible factors hidden in F_{off} (Stein and Alpert, 1993). For our purposes of better understanding the effect of resolution on the precipitation structure in F_{off}, the three factors considered in this chapter suffice.

3.2.3 Description of Experiments

Experiments for factor-separation

To obtain the factor-separated contributions, sensitivity experiments are performed with ECHAM6 using the T63L47 and T255L95 configurations. A summary is given in table

3.1. From the necessary simulations, only F_{AOS}, F_{off}, F_{AS}, F_{AO}, and F_A are performed. The simulations (F_{OS}, F_O, F_S) require a low resolution atmosphere with a high-resolution boundary, which is not possible. This means that we can isolate the effect of orography but including interactions with orography (equation 3.4), and the effect of surface including its interaction with the atmosphere (equation 3.5). We can, however, separate the effect of the atmosphere without the interaction terms by subtracting the control F_{off} from experiment F_A (equation 3.6), where the only difference is the high-resolution atmosphere.

$$F_{AOS} - F_{AS} = \hat{F}_O + \hat{F}_{AO} + \hat{F}_{OS} + \hat{F}_{AOS} \tag{3.4}$$

$$F_{AS} - F_A = \hat{F}_S + \hat{F}_{AS} \tag{3.5}$$

$$F_A - F_{off} = \hat{F}_A \tag{3.6}$$

Adding equations 3.4 to 3.6 simply gives us equation 3.1.

All simulations are run for one year with prescribed 1988 SSTs. The SST data is taken from the PCDMI Atmospheric Intercomparison Project (http://www-pcmdi.llnl.gov/projects/amip/). In the control simulations F_{off} and F_{AOS}, the model is run using the standard T63L47 and T255L95 configurations, respectively. In the sensitivity experiments, the model is run at T255L95 but with lower resolution boundary conditions at T63, similar to the approach by Schiemann et al. (2013). In the experiment F_{AS}, the high-resolution orography factor is turned off by running the model at T255 with T63 orography. The T255 geopotential is truncated to T63 by setting higher wave numbers to zero. Other orographic fields in the surface input file, which are used in the subgrid orography scheme, are obtained from a Gaussian grid corresponding to T63 that is then bilinearly interpolated to a grid corresponding to T255. In the experiment F_{AO}, the high-resolution surface factor is turned off by taking JSBACH land surface parameters from a T63 Gaussian grid and bilinearly interpolating to a T255 Gaussian grid. Among these parameters are land-sea mask, surface albedo and temperature, vegetation ratio, and soil moisture. The F_{AS} and F_{AO} setups are simply combined for the experiment F_A, with both the orography and surface in T63.

Table 3.1: Summary of simulations with the atmosphere(A), orography(O), and land surface(S) in high(255) or low(63) resolution. The last column denotes the operating factors in each simulation following the framework of Stein and Alpert (1993).

Name	**Resolution combination**	**Factors**
F_{AOS}	A_{255}+O_{255}+S_{255}	all factors operate
F_{off}	A_{63}+O_{63}+S_{63}	all factors off
F_{AS}	A_{255}+O_{63}+S_{255}	high-res orography off
F_{AO}	A_{255}+O_{255}+S_{63}	high-res land surface off
F_A	A_{255}+O_{63}+S_{63}	high-res orography and surface off

Additional experiments with orography and convection scheme

Additional sensitivity experiments are performed for Sections 3.4 and 3.5 to expound on the results of the decomposition analysis described above. These experiments are outlined in table 3.2. The $F_{AS[O_{63}^{Afr}]}$ and $F_{AS[O_{63}^{SAm}]}$ experiments are similar to F_{AS}, except that T63 orography is prescribed only over Africa or only over South America. The rest of the orography, as well as the atmosphere and surface, are in T255 such that the difference between F_{AOS} and $F_{AS[O_{63}^{Afr}]}$, and between F_{AOS} and $F_{AS[O_{63}^{SAm}]}$, give us the contribution due to high-resolution orography including its interactions over Africa and over South America, respectively.

The rest of the experiments in table 3.2 involve changes related to the convective parameterization. In F_{off}_Tiedtke, ECHAM is run using the Tiedtke scheme for deep convection instead of the default Nordeng scheme. Note that in the Tiedtke scheme, cloud base mass-flux and organized entrainment are proportional to moisture convergence. Compared to Nordeng, the Tiedtke scheme has a tendency to produce higher cloud tops in drier atmospheres, as discussed in Moebis and Stevens (2012). The F_{off}_NoConv experiment does not employ any deep convection scheme at all and only large-scale precipitation is produced by the model.

Table 3.2: Summary of additional sensitivity tests with orography and convective parameterization.

Name	**Modification**
$F_{AS[O_{63}^{Afr}]}$	F_{AS} w/ high-res African orography off
$F_{AS[O_{63}^{SAm}]}$	F_{AS} w/ high-res South American orography off
F_{off}_Tiedtke	F_{off} w/ Tiedtke convective parameterization
F_{off}_NoConv	F_{off} w/ no parameterized convection

3.3 Relative roles of atmosphere, orography, and surface

Although the models were run for only a year, precipitation biases similar to the climatological biases described in the previous chapter are already apparent. Figure 3.1 shows the 1988 boreal summer precipitation structure in the control runs and in GPCP. The shadings start from 4 mm/day in order to highlight the most intense precipitation values. The simulation F_{off} has excessive precipitation at the West Atlantic, whereas both GPCP and F_{AOS} rain more over the East Atlantic. While F_{AOS} has the maximum at the East Atlantic like GPCP, it still produces precipitation along the west coast whereas GPCP does not. The East Atlantic ITCZ in GPCP is linked with the precipitation over West Africa, which is more intense in GPCP compared to F_{off} and F_{AOS}. Both F_{off} and F_{AOS} actually underestimate precipitation over land, but F_{AOS} rains more than F_{off} over West Africa and South America.

It must be noted that the F_{off} and F_{AOS} control simulations differ not only in horizontal resolution but also in the number of vertical levels. To check whether the difference between figure 3.1a and b is influenced by vertical resolution, we reran F_{off} but with 95 vertical levels. The precipitation structure in F_{off} with 95 vertical levels is found to be similar to that with

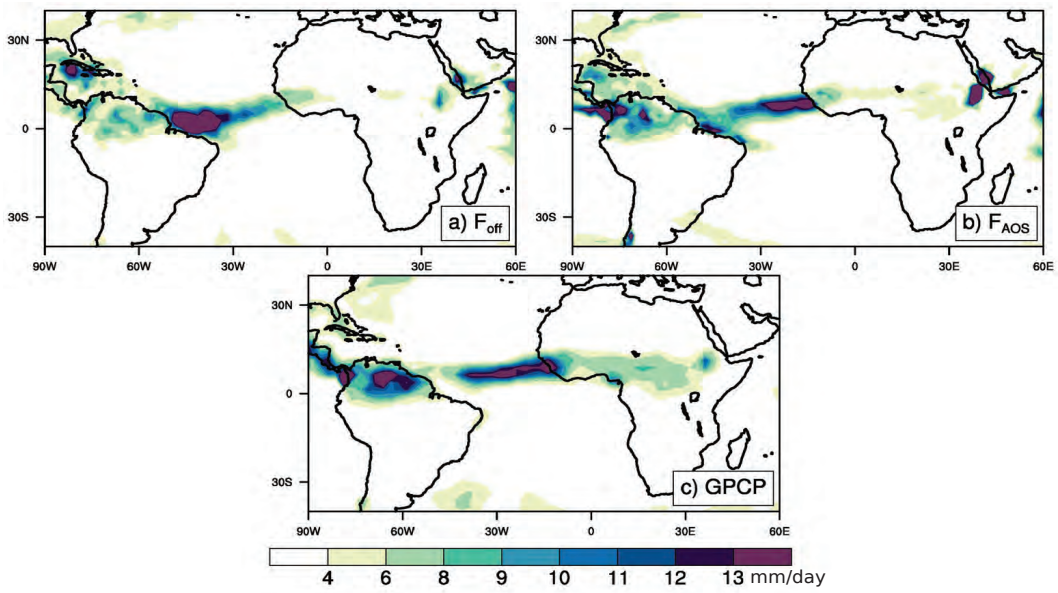

Figure 3.1: Boreal summer precipitation from the control simulations in a) F_{off} and b) F_{AOS} with 1988 prescribed SSTs, compared to observations c) GPCP. Shadings start from 4 mm/day.

47 levels. It is thus the horizontal resolution which has a major effect on the difference between figure 3.1a and b.

To better understand why F_{AOS} rains more over the East Atlantic than F_{off}, we use the factor separation approach outlined in the previous section. The factor-separated contributions of a high-resolution atmosphere, orography, and surface are shown in figure 3.2. With a high-resolution atmosphere, intense convection occurs starting at East Africa and continues downstream of the mean easterly flow up to the West African coast. Further downstream, at the coast of Brazil, there is a substantial decrease in precipitation of more than 5 mm/day at the West Atlantic basin (figure 3.2a). With a high-resolution orography, the precipitation response is dominated by the enhanced convection at the East Atlantic basin. There is also more precipitation over the continents, especially near orographic regions (figure 3.2b). In contrast to the atmospheric and orographic responses, the effect of a high-resolution land surface is minimal. This is probably because the surface over South America and Africa are more homogeneous compared to other areas such as the Maritime Continent. While the resolution of land-sea mask, for instance, is a major factor over the Maritime Continent (Schiemann et al., 2013), its role is not as important over South America or Africa. Lenters and Cook (1995) also find that prescribing simple boundary conditions over South America, such as uniform albedo and surface drag, does not have as much of an effect compared to that of orography or SST. The slight decrease over northern Africa in figure 3.2c is most likely an atmosphere-surface interaction effect.

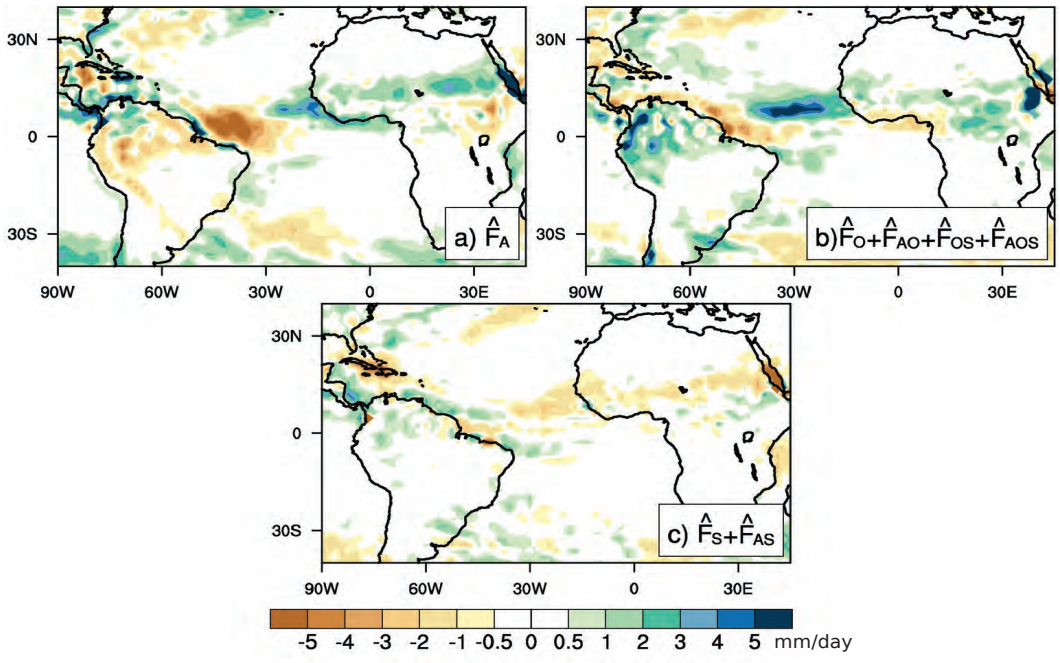

Figure 3.2: Factor-separated boreal summer precipitation contribution from a high-resolution a) atmosphere ($\hat{F}_A$), b) orography ($\hat{F}_O$) + interactions ($\hat{F}_{AO}$+$\hat{F}_{OS}$+$\hat{F}_{AOS}$), and c) surface ($\hat{F}_S$) + interaction with atmosphere ($\hat{F}_{AS}$).

To assess the role of intrinsic variability in the results of figure 3.2, we performed 5 additional F_{off} simulations with 1988 prescribed SSTs but with slightly different initial conditions. The precipitation structures of the ensemble are similar to figure 3.1a, with a standard deviation of around 1.5 mm/day over the West Atlantic. This means that the variability is small compared to the atmospheric and orographic contributions in figure 3.2.

The analysis highlights the fact that over the Atlantic, there are two main contributions to the high-resolution precipitation response: the West Atlantic precipitation decrease as an atmospheric effect, and the East Atlantic precipitation increase as an orographic effect. In the succeeding sections, we will try to understand the mechanisms behind the two precipitation structures.

3.4 The orographic effect on the East Atlantic

Previous studies have investigated the role of orography on the tropical Atlantic climate (Semazzi, 1980a,b; Hagos and Cook, 2005; Richter et al., 2007; Walsh, 1994). In January, heating over the south African orography enhances the South Atlantic high (thermal effect), while a weak low is induced north of the equator due to flow over the north African orography (mechanical effect). The combined orographic effect sets up a meridional pressure gradient, shifting the ITCZ northward (Hagos and Cook, 2005). In boreal summer, such orographically-induced effects hinge on large-scale circulation changes associated with the monsoon. As the northern hemisphere insolation increases, a monsoon circulation over West

Africa is established, reversing the prevailing easterly flow northeast of the equator (see figure 3.3a).

Figure 3.3b shows the effect of a high-resolution orography on the circulation over the Atlantic during the West African monsoon. With better resolved orography everywhere, the monsoon circulation is strengthened. A stronger westerly flow is induced along the equator, straddled by a pair of cyclonic circulations which further strengthen the westerly flow. The circulation response is consistent with increased convection in the eastern Atlantic (figure 3.2b), which might explain its similarity to a Gill model response (Gill, 1980). Apart from the monsoon enhancement, the subtropical highs in figure 3.3b are also intensified. The South Atlantic anticyclone becomes more confined to the ocean, although this does little to improve the too zonal, too westward anticyclone structure that is apparent in figure 3.3a, a problem common to other GCMs (Richter et al., 2007).

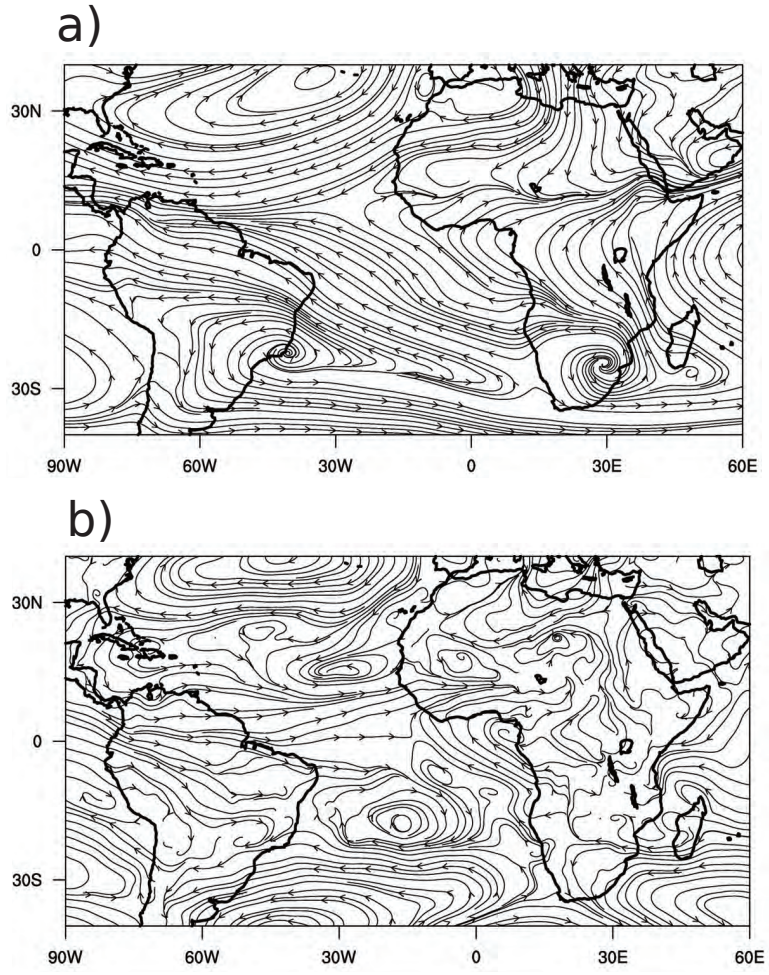

Figure 3.3: Horizontal streamline wind pattern at 850hPa during boreal summer from a) F_{off} and b) the difference of F_{AOS}-F_{AS} (contribution from high-resolution orography).

Although high-resolution orography is imposed everywhere, our hypothesis is that the circulation enhancement in figure 3.3b and the East Atlantic precipitation increase in figure 3.2b are responses to better resolved orography over South America and Africa in particular.

Additional experiments as described in Section 3.2.3, where orography is smoothed only over South America or only over Africa, are used to test this hypothesis.

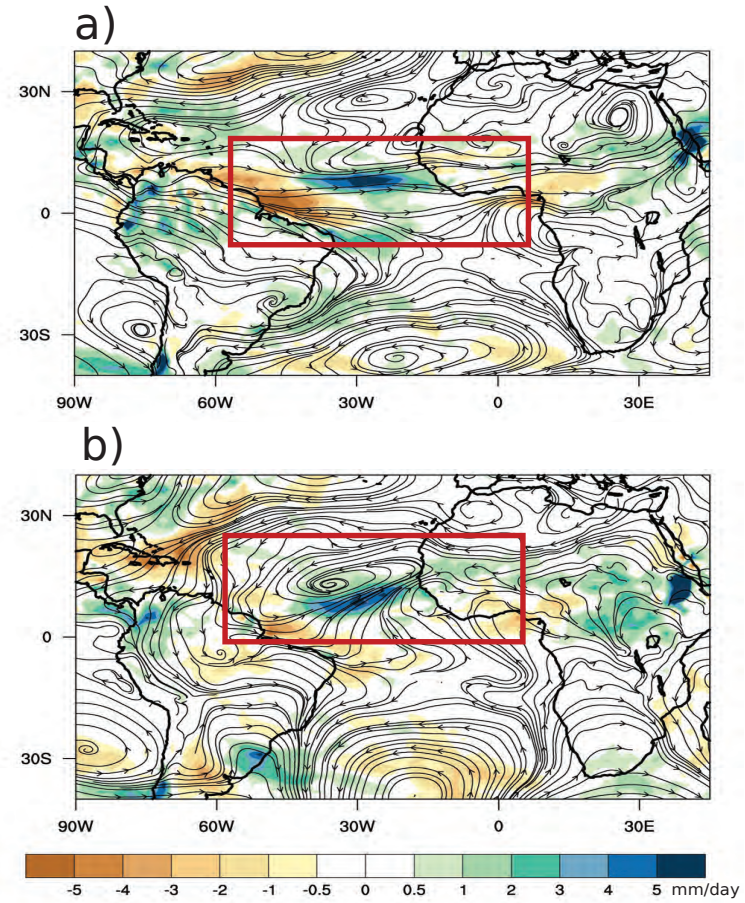

Figure 3.4: Horizontal streamline wind pattern at 850hPa and precipitation difference of a) F_{AOS}-$F_{AS[O_{63}^{SAm}]}$ (contribution from high-resolution orography over South America) and b) F_{AOS}-$F_{AS[O_{63}^{Afr}]}$ (contribution from high-resolution orography over Africa).

The effect of a high-resolution orography over South America during boreal summer is shown in figure 3.4a. Since the Andes are the most prominent orographic feature over South America, we attribute most of the changes in figure 3.4a to the Andes. Much of the literature on the Andes have focused on their local effects during the austral summer season. These studies show that while the Andes seem to have little influence on the large-scale circulation over the Atlantic (Walsh, 1994), they play a major role in the South American climate through their impact on the low-level jet (Virji, 1980; Lenters and Cook, 1995; Insel et al., 2009). However, there are very few studies regarding the effect of the Andes during boreal summer. In this season, and as compared to the large-scale circulation in austral summer, there is an overall northward shift of convergence zones throughout the tropical Atlantic (Hastenrath, 1984). In contrast to austral summer when the Andes affect the southern inland regions, we thus expect that the Andes would have more influence northwards along the equator and over the ocean during boreal summer. Indeed, figure 3.4a shows that with a high-resolution Andes, there is a strong westerly flow along the equator accompanied by a precipitation decrease

in the West Atlantic and an increase in the East Atlantic. The strong westerly flow likely results from the blocking of the mean easterly flow by the better resolved northern Andes. This leads to convergence in the east and divergence in the western basin. Xu et al. (2004) point out that resolution is especially important in the northern portion of the Andes, where the mountains cover only about 200 km and would be hardly resolved by a low resolution model (e.g. T63). They find that a low resolution Andes has less blocking of the easterly flow and advects warm continental air into the Pacific, thus contributing to the anomalous southern Pacific ITCZ. This bias is reduced with a high-resolution Andes as it blocks the easterly flow more effectively. The same mechanism applies in figure 3.4a, except that the blocking effect is on the Atlantic ITCZ. The blocking effect acts to further strengthen the westerly monsoon flow and brings rain into the eastern Atlantic.

The effect of a high-resolution orography over Africa is shown in figure 3.4b. The better resolved orography over Africa results in a cyclonic circulation, accompanied by increased rainfall over the eastern Atlantic. This orographically-induced cyclonic circulation has been investigated by Semazzi and Sun (1997). By comparing simulations with and without African topography, they demonstrate that the Atlas-Ahaggar mountain complex is responsible for setting up a windward high-pressure (anticyclonic) and a leeward low-pressure (cyclonic) distribution in northwest Africa during boreal summer. The dry northeasterly Harmattan flow, intensified by the high-pressure, meets the moist southwesterly monsoon flow, enhanced by the low-pressure and its accompanying cyclonic circulation. The low-level cyclonic circulation interacts with the Saharan heat low and transports moisture from the mid-Atlantic to the Sahel (Sultan and Janicot, 2003). We suggest a similar mechanism for the cyclonic circulation in figure 3.4b. It is likely the result of a stronger leeward mechanical forcing of the better resolved orography over north Africa.

Since the Andes blocking and Atlas-Ahaggar leeward effect are both mechanical effects which impact the circulation, the orographic contribution to the East Atlantic precipitation increase in figure 3.2b likely comes from changes in mean circulation dynamics rather than changes in moisture. To confirm this, we apply the decomposition analysis of Seager et al. (2010). The precipitation change due to changes in moisture (δTH) is calculated as:

$$\delta TH = \int_{P_{bot}}^{P_{top}} \nabla \cdot (u_{F_{AS}}[q_{F_{AOS}} - q_{F_{AS}}])\,\mathrm{d}p \tag{3.7}$$

where u and q denote the horizontal wind and humidity, respectively. Similarly, the precipitation change due to changes in mean circulation dynamics (δMCD) is calculated as:

$$\delta MCD = \int_{P_{bot}}^{P_{top}} \nabla \cdot ([u_{F_{AOS}} - u_{F_{AS}}]q_{F_{AS}})\,\mathrm{d}p. \tag{3.8}$$

The decomposition in figure 3.5 shows that the orographic effect comes mainly from changes in mean circulation dynamics. There is more precipitation over the East Atlantic not because it is moister with a high-resolution orography. Rather, there is more convergence eastwards from the mechanical forcing of orography.

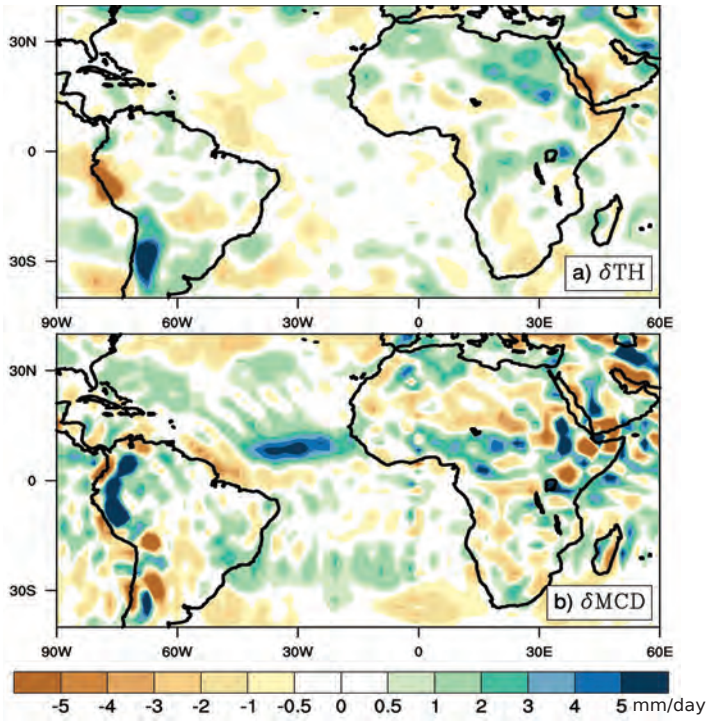

Figure 3.5: Decomposition into a) thermodynamic (TH) and b) mean circulation dynamics (MCD) component of the precipitation change in boreal summer due to the high-resolution orography factor.

In contrast to the orographically-induced meridional shift of the austral summer ITCZ discussed in Hagos and Cook (2005), we find that the combined effect of the Andes and the Atlas-Ahaggar mountains leads to the zonal shift of the boreal summer ITCZ, enhancing the monsoon precipitation in the East Atlantic. However, the full system includes nonlinearities which may amplify, destroy, or distort the individual contributions from South America and Africa discussed above. Nevertheless, comparisons between the full orographic response in figure 3.3b and the individual contributions from South American and African orography in figure 3.4 seem to indicate that the total forcing can be approximated as the sum of the individual responses.

3.5 The atmospheric effect on the West Atlantic

It is not obvious at the outset why an increase in atmospheric resolution would lead to a decreased rainfall over the West Atlantic (figure 3.2a). To get ideas on why the east-west partitioning of precipitation changes with a smaller grid spacing, we look at convection as it occurs in a gridbox and test the influence of the convection scheme. Additional experiments in low resolution with convection scheme off (F_{off}_NoConv) and with the Tiedtke scheme (F_{off}_Tiedtke) are performed, as described in Section 3.2.3. We chose the two set-ups because of their different conditions for convection. In F_{off}_NoConv, it is harder to rain because the lack of parameterization means that the full gridbox must be saturated for rain to occur. In F_{off}_Tiedtke, it is easier to rain because the convective updrafts are less sensitive to free

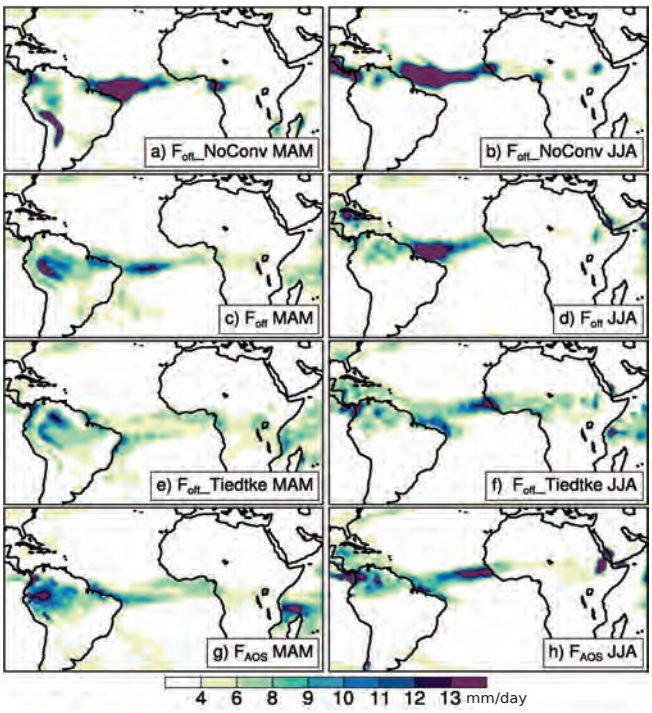

Figure 3.6: Boreal spring (a,c,e) and summer (b,d,f) precipitation in F_{off} without convective parameterization (a,b), with default Nordeng (c,d), with Tiedtke (e,f), and in F_{AOS} with default Nordeng (g,h)

.

tropospheric humidity compared to case in the default Nordeng scheme (Moebis and Stevens, 2012).

Figure 3.6 shows the effect of the convection scheme on the precipitation distribution in boreal spring (MAM) and summer (JJA). When the convection scheme is turned off and precipitation is produced only through grid-scale saturation, there is excessive precipitation over the West Atlantic in both seasons (figures 3.6a,b). With the default Nordeng scheme, the precipitation maximum is located over the south coast of Brazil in spring and over the western Atlantic basin in summer (figures 3.6c,d), characteristic of West Atlantic model biases described in the previous chapter. When we switch to the Tiedtke scheme, the westward bias is reversed: there is more precipitation on the eastern basin in both spring and summer (figures 3.6e,f). Recall that the precipitation maximum over the Gulf of Guinea in spring and over the eastern Atlantic basin in summer are characteristic behaviors of high-resolution models in the East Atlantic class. We see then that precipitation structures typical of high-resolution models can also emerge in low-resolution depending on the convection scheme. More importantly, we see that by making it harder to convect (Tiedtke $\rightarrow$ Nordeng $\rightarrow$ NoConv), we get a more and more pronounced West Atlantic bias.

If it is easier to rain, and if the flow is easterly, it will first rain east rather than west. A similar argument may explain the atmospheric contribution. Because it is easier to trigger convection within a smaller gridbox such as in T255, there is more rain east and less rain west (figures 3.6g,h). The ease by which convection occurs, set by the convection scheme or

by its response to increased resolution, together with the background easterly flow, determine the east-west partitioning of the atmospheric contribution on precipitation.

Because the atmospheric contribution in figure 3.2a depends on the interaction of convection with the background flow, its precipitation response mostly comes from changes in mean circulation dynamics (δMCD), instead of changes in moisture (δTH) (see figure 3.7). There is less precipitation over the West Atlantic not because it is drier westwards. Rather, since there is more convergence of winds over the east and less over the western basin, it rains more east and less west. The rainfall response induces further convergence east and divergence west, leading to a positive feedback between convection and circulation over the Atlantic. The convection scheme exerts a strong influence on this feedback mechanism by controlling the tendency to rain east, hence determining whether the circulation diverges downstream at the west coast.

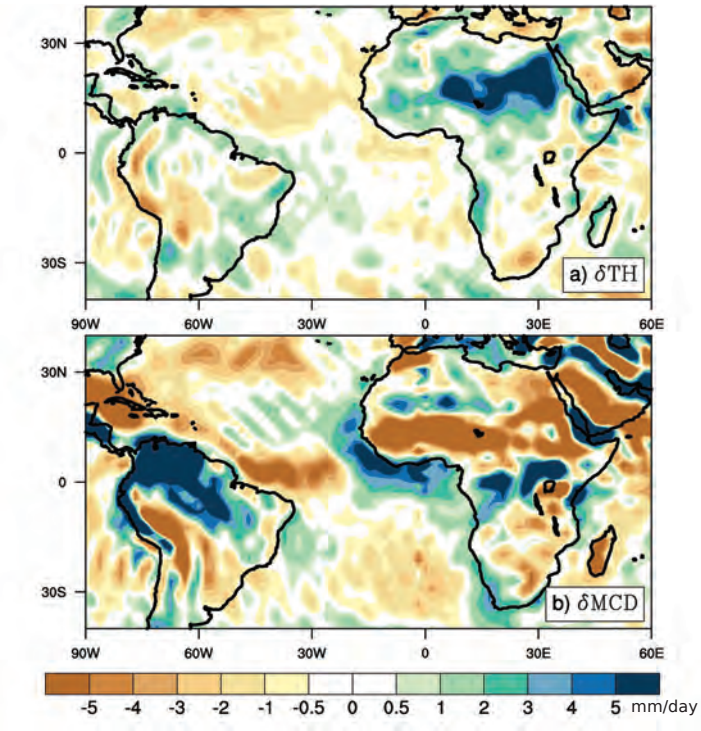

Figure 3.7: Decomposition into a) thermodynamic (TH) and b) mean circulation dynamics (MCD) component of the precipitation change in boreal summer due to the high-resolution atmosphere factor.

The atmospheric effect of suppressing convection over the West Atlantic and the orographic effect of enhancing convection over the East Atlantic both lead to a stronger westerly flow, but at different latitudes, as shown in figure 3.8. Because the orography directly impacts the monsoon, its westerly effect is northwards, near West Africa. In contrast, the atmosphere follows the background flow and convection is suppressed near Brazil, more southwards than the monsoon area.

The atmospheric effect is active both in spring and summer. In contrast, the orographic effect on the East Atlantic precipitation (Section 3.4) dominates only in the summer season, when orography-monsoon interactions are strongest. Applying the factor separation on bo-

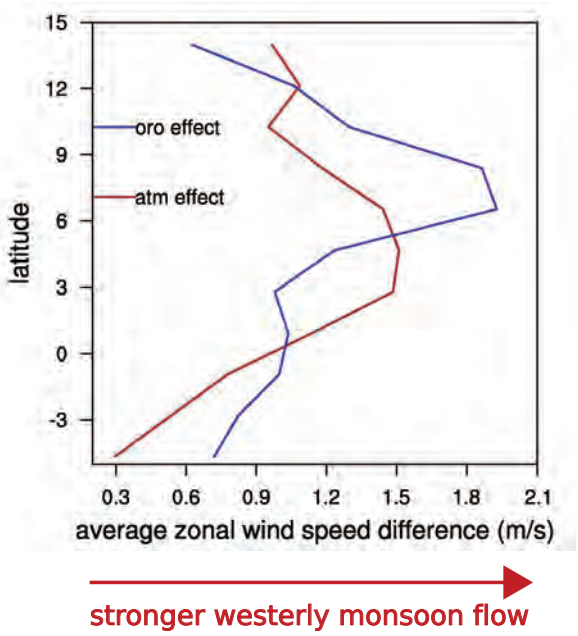

Figure 3.8: Boreal summer zonal wind speed difference of F_{AOS}-F_{AS} (orographic effect, blue) and F_A-F_{off} (atmospheric effect, brown), averaged over 20-40°W and plotted against latitude.

real spring precipitation confirms that the dominant contribution is the atmospheric effect, whereas the orographic effect is weaker and more southwards compared to its contribution during summer (see figure 3.9).

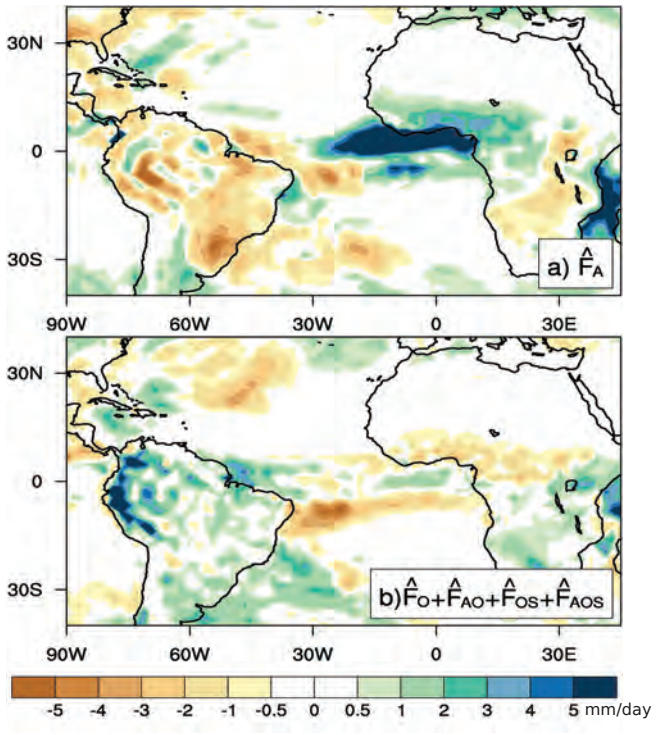

Figure 3.9: Factor-separated boreal spring precipitation contribution from a high-resolution a) atmosphere ($\hat{F}_A$) and b) orography ($\hat{F}_O$) + interactions ($\hat{F}_{AO}$+$\hat{F}_{OS}$+$\hat{F}_{AOS}$).

The combined effect of a convection scheme where deep convection can occur more easily and of a large-scale circulation with a mean easterly flow is to increase the tendency to rain east. The circulation responds and the resulting convergence further increases rain east and decreases rain west. In boreal spring, increased tendency to rain east results in excessive precipitation over the coast of Guinea, whereas a reduced tendency will overestimate rain on the opposite coast. In boreal summer, when the West African monsoon sets in, increased tendency to rain east results in a better precipitation distribution. Otherwise, the model would have deficient precipitation in the monsoon area and would instead rain excessively near Brazil, where observations show little precipitation.

3.6 Summary

Models fail to capture the east-west partitioning of precipitation over the Atlantic in the mean state. Biases emerge in boreal spring and continue during summer, when monsoon heating over West Africa is at its peak. A model with a higher horizontal resolution has more tendency to rain east. In this chapter, we investigated how horizontal resolution influences the east-west structure of the Atlantic ITCZ, with a focus on the boreal summer season. Our aim was to better understand the mechanisms behind the precipitation distribution.

Using ECHAM6, we performed three sensitivity experiments to infer the relative contributions from a high-resolution atmosphere, orography, and surface. These experiments were analyzed using the factor separation approach of Stein and Alpert (1993). Results showed two major contributions: a high-resolution atmosphere decreases rain on the West Atlantic, whereas a high-resolution orography increases rain on the East Atlantic. A high-resolution surface plays a minimal role.

The increase in precipitation over the East Atlantic was found to be a response to the stronger monsoon flow induced by better resolved orography. It is the better resolved orography over two continents, South America and Africa, which increases precipitation over the East Atlantic during the summer season. We suggested the following mechanisms: a) a better resolved Andes blocks the mean easterly flow from the Atlantic and induces convergence in the eastern basin, and b) a better resolved Atlas-Ahaggar complex intensifies the orographic effect and increases precipitation in the eastern basin. The combined effect leads to a stronger monsoon circulation and a wetter East Atlantic.

The decrease in precipitation over the West Atlantic was found to result from the easier occurrence of convection with a smaller grid spacing. With the background easterly flow, this results in more rain starting in East Africa, ending with less rain downstream over the West Atlantic coast. A similar response can also be obtained with a coarser grid spacing in T63 by making it easier to rain through changes in the convection scheme.

We can think of the problem as: given two asymmetrically distributed landmasses, such that in the eastern side there is more landmass north of the equator, and in the western side there is more landmass south of the equator, what happens to the precipitation distribution

when there is more heating northwards? The answer is that first, the monsoon develops over the greater landmass area east and north. This interacts with northern orography and brings rain into the East Atlantic coast. Second, following the background flow, more precipitation starting at the landmass east and north translates to less precipitation near the landmass west and south (see sketch in figure 3.10). The rainfall response in the east further enhances convergence eastward, whereas westward, the easterly flow decelerates and enhances divergence (Cook et al., 2004). From a modelling perspective, the spatial resolution contributes to the improvement of circulation dynamics related to the first aspect (orographic effect). For the second aspect, it is the convective parameterization which mostly influences the interaction between convection and the circulation (atmospheric effect).

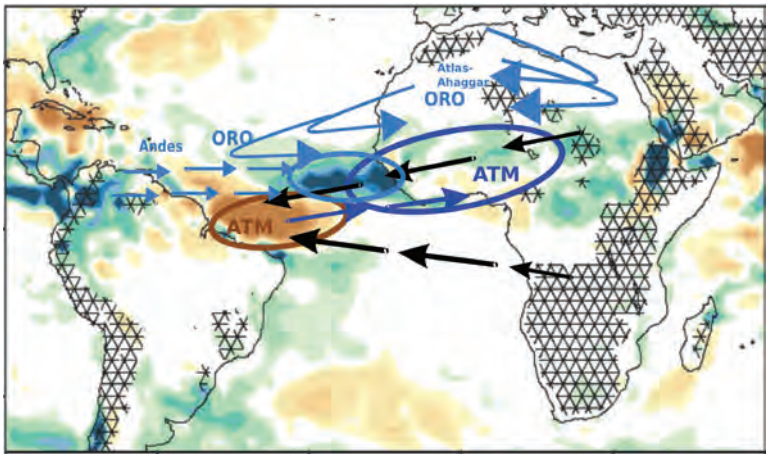

Figure 3.10: Sketch of the low-level wind and centers of convergence (blue) and divergence (brown) superimposed on the precipitation difference between F_{AOS} and F_{off} (i.e. sum of figure 3.2a-c). Hatched areas mark the location of orographic features higher than 800m.

With a different heating distribution, interactions involving convection, dynamics, and the large-scale flow would also change and some aspects of the circulation may be more important in one season than the other. For instance, we showed that in boreal spring, orography in the model does not have as much importance as the convection scheme. In this season, precipitation over the continents goes into a transition period, with the weakening of South American precipitation and the onset of West African precipitation. Over the ocean, the Atlantic ITCZ forms as a band extending across the equator, a feature which models fail to capture as they rain excessively over the coasts. The convection scheme may be key to understanding some of the persistent model biases in boreal spring. In other seasons such as austral summer, continental heating is concentrated through much of South America and parts of South Africa. Other circulation features, such as the South Atlantic High and its interaction with the Andes, become more prominent (Lenters and Cook, 1995; Rodwell and Hoskins, 2001). How well our models represent the precipitation distribution, in different seasons and over a particular area such as the Atlantic, ultimately rests on our basic understanding of how convection couples with the large-scale circulation and of how this coupling adapts to different heating distributions and continental geometries.

Chapter 4

Role of convection scheme on the simulated tropical Atlantic precipitation distribution: case of boreal summer

4.1 Introduction

The set of criteria in a given convection scheme which determines if and how convection occurs has a major influence on the resulting precipitation distribution. There are three main components of a convection scheme: 1) the trigger, which decides whether convection is possible, 2) the cloud model, which controls how the convective updraft mixes with the environment, and 3) the closure, which sets the strength of convection. Different parts of the convection scheme can impact different aspects of the simulated precipitation distribution. The trigger, for instance, is known to influence the phase speed of convectively coupled equatorial waves (CCEWs) and the strength of the Madden-Julian oscillation (MJO) (Lin et al., 2008; Frierson et al., 2010). Entrainment rates, when underestimated, decrease the sensitivity of the updraft to free tropospheric humidity and lead to a double ITCZ bias over the tropical Pacific (Moebis and Stevens, 2012; Oueslati and Bellon, 2013). As for the closure, there is no consensus as to which of the commonly used assumptions- quasi-equilibrium based on CAPE (Arakawa and Schubert, 1974; Zhang and Mu, 2005; Nordeng, 1994) or moisture convergence (Tiedtke, 1989), can best capture the mean climate and variability of the tropics (Slingo, 1996; Lin et al., 2008; Song and Zhang, 2009).

In the previous chapter, we have found that the east-west structure of the Atlantic ITCZ is influenced, in part, by how easy convection occurs in the model. The two convection schemes in ECHAM, Tiedtke and Nordeng, produce different Atlantic ITCZ structures during boreal summer. The easier occurrence of deep convection in the Tiedtke scheme compared to the Nordeng scheme results in an eastward shift of the Atlantic ITCZ. The eastward precipitation

maximum in Tiedtke is accompanied by decreased rainfall over the west Atlantic and a more northward ITCZ compared to Nordeng, as shown in figure 4.1. Tiedtke also rains more over land, both over West Africa and South America.

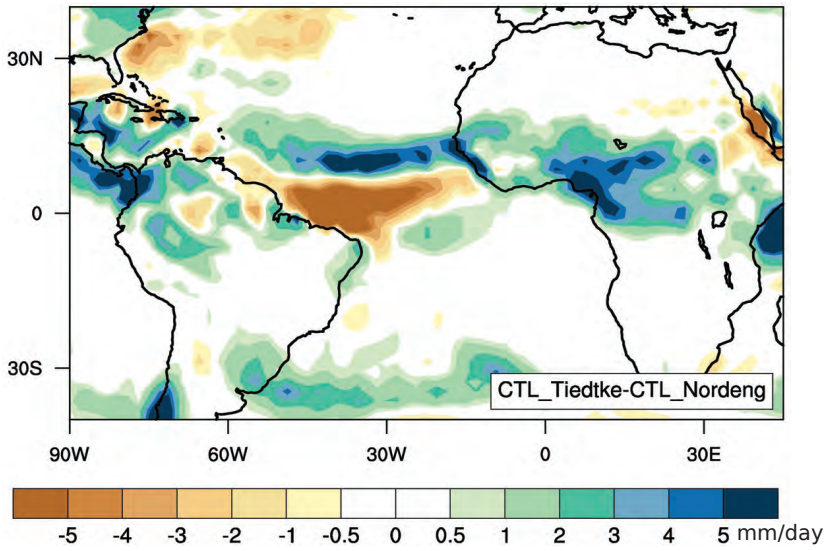

Figure 4.1: CTL_Tiedtke minus CTL_Nordeng boreal summer precipitation.

In this chapter, we investigate how different parts of the convection scheme determine the occurrence of deep convection and the resulting precipitation distribution during boreal summer. We perform a suite of experiments where different parts of the Nordeng scheme are modified during summer to make it easier to rain. The aim is to decompose the better boreal summer precipitation in Tiedtke (figure 4.1) in terms of differences in the trigger, entrainment, and closure parameters. Moreover, the Nordeng scheme is modified separately over land and over ocean in order to study the relative importance of, and interaction between, continental and oceanic convection. Finally, the modified Nordeng approach also allows us to test the spring-summer relationship as proposed in Chapter 2. To verify whether spring impacts the summer precipitation, we perform an additional experiment with the Nordeng scheme modified only in boreal spring.

The outline of the chapter is as follows: Section 4.2 provides a brief review of the Tiedtke and Nordeng convection schemes and describes the sensitivity experiments involving modifications to the Nordeng scheme. Results are presented in Section 4.3. This section is divided into three parts discussing the roles of trigger, entrainment, and closure (Section 4.3.1), the interaction between land and ocean (Section 4.3.2), and the effect of boreal spring on the summer precipitation (Section 4.3.3). A summary is given in Section 4.4.

Table 4.1: A comparison of the trigger, organized entrainment, turbulent entrainment, and closure formulations in the Nordeng and Tiedtke schemes.

	Trigger	Entrainment$_{org}$	Entrainment$_{trb}$	Closure
Nordeng	buoyancy$_{LCL}$+zlift	buoyancy	strong	CAPE
Tiedtke	buoyancy$_{LCL}$+zlift	qconv	weak	qconv

4.2 Methods

4.2.1 Convective parameterization in ECHAM

As described in Chapter 3, ECHAM6 employs two deep convection schemes: the Nordeng scheme, which is used by default, and the alternative Tiedtke scheme. Table 4.1 summarizes the trigger, entrainment, and closure formulations in the two schemes. The trigger is computed based on the buoyancy of the updraft at the lifting condensation level. In both schemes, an additional buoyancy (zlift) is added based on the variance of potential temperature in the boundary layer to account for subgrid variability. The organized entrainment in Nordeng is based on updraft buoyancy, whereas it is computed based on moisture convergence (qconv) in Tiedtke. The turbulent entrainment parameter is the same for both schemes, but a mistake in the implementation in Tiedtke results in a weakened entrainment effect compared to Nordeng (see Moebis and Stevens (2012)). The closure in Nordeng is based on a quasi-equilibrium assumption such that it removes CAPE over a prescribed relaxation time. In Tiedtke, the closure is based on the amount of moisture convergence in the boundary layer.

4.2.2 Description of Experiments

Simulations are performed using the model ECHAM6 as described in Chapter 3. We use the standard configuration in T63 with 47 levels in the vertical. Table 4.2 lists the sensitivity experiments performed over land and over ocean for the case of boreal summer. All experiments are run for one year using prescribed 1988 SSTs, as in the simulations of the previous chapter. To make it easier to rain, the criteria for deep convection in the Nordeng scheme is relaxed by modifying the trigger, closure, and entrainment parameters. The modifications are applied only during the months June-July-August (JJA) and the Nordeng scheme remains unchanged for the other months. In EXP_2xzlift, the added buoyancy to the test parcel "zlift" is doubled so that convection can be triggered more easily. In EXP_2xCAPE, the cloud base mass flux is set to twice its value to enhance the strength of convection. In EXP_noEntr, the turbulent entrainment is set to zero to decrease the mixing with the environment. This results in less diluted updrafts in theory, which means an easier production of deep convection. Because Tiedtke and Nordeng also differ in their closure, we perform EXP_qconv, where the default CAPE closure in Nordeng is replaced by the moisture convergence closure used in Tiedtke. The letters L and O denote whether the convection scheme is modified only over land or over ocean, respectively.

To test specific results, we perform additional experiments. The EXP_noEntr_O and EXP_qconv_O set-ups are combined in EXP_noEntr_O_qconv_O. In EXP_noEntr, turbulent entrainment is set to zero globally. This is combined with a moisture convergence closure over ocean in EXP_noEntr_qconv_O. To test whether spring has an impact on summer, we follow the set-up of EXP_noEntr_qconv_O, but apply the changes only during the months March-April-May (EXP_noEntr_qconv_O$_{MAM}$). In EXP_noEntr_SAM+AFR, entrainment is turned off only over South America and Africa.

As reference, we use the control simulations from the previous chapter and rename F$_{off}$ as CTL_Nordeng and F$_{off}$_Tiedtke as CTL_Tiedtke. To account for intrinsic variability, we compare the results to the standard deviation of the ensemble of five CTL_Nordeng simulations from the previous chapter.

Table 4.2: Summary of boreal summer simulations.

Name	**Convection scheme**	**Description**
CTL_Nordeng	Nordeng	control simulation with 1988 SSTs
CTL_Tiedtke	Tiedtke	control simulation with 1988 SSTs
EXP_2xzlift_L	Nordeng	doubled buoyancy perturbation (zlift) in convective trigger over land
EXP_2xCAPE_L	Nordeng	doubled CAPE closure over land
EXP_qconv_L	Nordeng	moisture convergence closure over land
EXP_noEntr_L	Nordeng	no turbulent entrainment over land
EXP_noEntr_SAM+AFR	Nordeng	no turbulent entrainment over South America and Africa
EXP_2xzlift_O	Nordeng	doubled buoyancy perturbation (zlift) in convective trigger over ocean
EXP_2xCAPE_O	Nordeng	doubled CAPE closure over ocean
EXP_qconv_O	Nordeng	moisture convergence closure over ocean
EXP_noEntr_O	Nordeng	no turbulent entrainment over ocean
EXP_noEntr_O_qconv_O	Nordeng	no turbulent entrainment over ocean moisture convergence closure over ocean
EXP_noEntr	Nordeng	no turbulent entrainment globally
EXP_noEntr_qconv_O	Nordeng	no turbulent entrainment globally moisture convergence closure over ocean
EXP_noEntr_qconv_O$_{MAM}$	Nordeng	no turbulent entrainment globally moisture convergence closure over ocean during MAM

4.3 Results

4.3.1 Sensitivity to trigger, entrainment, and closure

In the previous chapter, we found that if deep convection can occur more easily in ECHAM, either by having a smaller grid spacing or by switching to the Tiedtke scheme, the precipitation distribution during boreal summer improves. How different parts of the convection

scheme contribute to the improved summer precipitation remains unclear. We explore this idea in this section by using the modified version of Nordeng (see Section 4.2). We evaluate the impact of modifications to the convection scheme over land on the amount of rainfall over land. Similarly, we look at how changes to the convection scheme applied over ocean impact the amount of rainfall over ocean, as well as the longitudinal and latitudinal position of the Atlantic ITCZ.

Over land, the area averaged precipitation over South America and Africa is underestimated in CTL_Nordeng, whereas CTL_Tiedtke shows rainfall values much closer to GPCP observations (figure 4.2). The vertical gray bar indicates the standard deviation of an ensemble of CTL_Nordeng simulations, as a measure of intrinsic variability. Modifications in the trigger (EXP_2xzlift_L) and closure (EXP_2xCAPE_L, EXP_qconv_L) of the Nordeng scheme have minimal impact on the rainfall amount. This means that the low value of precipitation in CTL_Nordeng is neither a consequence of the inability to trigger convection nor of insufficient cloud base mass flux. When turbulent entrainment is turned off (EXP_noEntr_L), the average precipitation over land increases by about 1.5 mm/day, and ends up producing more rain than GPCP. Only through entrainment can Nordeng significantly increase the precipitation over land. This shows that deep convection over land in ECHAM is mostly controlled by the updraft's sensitivity to free tropospheric humidity, set by the entrainment parameter. In Tiedtke, entrainment is weakened due to mistake in the computation of the entrainment value (Moebis and Stevens, 2012). Removing turbulent entrainment as in EXP_noEntr_L, although unphysical, has the expected effect of increasing the fraction of triggered convective events over land which reach high ($\leq$ 250hPa) cloud tops (figure 4.3). We choose 250hPa as a measure for deep convection as it is found to adequately represent the spatial distribution of precipitation events $>$ 4 mm/day. Setting the turbulent entrainment to zero effectively raises the depth of convection and as a consequence, increases the rainfall amount and net convective heating over land. Conversely, having a strong entrainment caps the convection to lower heights and leads to reduced rainfall over land. The different behavior of CTL_Tiedtke and CTL_Nordeng over land in figure 4.2 can thus be interpreted as a result of their different entrainment formulations.

Over ocean, precipitation over the western Atlantic is overestimated in CTL_Nordeng, whereas both CTL_Tiedtke and especially GPCP show lower values (figure 4.4). The west Atlantic bias is indicative of oversensitivity to SST, which are warmest over the west Atlantic during boreal summer (see figure 2.10). This bias persists in the simulations where the trigger (EXP_2xzlift_O) and CAPE closure (EXP_2xCAPE_O) are modified. By setting the turbulent entrainment to zero (EXP_noEntr_O), or by switching to a moisture convergence closure (EXP_qconv_O), or through the combination of both (EXP_noEntr_O_qconv_O), the bias with respect to GPCP is halved and values close to CTL_Tiedtke are obtained. A lower west Atlantic rainfall is a consequence of an improved Atlantic ITCZ structure, as shown in figure 4.5. In the latter, the Atlantic ITCZ is evaluated in terms of its northernmost latitude and the longitude of its main ocean object. Recall from Chapter 2 that the main ocean object is defined as the largest rainy cluster. CTL_Tiedtke and GPCP both have a northwards ITCZ

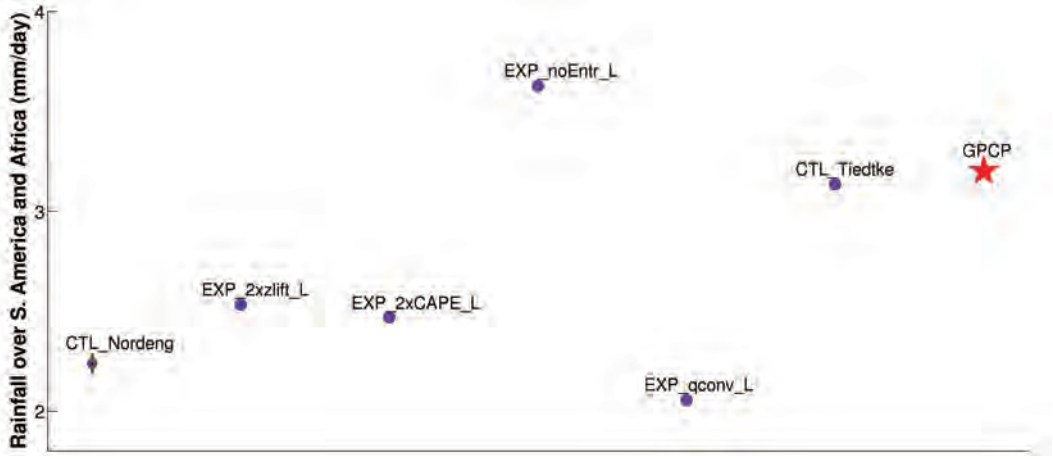

Figure 4.2: Area-averaged rainfall over Atlantic land areas, South America and Africa (Lon -90°:60°, Lat -30°:30°) in boreal summer experiments over land. The vertical gray bar shows the standard deviation of the ensemble mean of CTL_Nordeng.

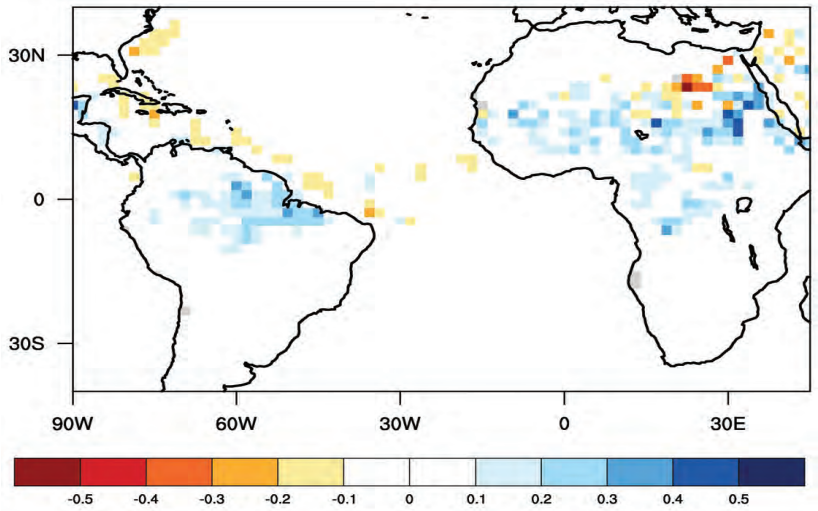

Figure 4.3: EXP_noEntr_L minus CTL_Nordeng fraction of triggered convective events which reach cloud tops $\leq$ 250hPa during boreal summer.

and an eastward ocean object. CTL_Nordeng fails to capture both characteristics and instead rains more southward and westward. EXP_noEntr_O and EXP_qconv_O both shift the ITCZ northwards and eastwards, well beyond the intrinsic variability of the ITCZ in CTL_Nordeng. A similar response is obtained from the combination of the two in EXP_noEntr_O_qconv_O. But the best result is achieved when entrainment is turned off globally, combined with a moisture convergence closure over ocean in EXP_noEntr_qconv_O.

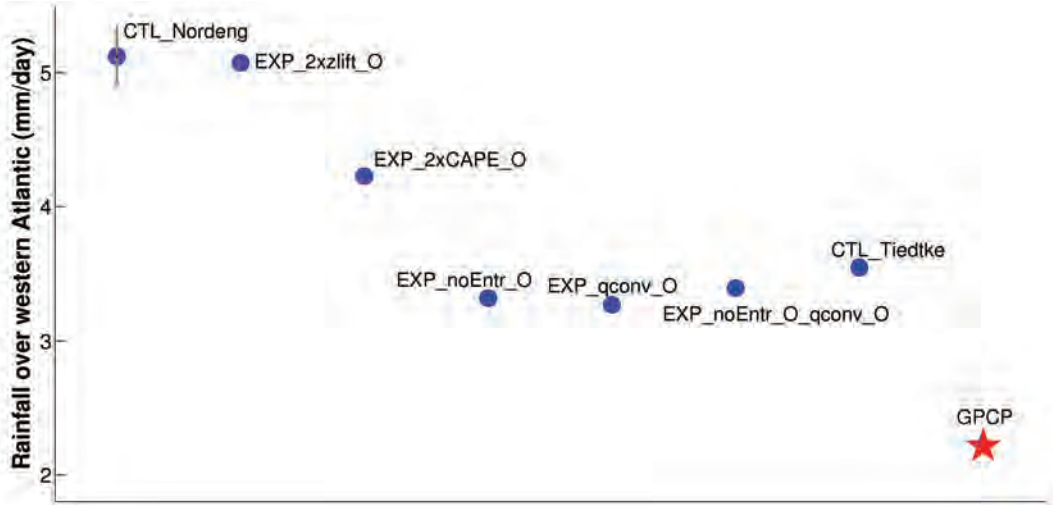

Figure 4.4: Area-averaged rainfall over west Atlantic ocean (Lon -50°:20°, Lat -15°:5°) in boreal summer experiments over ocean. The vertical gray bar shows the standard deviation of the ensemble mean of CTL_Nordeng.

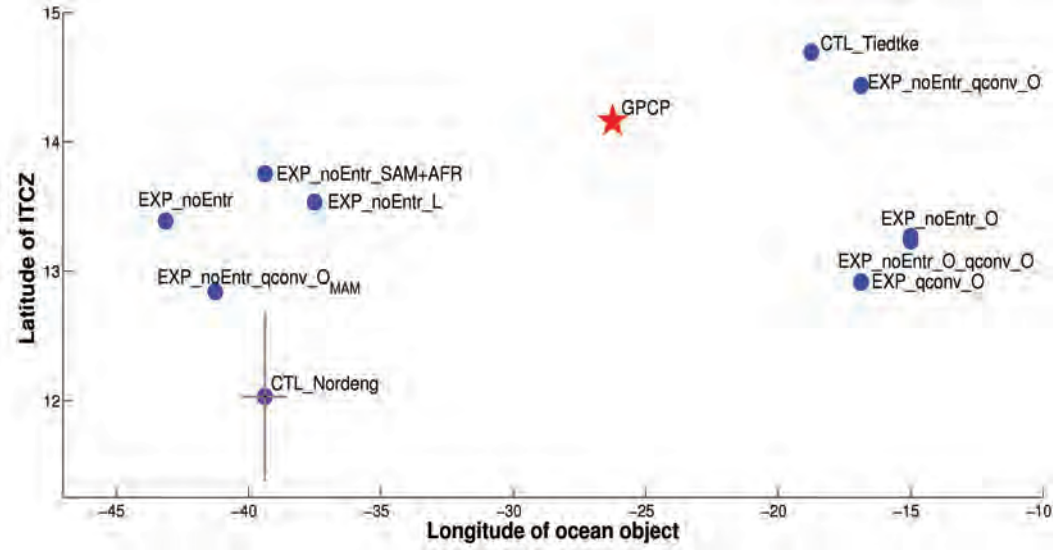

Figure 4.5: Longitude of Atlantic main ocean object plotted against the northernmost latitude of the Atlantic ITCZ (marked by the 2mm/day contour at 25°W). The red star marks the Atlantic ITCZ in GPCP observations. The gray bars show the standard deviation of the ensemble mean of CTL_Nordeng.

Although turning off entrainment or changing the closure have similar effects on the oceanic precipitation, the underlying mechanisms differ. By turning off turbulent entrainment, in

theory we make it easier to rain everywhere over the tropical Atlantic ocean. However, as figure 4.6 shows, the fraction of deep convective events with high cloud tops ($\leq$ 250hPa) actually decreases when there is no turbulent entrainment. How is this possible? As it is easier to rain everywhere, EXP_noEntr_O can start raining over the East Atlantic. As suggested in Chapter 3, raining east steals moisture that would have otherwise been available to the West Atlantic, leading to less rain downstream. If updrafts are fed with less moisture, they would tend to be less buoyant and would not penetrate as deep in the atmosphere. This is consistent with figure 4.6 and with the decreased rain over the West Atlantic.

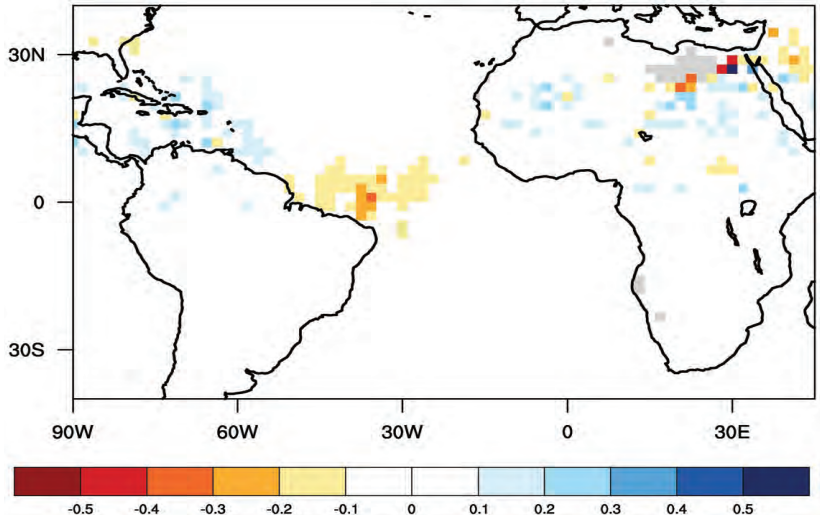

Figure 4.6: EXP_noEntr_O minus CTL_Nordeng fraction of triggered convective events which reach cloud tops $\leq$ 250hPa during boreal summer.

Concerning the effect of closure, figure 4.7 indicates that EXP_qconv_O has a strong westerly flow in the inner tropics, peaking at 8°N, indicating a potential positive feedback with the West African monsoon. With a closure based on moisture convergence, EXP_qconv_O can explicitly detect the convergence associated with the monsoon, and starts raining at the east coast. The rain on the east coast increases convergence, which enhances the monsoonal flow. This results in increased moisture convergence, sustaining a positive feedback and decisively shifts the precipitation maximum towards the east coast. Although the main ocean object shifts eastward in EXP_noEntr_O, this is not related to a strengthening of and feedback with the monsoonal flow, as can be seen in figure 4.7. The background flow is only slightly enhanced at latitudes above 8°N and remains overall much weaker than EXP_qconv_O. Moreover, EXP_noEntr_O exhibits a secondary maximum over the west Atlantic, unlike the case for EXP_qconv_O (figure 4.8). That a CAPE closure translates to a decreased sensitivity to the large-scale circulation has been demonstrated by Song and Zhang (2009) for the case of the double ITCZ bias in the Pacific. In their study, a convection scheme with a CAPE closure collocated precipitation and SST too strongly, whereas one with a closure based on large-scale free tropospheric processes was less sensitive to SST and had a reduced southward ITCZ bias.

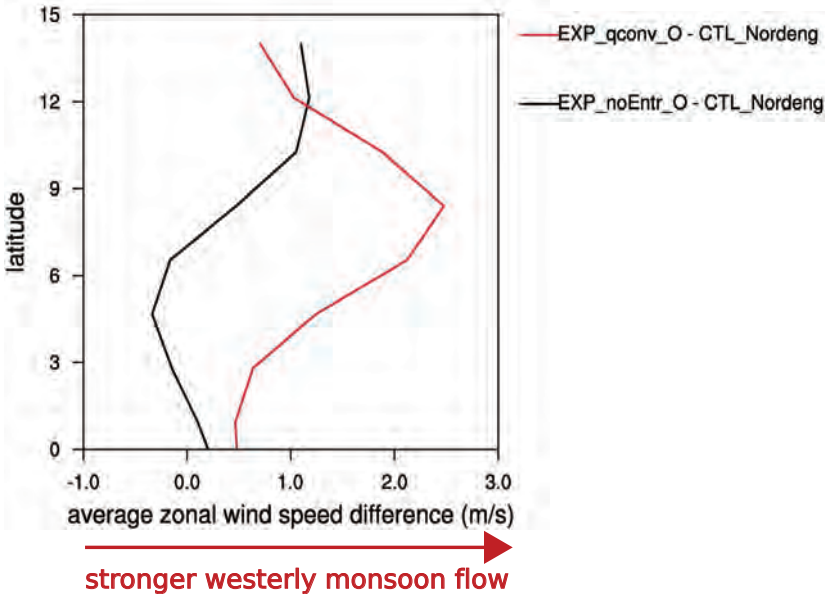

Figure 4.7: Zonal wind difference averaged over 20°-40°W plotted against latitude. The red line shows the difference between EXP_qconv_O and CTL_Nordeng and the black line shows the difference between EXP_noEntr_O and CTL_Nordeng during boreal summer.

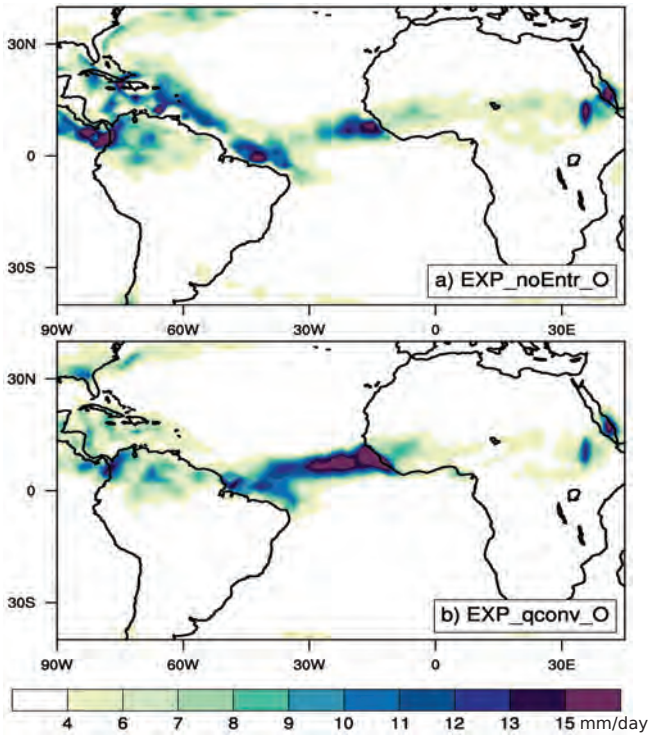

Figure 4.8: Boreal summer precipitation in a) EXP_noEntr_O and b) EXP_qconv_O.

4.3.2 Interaction of continental and oceanic precipitation

Changes to the convection scheme applied separately for land and ocean also give us an opportunity to understand how land affects the Atlantic ITCZ and vice versa. Figure 4.5 shows that increased rainfall over land through entrainment shifts the ITCZ northwards. A similar northward shift can be reproduced when turbulent entrainment is turned off only over South America and Africa. Both continents are nevertheless crucial for such a response, as setting the turbulent entrainment to zero separately over South America and over West Africa only results in a minimal northward and eastward shift, respectively (not shown). Increased rainfall over both continents decreases rainfall over ocean, especially over the west Atlantic, as the total amount of rain falling on the Atlantic sector tends to remain conserved. Finally, while rain over land can affect the latitude of Atlantic ITCZ, it cannot significantly shift the longitudinal position eastwards (figure 4.5).

Improvements in the Atlantic ITCZ structure in EXP_qconv_O and EXP_noEntr_O have minimal impact on rainfall over land. Rainfall over South America and Africa is around 2.5 mm/day in EXP_qconv_O and around 2.3 mm/day in EXP_noEntr_O, having the same dry bias over land as CTL_Nordeng (figure 4.2).

Although their experimental framework is different, Biasutti et al. (2004) arrive at similar conclusions regarding changes in precipitation amount between land and ocean over the tropical Atlantic. Using the CCM3 model, they first show that continental precipitation is controlled mainly by insolation, whereas oceanic precipitation strongly follows SST. By varying insolation and fixing SST, they find that as continental precipitation decreases, so does the atmospheric stability over ocean, leading to an increase in oceanic precipitation. Correspondingly, increasing continental precipitation would decrease oceanic precipitation. In another experiment, with varying SSTs but fixed insolation, their results show that oceanic convection does not have a strong impact on continental precipitation, except in coastal regions.

Setting the turbulent entrainment to zero globally (EXP_noEntr) results in a northward but westward Atlantic ITCZ. But when combined with a moisture convergence closure over ocean that shifts the ITCZ eastward, EXP_noEntr_qconv_O successfully reproduces the Atlantic ITCZ in CTL_Tiedtke (figure 4.5). The contribution from entrainment over land is important in such a response, since when entrainment is only turned off only over ocean as in EXP_noEntr_O_qconv_O, the ITCZ does not shift as far north.

4.3.3 Effect of spring on summer

In Chapter 2, we found that models tend to lock their precipitation maximum eastwards or westwards during boreal spring and summer. For instance, ECHAM with the default Nordeng scheme rains more over the coast of Brazil during spring, and continues to rain west in the next season. Similarly, the eastward maximum in Tiedtke during spring is carried over to the summer. How does the precipitation distribution in spring impact the summer season?

To answer this question, we modify the Nordeng scheme during boreal spring and look at its effect on the precipitation during summer. We use Nordeng with a moisture convergence closure over ocean and zero turbulent entrainment globally (EXP_noEntr_qconv_O_{MAM}), as we have previously demonstrated that this combination can best reproduce a Tiedtke-like behavior during summer. The resulting precipitation distribution in spring shows a Tiedtke-like behavior, with rainfall concentrated on the Gulf of Guinea, reminiscent of East Atlantic models (Chapter 2). The spring eastward maximum in EXP_noEntr_qconv_O_{MAM} leads to some improvements on the precipitation distribution in summer. Rainfall over the west Atlantic is reduced and there is more rain northwards compared to CTL_Nordeng (figure 4.9), in agreement with different behavior of CTL_Nordeng and CTL_Tiedtke. However, the Atlantic ITCZ in EXP_noEntr_qconv_O_{MAM} fails to shift eastward (figure 4.5). Hence, while spring does have an impact on the latitude of the ITCZ in summer, it plays a minimal role on the longitudinal position. This means that the apparent locking of the east/west precipitation maximum in CTL_Tiedtke and CTL_Nordeng happens simply because both spring and summer seasons are guided by the same convection scheme. If we would use the Tiedtke scheme in spring and the Nordeng scheme in summer, the longitude of the Atlantic ITCZ would be eastwards in spring and westwards in summer.

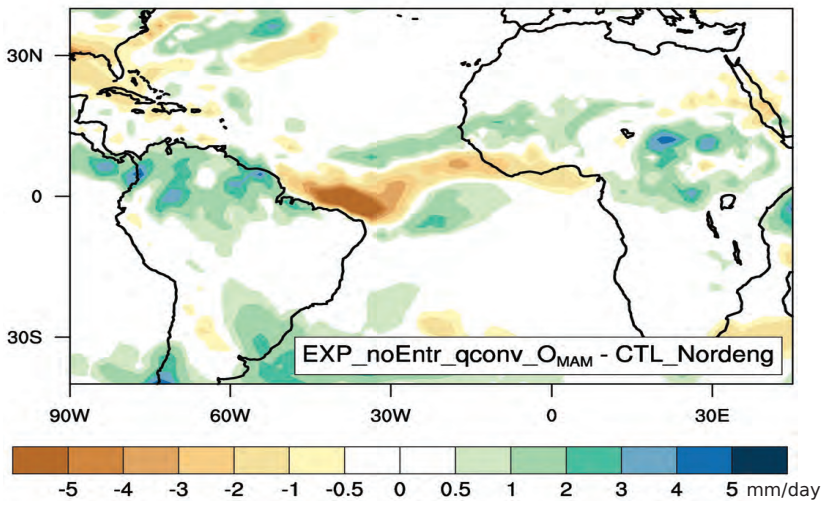

Figure 4.9: EXP_noEntr_qconv_O_{MAM} minus CTL_Nordeng boreal summer precipitation.

4.4 Summary

During boreal summer, the observed Atlantic ITCZ shifts northwards and eastwards towards West Africa, in accordance with the onset of the monsoon. The model ECHAM, which employs the Nordeng scheme by default, fails to capture such a shift, as the simulated Atlantic ITCZ remains westward and southward near the coast of Brazil. This erroneous Atlantic ITCZ position is accompanied by deficient rainfall over land areas, including South America

Table 4.3: Summary of results over land: experiment name, triggering of convective events, effective entrainment value, type of closure, rain rate over South America and Africa, Atlantic ITCZ over ocean.

Name	Trigger	Entrainment	Closure	$RR_{SAm+Afr}$	Atl ITCZ
CTL_Nordeng	infrequent	strong	CAPE	low	west, south
EXP_noEntr_L	infrequent	weak	CAPE	high	west, partially north
CTL_Tiedtke	infrequent	weak	qconv	high	east, north
GPCP	–	–	–	high	east, north

Table 4.4: Summary of results over ocean: experiment name, triggering of convective events, effective entrainment value, type of closure, rain rate over West Atlantic, Atlantic ITCZ over ocean.

Name	Trigger	Entrainment	Closure	$RR_{WestAtl}$	Atl ITCZ
CTL_Nordeng	frequent	strong	CAPE	high	west, south
EXP_noEntr_O	frequent	weak	CAPE	low	partially east, partially north
EXP_qconv_O	frequent	strong	qconv	low	east, partially north
EXP_noEntr_qconv_O	frequent	weak	qconv	low	east, north
CTL_Tiedtke	frequent	weak	qconv	low	east, north
GPCP	–	–	–	low	east, north

and Africa. When we use a convection scheme where deep convection occurs more easily (Tiedtke) such precipitation biases are significantly reduced and a better precipitation distribution is obtained. In this chapter, we investigated why and how the precipitation distribution changes as we switch from Nordeng to Tiedtke. Our aim was to understand how different components of a convection scheme impact the simulated precipitation distribution in the tropical Atlantic. To this end, we employed a modified Nordeng scheme where the trigger, entrainment, and closure are modified to mimic the easier deep convection in Tiedtke. The modifications were applied separately over land and over ocean. This also allowed us to investigate the interaction of precipitation over land and over ocean.

The main findings of this chapter are summarized in tables 4.3 and 4.4. Over land, entrainment was identified as the key parameter which controls the amount of rainfall. A high entrainment rate prevents convective updrafts from reaching high cloud tops and decreases the total amount of precipitation. Setting the turbulent entrainment to zero has the opposite effect. This explains why Tiedtke, which has a relatively weaker entrainment, has more rain over land compared to Nordeng. Increased rainfall over land through entrainment broadens the Atlantic ITCZ and shifts it northwards, but fails to displace it eastwards. Over ocean, the value of the entrainment parameter affects the longitudinal position of the Atlantic ITCZ. A weaker entrainment enhances convection everywhere, allowing rain to form over the East Atlantic and as a consequence, reduces rain over the West Atlantic. Entrainment works slightly differently over land and over ocean because of differences in one, the frequency of triggered convective events, and two, the spatial structure of precipitation between land and ocean. Deep convection is triggered less frequently over land due to the limited moisture supply. As such, suppressing these already too few events through strong entrainment leads

to very dry conditions over land. Over ocean, convection is triggered more frequently, but the resulting amount of precipitation is overestimated in regions of high SSTs such as the west Atlantic. This oversensitivity to SSTs is partially alleviated by making it easier to rain elsewhere through entrainment. Hence, over ocean, entrainment plays a partial role in the structure of precipitation, whereas over land, it acts as the primary control on the amount of rainfall.

The closure is key in determining the longitudinal position of the Atlantic ITCZ. A closure based on CAPE directly incorporates local thermodynamic instability, hence increasing the sensitivity to SST (Song and Zhang, 2009), whereas such relationships are less direct when moisture convergence is used. Which type of closure we use becomes a decisive factor when, for instance, there is more convergence on one side and warmer SSTs on the other. Such is the case during boreal summer over the Atlantic. Convection is then favored eastwards with a moisture convergence closure, and westwards with a CAPE closure. This explains why the too strong collocation of SST and precipitation proposed by Biasutti et al. (2006) cannot fully explain the precipitation biases found in models- the type of closure, and to some degree the entrainment, modulate the sensitivity of convection to SST.

The synoptic situation during boreal summer over the Atlantic, with high SSTs over the West Atlantic and high moisture convergence over the East Atlantic, provides an ideal situation for Tiedtke and Nordeng to have different precipitation distributions. This may not be the case in other seasons. For instance, in the absence of a monsoon, it becomes less obvious why regions of warm SST would differ from regions of enhanced low-level convergence. As such, there is also no assurance that a convergence-sensitive scheme will have a better precipitation than an SST-sensitive scheme in the mean state. In the succeeding chapter, we will tackle the need for a physical basis of alleviating precipitation biases in more detail.

Chapter 5

Role of convection scheme on the simulated tropical Atlantic precipitation distribution: case of boreal spring

5.1 Introduction

Biases in the precipitation distribution and surface winds during boreal spring are ubiquitous problems present in most climate models. Because it has serious repercussions on SSTs in coupled models, reducing the westerly wind bias in the uncoupled mode has been the focal point of recent studies. Several authors have identified the erroneous representation of deep convection over the tropical Atlantic as the root cause of the westerly wind bias (Chang et al., 2008; Wahl et al., 2011; Richter and Xie, 2008; Richter et al., 2013; Zermeno-Diaz and Zhang, 2013). There are two open issues. First, as exemplified in figure 5.1a with ECHAM Nordeng, there is more than one precipitation bias over the Atlantic. In addition to the southward shift of the Atlantic ITCZ, there is also the dry bias in the Amazon region over northeast Brazil. Some models also have a wet bias over Congo (Richter et al., 2012), though this feature is less robust than the Amazon bias. Proposed mechanisms on the origins of the westerly wind bias vary depending on the supposed location of the precipitation bias. For instance, in Richter et al. (2012), it is the deficient convective heating over South America and excessive heating over Africa which weaken the Atlantic Walker circulation and drive anomalous westerly winds towards Africa. A different mechanism is highlighted in Richter et al. (2013), where the southward shift of the ITCZ is presumed to be the main driver of the wind bias. Because meridional winds advect easterly momentum (Okumura and Xie, 2004), an ITCZ shifted southwards would pull southeasterly winds away from the equator and weaken the equatorial easterlies. However, Richter et al. (2013) note that this mechanism fails to explain why a corresponding northward shift away from the equator does not result in

a similar weakening of the equatorial easterlies. Aside from the lack of a clear-cut mechanism, there is also some circularity in the argument that biases in convection drive biases in winds, which brings us to the second issue: convection is strongly coupled to the circulation, and the precipitation biases themselves contain the imprint of wind biases. In this chapter, we hope to evaluate some of these issues from the perspective of the convection scheme.

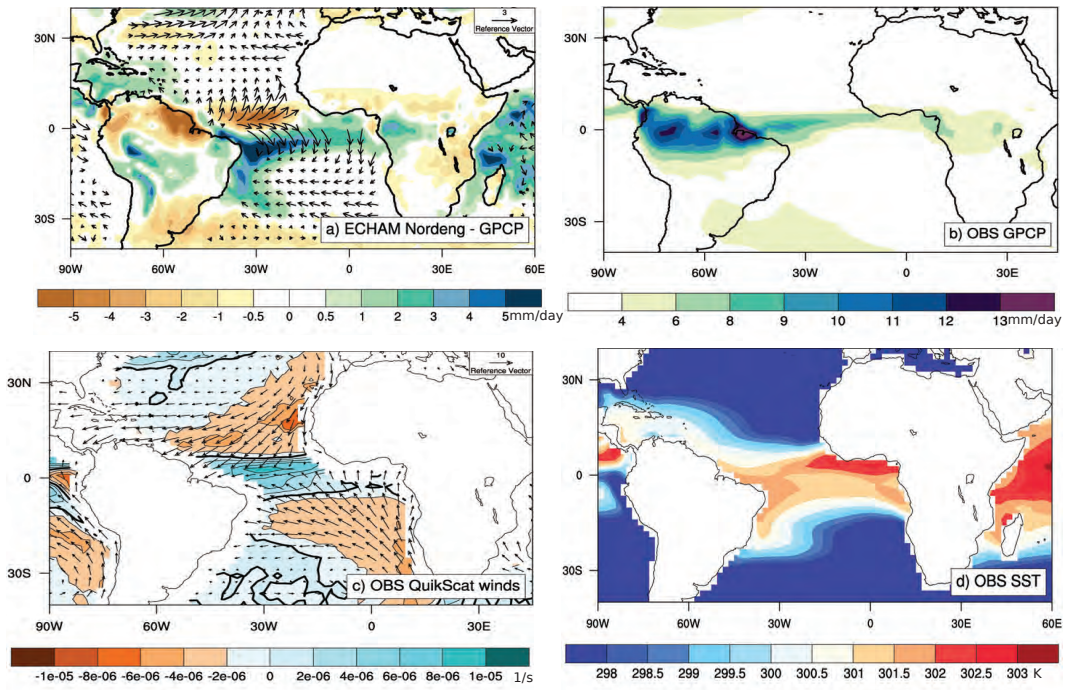

Figure 5.1: 10-year mean (1999-2009) boreal spring a) difference in precipitation and surface wind between ECHAM Nordeng and observations (GPCP precipitation, QuikScat winds), b) GPCP precipitation, c) Quikscat surface winds (vectors) and convergence (shaded contours), and d) observed SSTs (Hurrell et al., 2008).

Unlike the boreal summer case, switching to the Tiedtke scheme in ECHAM does not lead to a better precipitation distribution during boreal spring (figure 5.2). The only difference in terms of rainfall amount is that, Nordeng rains slightly more over the western basin compared to Tiedtke, whereas Tiedkte rains more over the Gulf of Guinea, corresponding to differences between West and East Atlantic models described in Chapter 2. But in terms of the structure of precipitation, the two schemes are quite similar in that rain is preferred over the coasts, instead of along the equator where the observed band of precipitation is located (figure 5.1b). The erroneous Atlantic ITCZ structures in Tiedtke and Nordeng roughly follow the contours of SSTs warmer than 301.5 K (figure 5.2), whereas the observed band is found over the SST gradient and maximum surface convergence near the equator (figure 5.1c,d). Because both schemes fail to capture the observed precipitation distribution in boreal spring, our focus is no longer directed at modifying Nordeng to mimic Tiedtke. Rather, we will modify the Nordeng scheme and other parameters of the ECHAM model to test hypotheses on factors controlling the erroneous Atlantic ITCZ structure during boreal spring.

In this chapter, we aim to answer three main questions. Firstly, do our choices of trigger, entrainment, and closure parameters influence the model's oversensitivity to SST? Previously,

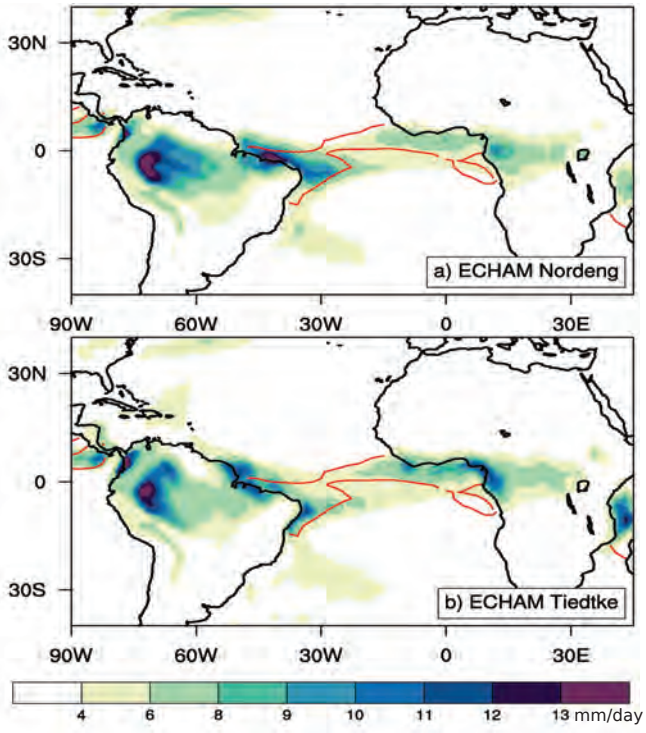

Figure 5.2: 10-year mean (1999-2009) boreal spring precipitation in a) ECHAM with Nordeng scheme and b) ECHAM with Tiedtke scheme. The red contours mark the SST contour at 301.5 K.

we have shown that with a monsoon circulation on the eastern side, a low entrainment rate and moisture convergence closure would favor convection eastwards and effectively decrease the sensitivity to high SSTs in the west during boreal summer. Secondly, we will explore the effect of continental precipitation on the Atlantic ITCZ and circulation to test the hypothesis that the dry bias over the Amazon in northeast Brazil (see figure 5.1a) is a possible root cause of the anomalous westerly wind and southward ITCZ bias. Finally, we will test the importance of cloud radiative effects (CRE), which have been shown to have an influence on westerly winds and ITCZ over the Pacific, as well as on the strength of MJOs (Crueger and Stevens, 2015).

The outline of this chapter is as follows: Sensitivity experiments are described in Section 5.2. Results are presented in the next section, divided into three parts corresponding to our three main questions regarding the roles of: trigger, entrainment, and closure (Section 5.3.1), convection over South America (Section 5.3.2), and cloud radiative effects (Section 5.3.3). A summary is given in Section 5.4.

5.2 Description of Experiments

Simulations are performed using the model ECHAM6 in its T63L47 configuration. Table 5.1 lists the sensitivity experiments performed for the case of boreal spring. Following the framework of the previous chapter, we modify different components of the Nordeng scheme such as the trigger, entrainment, and closure during the months March-April-May (MAM).

These modifications are performed as a first step over ocean only. The experiments are run for one year using prescribed 2001 SSTs. We choose the year 2001 in order to compare the simulated surface winds with observed near-surface ocean winds from the QuikSCAT L2B dataset[1], which covers the period 1999-2009. The trigger and entrainment are modified in two ways, by imposing either a stricter or a more lenient criteria for deep convection. The criteria is relaxed in EXP_4xzlift_O and in EXP_noEntr_O by quadrupling the added buoyancy for convective triggering and by removing turbulent entrainment, respectively. In contrast, a more stringent criteria is employed in EXP_nozlift_O and EXP_entrscv_O by removing the added buoyancy and by using the turbulent entrainment for shallow convection ($\sim$3xEntr$_{deep}$), respectively. In EXP_qconv_O, a moisture convergence closure is employed instead of the default CAPE.

Additional experiments are performed to explore the role of continental precipitation and cloud radiative feedbacks. The influence of land, in particular South America, is tested in EXP_noEntr_SAM, where we set the turbulent entrainment to zero over South American land points (90°W-30°E,30°S-30°N) to artificially enhance convection over that region. In EXP_noCRE$_{LW}$, cloud radiative effects (CRE) are turned off in the longwave. Clouds are made transparent to radiation by setting the cloud cover to zero within the radiation code, following the protocol of the Clouds On/Off Climate Interaction Experiment (COOKIE) (Stevens et al., 2012), but only in the longwave. This weakens the positive feedback between circulation and convection due to the removal of longwave radiative heating from deep convective clouds. Both EXP_noEntr_SAM and EXP_noCRE$_{LW}$ are run five times with 2001 SSTs and with varying initial conditions to account for internal variability. As reference, we run a control simulation using 2001 SSTs, CTL_Nordeng, and average over five realizations.

Table 5.1: Summary of boreal spring simulations

Name	**Convection scheme**	**Description**
CTL_Nordeng	Nordeng	control simulation with 2001 SSTs
CTL_Tiedtke	Tiedtke	control simulation with 2001 SSTs
EXP_4xzlift_O	Nordeng	quadrupled buoyancy perturbation (zlift) in convective trigger over ocean
EXP_nozlift_O	Nordeng	zero buoyancy perturbation (zlift) in convective trigger over ocean
EXP_noEntr_O	Nordeng	no turbulent entrainment over ocean
EXP_entrscv_O	Nordeng	shallow convection turbulent entrainment over ocean
EXP_qconv_O	Nordeng	moisture convergence closure over ocean
EXP_noEntr_SAM	Nordeng	no turbulent entrainment over South America
EXP_noCRE$_{LW}$	Nordeng	no cloud radiative effects in the longwave

[1]QuikScat (or SeaWinds) data are produced by Remote Sensing Systems and sponsored by the NASA Ocean Vector Winds Science Team. Data are available at www.remss.com.

5.3 Results

5.3.1 Sensitivity to trigger, entrainment, and closure

The precipitation bias in CTL_Tiedtke and CTL_Nordeng with respect to GPCP observations is shown in figures 5.3a and b. Both show a southward Atlantic ITCZ displacement, which is accompanied by a dry bias over ocean northwest of the equator and deficient rainfall over Amazon, similar to the bias found in the 10-year simulation in figure 5.1.

None of the modifications applied over ocean lead to substantial changes in the Atlantic ITCZ structure (figure 5.3c-g). In all of the simulations, the deficient rainfall northwest of the equator persists, accompanied by excessive rainfall southwards and eastwards. The actual precipitation structure can be seen in figure 5.4. Changing the trigger, entrainment, and closure at best impacts the east-west partitioning of precipitation. We see that turning off turbulent entrainment (EXP_noEntr_O) or switching to a moisture convergence closure (EXP_qconv_O) leads to a stronger precipitation maximum over the east coast. This is reminiscent of the previous chapter, and results in a Tiedtke-like behavior (figure 5.4d,g). Conversely, a stronger entrainment (EXP_entrscv_O) puts the precipitation maximum over the west coast, a Nordeng-like behavior (figure 5.4c). Interestingly, strengthening and weakening the trigger through the buoyancy perturbation (zlift) both result in an increase in rainfall over the Gulf of Guinea (figure 5.4e,f). That the modifications only lead, at best, to either a Nordeng-like or Tiedtke-like behavior stresses the fact that the structure of precipitation remains essentially unchanged in all these simulations. The latitudinal position of the ITCZ appears mostly independent of its longitudinal position and vice versa. This is different to the summer season, when the simulated ITCZ appears as one band located either northeast or southwest. In spring, the ITCZ has a tilted structure, with rainfall concentrated over both coasts.

Although a weakening of entrainment shifts the precipitation maximum from the west to the east coast, as in the case for summer, there is one subtlety. During spring, the SST is actually warmer over the Gulf of Guinea (figure 5.1d). The response to entrainment over the Gulf of Guinea nevertheless implies that despite warmer SSTs, the free troposphere has to be drier such that convection is enhanced with a weakened entrainment, and suppressed with a stronger one.

A CAPE-based closure, related to local thermal instability, contributes to the sensitivity to SST that results in the coastal bias of CTL_Nordeng (figure 5.4a). Unlike the case of summer, switching to a moisture convergence closure cannot counteract such a sensitivity to SST and instead appears to even have a positive feedback with it, especially over the warmest SST regions. The high SSTs over the Gulf of Guinea enhances deep convection, resulting in more convective heating. The heating leads to increased moisture convergence which further enhances deep convection over the Gulf of Guinea (figure 5.4g). This positive feedback prevents the model from capturing the observed maximum of surface convergence, which lies along a narrow band near the equator, over the SST gradient (figure 5.1c,d). In

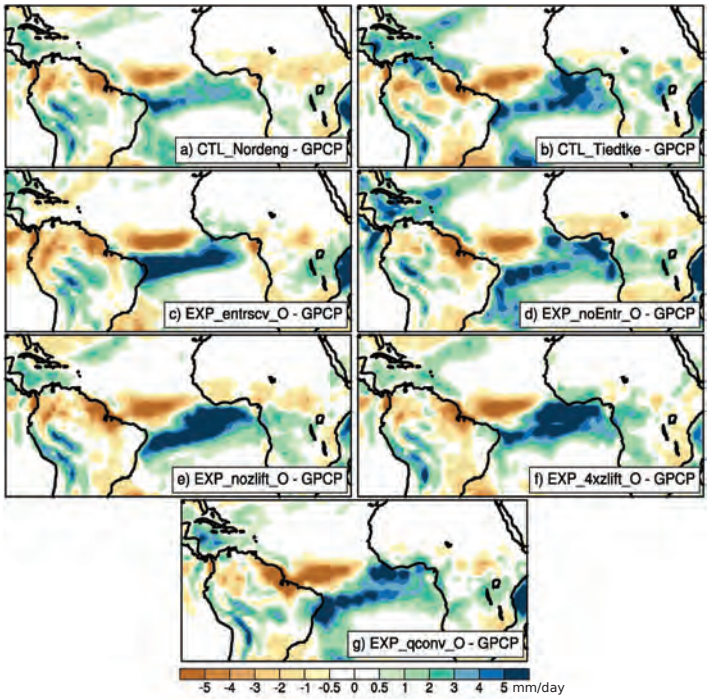

Figure 5.3: Boreal spring precipitation difference with respect to GPCP in control simulations (a,b), experiments with entrainment (c,d), trigger (e,f), and moisture convergence closure (g).

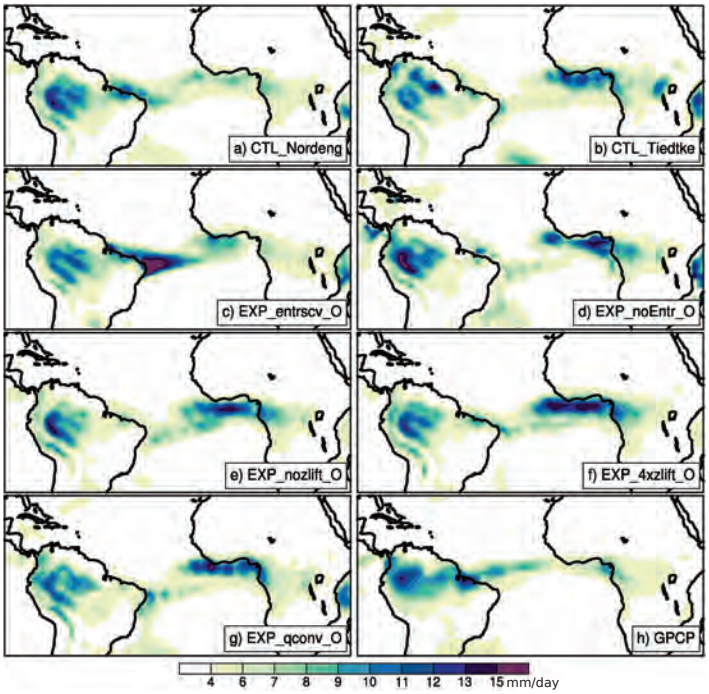

Figure 5.4: Boreal spring precipitation in control simulations (a,b), experiments with entrainment (c,d), trigger (e,f), and moisture convergence closure (g), and GPCP observations (h).

summer, the convergence associated with the monsoon covers a much larger area, which effectively counteracts the warm SSTs to the west.

Increasing or removing the buoyancy perturbation to the convective trigger both enhance precipitation over the warmest SSTs over the Gulf of Guinea. The buoyancy perturbation is computed based on the variance of potential temperature in the boundary layer. On the one hand, quadrupling this value likely means that the perturbation is increased most over the warmest areas. On the other hand, without any perturbation, convection will be triggered only over the most buoyant, warmest areas. Hence, in both cases, convection over the Gulf of Guinea will tend to be enhanced.

That adjustments in the trigger, entrainment, and closure do not substantially impact the oversensitivity of precipitation to SST does not mean that the convection scheme itself has no role. If anything, these results indicate that there is something more fundamental in the convection scheme which supports the collocation of SST and precipitation. In summer, the strong large-scale forcing from the monsoon can break this collocation. In spring, such a forcing is absent and the influence of SSTs prevails. The convection scheme does not see SSTs directly, but feels their impact through the boundary layer moist static energy, h_{PBL}. The h_{PBL} influences the convection scheme through (1) the trigger, when convective instability in the PBL is computed, (2) the closure, when CAPE is used, and (3) the updraft model itself, when the cloud top height is calculated. We have shown that neither changes to the trigger nor changes to the type of closure can offset the oversensitivity to SST. The impact of SSTs on the convection scheme must then come from their influence on cloud top height. In ECHAM, the cloud top is determined in two steps, first through an initial guess based on the adiabatic cloud top height, and second after including of the effects of mixing with the environment. The initial cloud top guess serves as an upper bound for the final cloud top height. It is found that during boreal spring, high initial cloud tops occur most frequently over the warm SST regions in the coasts of Guinea and Brazil (figure 5.5a), resulting in high final cloud tops over these areas (figure 5.5b). It is through the cloud top height calculation that the convection scheme favors convection over the warmest SSTs.

5.3.2 Sensitivity to South American precipitation

Richter and Xie (2008) suggest the deficient South American precipitation in models as a possible root cause of the anomalous westerly wind and southward ITCZ bias. This is tested in Richter et al. (2012), where they set the albedo over Amazon rain forest areas to zero as a way to increase rainfall over the Amazon. However, this method failed to increase precipitation over northeast Brazil and instead enhanced convection in regions near the Andes. Moreover, this method directly impacts the circulation by changing the temperature gradient between land and ocean. Our modified Nordeng scheme approach gives us a better method of testing the effects of the dry Amazon bias on the circulation. From the previous chapter, we have learned that entrainment strongly influences the amount of rain over land. In EXP_noEntr_SAM, we remove turbulent entrainment over South America to support higher

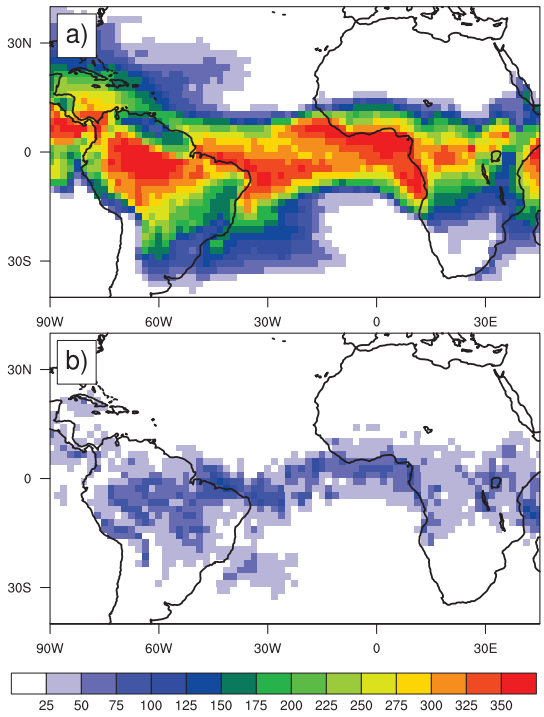

Figure 5.5: Number of convective updrafts with a) initial cloud top heights $\leq$ 250hPa and b) final cloud top heights $\leq$ 250hPa .

cloud tops. In response, compared to the Nordeng simulation, the rainfall amount increases and the dry bias is reduced in figure 5.6a, with the hatched areas marking significant changes with 90% confidence level.

However, the improved rainfall over Amazon does not have a huge impact on the precipitation over the adjacent ocean. The southward Atlantic ITCZ bias persists and even worsens. The westerly wind anomaly is also exacerbated and increases by about 1 m/s, as shown in figure 5.6c. It is possible that as rainfall increases over northeast Brazil, instability over the adjacent ocean decreases (Biasutti et al., 2004), further decreasing precipitation over the northwest side of the Atlantic and worsening the wind bias. Another possibility is that, as Zermeno-Diaz and Zhang (2013) proposed, the westerly wind problem is not about getting the correct rainfall amounts, but is rather an issue of getting the correct diabatic heating profile over Amazon. This may also explain the results of Richter and Xie (2008) in the sense that the decreased westerly wind anomaly is due changes to the albedo (temperature gradient), rather than convection.

5.3.3 Sensitivity to cloud radiative effects

In an aquaplanet, the existence of a double ITCZ not only depends on the convection scheme's ability to initiate an off-equatorial ITCZ, but also on the feedbacks necessary to maintain an ITCZ away from the equator (Moebis and Stevens, 2012). Similarly, areas of convection over land and over ocean in the tropical Atlantic are maintained by a positive feedback

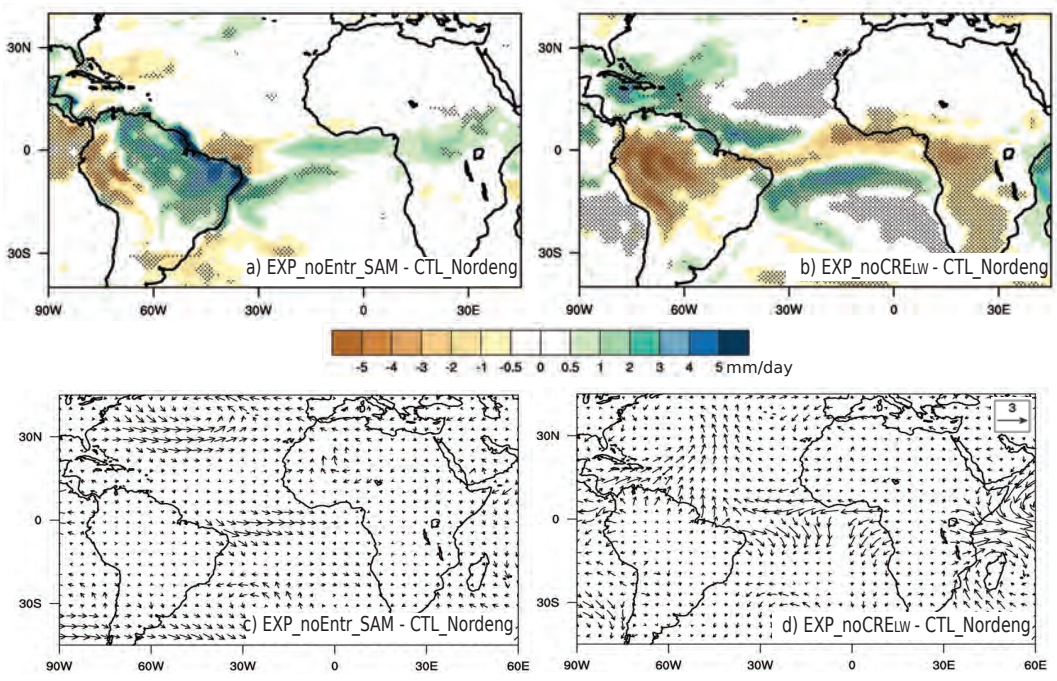

Figure 5.6: Boreal spring precipitation difference of a) EXP_noEntr_SAM - CTL_Nordeng, b) EXP_noCRE$_{LW}$ - CTL_Nordeng and the corresponding wind difference in c) and d). Hatched areas in a and b denote points with 90% confidence level.

mechanism. Convection heats the atmosphere in two ways: through latent heat release and through radiative heating from high level clouds. The total heating drives convergence and further strengthens convection. We can test the effect of this feedback on convection and circulation over the tropical Atlantic by artificially weakening it. In EXP_noCRE$_{LW}$, the longwave radiative heating from deep convective clouds is switched off. The idea is that a weakened coupling of convection and circulation will weaken convection itself and reduce the biases. This is indeed what happens in figure 5.6b; rainfall decreases over areas where it used to rain and increases over areas where it did not rain as much. Over ocean, a double ITCZ-like response is apparent, indicative of a broader ITCZ. Increased rain over the northwest Atlantic pulls the ITCZ northwards and reduces the westerly wind bias by more than 1 m/s (figure 5.6d). But the rain also increases south of the equator and induces a northerly wind bias, enhancing the already existing bias in CTL_Nordeng. This illustrates that part of the westerly wind-southward ITCZ problem comes from an incorrect coupling between circulation and convection possibly linked to the representation of cloud radiative effects.

5.4 Summary

Previous studies show that characteristic biases in coupled climate models, such as the reversed SST gradient and weak surface easterlies, originate from the erroneous boreal spring precipitation distribution in the atmospheric component of models. Interestingly, to date, the origins of the precipitation biases themselves have not been investigated in detail. In this chapter, we looked at how the convection scheme and its interaction with

the circulation impacts the precipitation biases over the tropical Atlantic, in particular the erroneous Atlantic ITCZ structure and the deficient rainfall over Amazon. To that aim, we modified the trigger, entrainment, and closure over ocean and over South America. In addition, we tested the effects of cloud radiative effects on the biases.

Our results show that:

- There is no effect of the trigger, closure, and entrainment on the latitudinal position of the ITCZ and westerly wind anomaly. At best, they influence the east-west partitioning of precipitation. Weakening entrainment results in a Tiedtke-like behavior, with more rain over the Gulf of Guinea than the other coast, whereas the opposite occurs when entrainment is strengthened. Increasing and removing the added buoyancy to the convective trigger result in increased rainfall rates over the Gulf of Guinea. Switching to a moisture convergence closure also results in a Tiedtke-like behavior.
- Reduction of the dry bias over South America can be achieved by weakening entrainment over the region. However, the resulting increase in rainfall amounts over South America does not have an impact on the latitudinal position of the ITCZ and westerly wind anomaly, in contrast to Richter and Xie (2008).
- Turning off cloud radiative effects in the longwave broadens the Atlantic ITCZ and reduces the westerly wind anomaly.

These results show that there is no simple way to adjust the convection scheme which would effectively reduce ITCZ bias, much unlike the case for boreal summer. In absence of a large-scale forcing such as the monsoon over West Africa, the simulated Atlantic ITCZ structure tends to follow the SST pattern during boreal spring. The issue comes from the fact that the convection scheme is more sensitive to SST peaks instead of SST gradients.

Chapter 6

Summary and Conclusions

In this thesis, our goal was to advance our understanding of factors controlling the tropical Atlantic precipitation distribution. The approach was to first test this understanding by evaluating the status of our current models in simulating the precipitation distribution. Robust precipitation biases in models were identified. Reasons behind these biases were explored, with the motivation that by diagnosing why our models rain incorrectly, we may learn more about how convection, SST, and circulation interact and thus determine the precipitation distribution. In this chapter, we revisit the three questions we raised in the beginning of this thesis. A summary of our findings and conclusions for each question is provided. General concluding remarks, followed by an outlook are given at the end of this chapter.

How well do state-of-the-art atmospheric models represent the tropical Atlantic distribution?

The precipitation distribution over the Atlantic in 24 atmosphere-only models was evaluated and compared to satellite observations. An object-based approach was used in order to have a detailed analysis of the structure, amplitude and location of precipitation in each model. Based on the distribution of precipitation objects, two classes of models emerge. The two classes of models differ in their annual mean state, and causes for their differences were traced to the boreal spring and summer season.

- West Atlantic models: In the annual mean, the precipitation object over ocean is found over the western Atlantic near the coast of Brazil, instead of the central Atlantic as observed. In boreal spring, these models show a strong southward shift of the ITCZ, with excessive precipitation near the south coast of Brazil. In boreal summer, rain is sustained over the west Atlantic, whereas the observed Atlantic ITCZ shifts to the eastern Atlantic towards the West African monsoon. In both spring and summer, a dry bias over Amazon exists.
- East Atlantic models: In the annual mean, the precipitation object over ocean is found over the eastern Atlantic. In boreal spring, these models have a less pronounced south-

ward bias of the ITCZ, but they place the precipitation maximum on the east over the Gulf of Guinea. In boreal summer, the Atlantic ITCZ remains located at the east coast, similar to observations. In both spring and summer, a dry bias over Amazon exists.

Since SSTs are prescribed, the emergence of the two model classes cannot be a result of a too strong collocation of SST and rainfall (Biasutti et.al, 2006) alone, suggesting that other mechanisms play a role. It is found that the east-west partitioning of the Atlantic ITCZ is dependent on horizontal resolution. Higher resolution models tend to fall in the East Atlantic class. This might be a result of better resolved boundary conditions such as orography and land-sea mask, a hypothesis addressed in the next question.

How does horizontal resolution impact the Atlantic ITCZ position?

The influence of horizontal resolution on the east-west structure of the Atlantic ITCZ was investigated, with a focus on the boreal summer season. Using ECHAM6, we performed three sensitivity experiments designed to isolate the relative contributions of a high-resolution atmosphere, orography, and land surface. Both high-resolution atmosphere and high-resolution orography contribute to an eastward precipitation maximum, but through different mechanisms. A high-resolution atmosphere tends to decrease rain on the West Atlantic, whereas a high-resolution orography increases rain on the East Atlantic. A high-resolution surface has a minimal effect.

- Orographic effect: The monsoon circulation is strengthened with an increased orographic resolution. A better resolved Andes blocks the mean easterly flow from the Atlantic and induces a stronger westerly wind. A better resolved African orography enhances the cyclonic circulation near West Africa and increases precipitation in the eastern Atlantic.
- Atmospheric effect: Convection is triggered more easily with a smaller grid-spacing. Following the background easterly flow, it starts to rain more east, resulting in less rain downstream over the west Atlantic.

During boreal spring, a high-resolution atmosphere has a similar effect as during summer. In contrast, a better resolved orography does not lead to a significant increase in precipitation in the eastern Atlantic, likely related to the fact that the monsoonal flow is absent in spring. It appears that making it easier to rain, as with a high-resolution atmosphere, leads to an increase in precipitation over the East Atlantic. A similar effect can be obtained by modifying the convection scheme. In fact, the Tiedtke convection scheme, which allows deep convection to occur more easily compared to the default Nordeng scheme, tends to rain more over the East Atlantic. This further motivates our last question.

How does the convection scheme influence the simulated precipitation over land and over ocean?

The relative roles of the trigger, entrainment (cloud model), and closure on the precipitation distribution was investigated by applying changes to the default Nordeng convection scheme in ECHAM. The modifications were applied separately over land and over ocean, which allowed us to study how changes to the scheme applied over ocean affect the precipitation over ocean, and how changes to the scheme over land affect the precipitation over land. In addition, with this method, the relationship between precipitation over land and over ocean was explored. We analyzed the impact of the convection scheme in two cases, one for the boreal summer season, and the other for spring.

- Over land during boreal summer: Entrainment is the only parameter that significantly affects the amount of precipitation. A strong entrainment effectively limits the depth of convection given the dryness of the environmental air and reduces the amount of precipitation over land. As a consequence, rain over the ocean increases, especially over the West Atlantic. The increased rainfall over the West Atlantic pulls the Atlantic ITCZ southward, but does not affect its longitudinal position.

- Over ocean during boreal summer: Both entrainment and closure affect the precipitation distribution, although the closure appears more important as it can directly influence the monsoon flow. Weakening entrainment enhances rain on the East Atlantic by making it easier to produce deep convection, an effect similar to that of a high-resolution atmosphere described previously. The design of the closure controls whether the precipitation maximum is located either over the west or over the east coast. The Atlantic ITCZ is situated over the West Atlantic with a CAPE closure, where the SST is maximum, and over the East Atlantic with a moisture convergence closure, where convergence is strongest due to the monsoonal flow.

- Over land during boreal spring: Similar conclusions as for the summer season apply, although removing the dry bias over South America via a weakened entrainment has little impact on the Atlantic ITCZ bias and the associated westerly wind anomaly. This is in contrast to what has been proposed in Richter et al. (2012) and supports the alternative view that it is the diabatic heating profile, rather than the amount of rainfall, that is important for the surface winds (Zermeno-Diaz and Zhang, 2013).

- Over ocean during boreal spring: The latitudinal and longitudinal position of the Atlantic ITCZ remain mostly insensitive to the changes applied to the convection scheme. One hypothesis is that the strong connection between SST and precipitation comes from the cloud top computation. It is found that during boreal spring, high initial cloud tops occur most frequently over the warm SST regions in the coasts of Guinea and Brazil, resulting in high final cloud tops over these areas. Higher clouds heat the atmosphere more, via condensational and radiative heating, which further enhance convection. This positive feedback is weakened by turning off cloud radiative effects in the

longwave, resulting in a reduction of the Atlantic bias and the accompanying westerly wind anomaly.

Our answers to the three questions help us to deconstruct some aspects of the complex interaction of convection, SST, and circulation over the tropical Atlantic. Two main points are drawn from our results. First, convection is not controlled by thermodynamical mechanisms alone. In observations, convection does not always occur over the warmest SSTs. During boreal spring, the observed band of convection lies over the SST gradient, rather than its peak. During boreal summer, the ITCZ is found in the eastern Atlantic, near the monsoon region, rather than the warm SST region over the western Atlantic. The East and West Atlantic ITCZ biases in our models express a fundamental gap between convection as observed and convection as parameterized. Our parameterizations reflect our view of convection as a result of thermodynamic instability within a column, rather than an outcome of dynamical mechanisms. Choices in the formulation of some components within the convection scheme can relax this viewpoint to increase the sensitivity to the large-scale circulation, as in the case for summer, but do not always suffice, as illustrated in spring. Second, convection strongly couples with the circulation, but whether this coupling is governed by the total amount of convective heating or by its vertical structure is unclear. In summer, higher rainfall amounts over the east resulting from an increased sensitivity to the monsoon flow further enhance the monsoon and cause a positive feedback. In spring, increased rain over the Amazon does not impact the circulation over the Atlantic. A better understanding of how convection controls the circulation is paramount for reducing wind biases in our models.

General concluding remarks

The precipitation distribution in our models reflect (1) how well we understand the interaction of convection with the large-scale circulation, (2) how well we resolve the large-scale, and (3) how well our parameterizations are designed and implemented. Accordingly, we make three final points on the tropical Atlantic precipitation biases studied in this thesis:

- *Convective heating profiles vs. rainfall amount (1)* Studies have pointed to the boreal spring precipitation bias in atmospheric models as the root cause of the westerly wind anomaly and reversed SST gradient. However, the precipitation biases are maintained by the wind biases and vice-versa. Precipitation biases do not emerge independently of biases in circulation, because the two are strongly coupled. Moreover, the surface winds also depend on the profile of convective heating, not just on the total rainfall amount. This is likely the reason for the minimal impact of the increased rainfall over Amazon on the circulation and Atlantic ITCZ. The results of Richter et al. (2012), which showed a reduction in the westerly wind anomaly from a reduced albedo over Amazon, can be explained as a direct impact of the imposed albedo on the circulation rather than a consequence of increased rainfall over Amazon.

- *Improved precipitation from better large-scale circulation (2)* Increased model resolution can indeed lead to a reduction of precipitation biases by providing a better large-scale circulation. This is illustrated in the case of the West African monsoon during boreal summer. A better resolved orography over Africa and South America leads to a stronger monsoon circulation. The stronger monsoon circulation helps in shifting the Atlantic ITCZ eastwards, similar to observations. However, such improvements are contingent on the large-scale circulation itself. Without a monsoon circulation that interacts with orography, the contribution of a better resolved orography will be minimal. Such is the case for boreal spring.

- *No quick fix for the convection scheme (3)* For the double ITCZ case, previous studies have suggested increasing entrainment rates (Oueslati and Bellon, 2013) or replacing the CAPE closure (Song and Zhang, 2009) as ways to reduce the bias. The former claims that sensitivity to free tropospheric humidity is underestimated, while the latter supposes that it is the CAPE closure which leads to oversensitivity to SSTs. For the Atlantic ITCZ bias, weakening entrainment reduces the dry bias over land and decreases the West Atlantic bias over ocean during boreal summer. In boreal spring, strengthening or weakening entrainment does not impact the southward Atlantic ITCZ bias. These results indicate that there is no simple adjustment to the convection scheme which would work for all areas and all seasons.

Outlook

For future work, we provide some suggestions regarding the previously mentioned three points.

- Simulations with prescribed diabatic heating profiles over South America during boreal spring can be performed to test the impact on the surface westerly wind bias. The effect of two types of heating profiles can be tested, one with a top-heavy profile, and the other with a bottom-heavy profile. An accompanying simulation, where observed winds are prescribed over ocean, can shed some light on the southward ITCZ bias and its coupling with the anomalous westerly wind bias. It would be interesting to see how the precipitation would respond to correct winds, given that its parameterization is biased towards warm SSTs.

- The effect of orography on the circulation in a changing large-scale circulation over the tropical Atlantic can be studied further with an idealized framework. The tropical Atlantic sector can be idealized as an ocean basin located between two idealized continents, the western continent with more landmass south, and the eastern continent with more landmass north. Idealized orography can be added as perturbations to the geopotential. With this set-up, we can impose varying SST and insolation and test the impact of the orographic effect on the circulation.

- Based on the results of this study, the convection scheme should take into account the dynamical aspect of convection based on moisture convergence. This can be done by imposing additional criteria on the trigger function that would incorporate the sensitivity to moisture convergence. From a theoretical perspective, this requires us to bridge the gap between our thermodynamic and dynamic perspectives on convection.

Bibliography

Adler, R., Huffman, G., Chang, A., Ferraro, R., Xie, P., Janowiak, J., Rudolf, B., Schneider, U., Curtis, S., Bolvin, D., Gruber, A., Susskind, J., and Arkin, P. (2003). The version 2 global precipitation climatology project (GPCP) monthly precipitation analysis (1979-present). *J. Hydrometeor.*, 4:1147–1167.

Alpert, L. (1945). The Intertropical Convergence Zone of the Eastern Pacific Ocean. *Bull. Amer. Meteor. Soc.*, 10:426–432.

Andersson, A., Fennig, K., Klepp, C., Bakan, S., Grassl, H., and Schulz, J. (2010). The Hamburg Ocean Atmosphere Parameters and Fluxes from Satellite Data - HOAPS-3. *Earth Syst. Sci. Data*, 2:215–234.

Arakawa, A. (2004). The cumulus parameterization problem: Past, present, and future. *J. Climate*, 17:2493–2525.

Arakawa, A. and Schubert, W. (1974). Interaction of a cumulus cloud ensemble with the large scale environment, Part I. *J. Atmos. Sci.*, 31:674–701.

Balogun, E. (1973). *A study of satellite-observed cloud patterns of tropical cyclones.* PhD thesis, SMRP Research Paper No. 109. Univ. Chicago, Dept of Geophys. Sci. 103 pp.

Bechtold, P., Bazile, E., Guichard, F., Mascart, P., and Richard, E. (2001). A mass-flux convection scheme for regional and global models. *Q. J. R. Meteorol. Soc.*, 127:869–886.

Betts, A. and Miller, M. (1986). A new convective adjustment scheme. Part II: Single column tests using GATE wave, BOMEX, ATEX and arctic air-mass data sets. *Q. J. R. Meteorol. Soc.*, 112:693–709.

Biasutti, M., Battisti, D., and Sarachik, E. (2004). Mechanisms Controlling the Annual Cycle of Precipitation in the Tropical Atlantic Sector in an Atmospheric GCM. *J. Climate*, 17:4708–4723.

Biasutti, M., Sobel, A., and Kushnir, Y. (2006). AGCM Precipitation Biases in the Tropical Atlantic. *J. Climate*, 19:935–957.

Bischoff, T. and Schneider, T. (2014). Energetic constraints on the position of the Intertropical Convergence Zone. *J. Climate*, 27:49374951.

Bjerknes, J., Allison, L., Kreins, E., Godshall, F., and Warnecke, G. (1969). Satellite mapping of the Pacific tropical cloudiness. *Bull. Amer. Meteor. Soc.*, 50:313–322.

Bony, S. and Emanuel, K. (2001). A parameterization of the cloudiness associated with cumulus convection: evaluation using TOGA COARE data. *J. Atmos. Sci.*, 58:3158–3183.

Bony, S., Stevens, B., Frierson, D., Jakob, C., Kageyama, M., Pincus, R., Shepherd, T., Sherwood, S. C., A.P. Siebesma, A. S., Watanabe, M., and Webb, M. (2015). Clouds, circulation and climate sensitivity. *Nature Geoscience*, 8:261–268.

Bordoni, S. and Schneider, T. (2008). Eddy-mediated regime transitions in the seasonal cycle of a Hadley circulation and implications for monsoon dynamics. *J. Atmos. Sci.*, 65:915934.

Bougeault, P. (1985). A simple parameterization of the large-scale effects of cumulus convection. *Mon. Wea. Rev.*, 113:2108–2121.

Bretherton, C., McCaa, J., and Grenier, H. (2004). A new parameterization for shallow cumulus convection and its application to marine subtropical cloud-topped boundary layers. Part I: Description and 1D results. *Mon. Wea. Rev.*, 132:864–882.

Chang, C., Carton, J., Grodsky, S., and Nigam, S. (2007). Seasonal climate of the tropical Atlantic sector in the NCAR community climate system model 3: error structure and probable causes of errors. *J. Climate*, 20:1053–1070.

Chang, C., Nigam, S., and Carton, J. (2008). Origin of the Springtime Westerly Bias in Equatorial Atlantic Surface Winds in the Community Atmosphere Model Version 3 (CAM3) Simulation. *J. Climate*, 21:4766–4778.

Chao, W. and Chen, B. (2001). The Origin of Monsoons. *J. Atmos. Sci.*, 58:3497–3506.

Chao, W. and Chen, B. (2004). Single and double ITCZ in an aquaplanet model with constant sea surface temperature and solar angle. *Climate Dynamics*, 22:447–459.

Charney, J. (1971). Tropical cyclogenesis and the formation of the Intertropical Convergence Zone. In Reid, W., editor, *Mathematical Problems of the Geophysical Fluid Dynamics, Lect. Appl. Math*, volume 13, pages 355–368, Providence, R.I. Am. Math Soc.

Chikira, M. and Sugiyama, M. (2010). A Cumulus Parameterization with State-Dependent Entrainment Rate. Part I: Description and Sensitivity to Temperature and Humidity Profiles. *J. Atmos. Sci.*, 67:2171–2193.

Cook, K., Hsieh, J., and Hagos, S. (2004). The Africa-South America Intercontinental Teleconnection. *J. Climate*, 17:2851–2865.

Crueger, T. and Stevens, B. (2015). The effect of atmospheric radiative heating by clouds on the Madden-Julian Oscillation. *J. Adv. Model. Earth Syst.*, 7:854864.

Dai, A. (2006). Precipitation Characteristics in Eighteen Coupled Climate Models. *J. Climate*, 19:46054630.

Davey, M., Huddleston, M., Sperber, K., and Coauthors (2002). STOIC: A study of coupled model climatology and variability in the tropical ocean regions. *Climate Dynamics*, 18:403–420.

Davis, C., Brown, B., and Bullock, R. (2006). Object-based verification of precipitation forecasts. Part I: Methodology and application to mesoscale rain areas. *Mon. Wea. Rev.*, 134:1772–1784.

Del Genio, A., Yao, M., and Jonas, J. (2007). Will moist convection be stronger in a warmer climate? *Geophys. Res. Lett.*, 34.

Demory, M., Vidale, P., Roberts, M., Berrisford, P., Strachan, J., Schiemann, R., and Mizielinski, M. (2014). The role of horizontal resolution in simulating drivers of the global hydrological cycle. *Climate Dynamics*, 42:22012225.

DeWitt, D. (2005). Diagnosis of the tropical Atlantic near-equatorial SST bias in a directly coupled atmosphere-ocean general circulation model. *Geophys. Res. Lett.*, 32.

Dirmeyer, P., Cash, B., et al. (2012). Simulating the diurnal cycle of rainfall in global climate models:resolution versus parameterization. *Climate Dynamics*, 39:399–418.

Donner, L. (1993). A cumulus parameterization including mass fluxes, vertical momentum dynamics, and mesoscale effects. *J. Atmos. Sci.*, 50:889–906.

Duffy, P. B., Govindasamy, B., Iorio, J. P., Milovich, J., Sperber, K. R., Taylor, K. E., Wehner, M. F., and Thompson, S. L. (2003). High-resolution simulations of global climate, part 1: present climate. *Climate Dynamics*, 21:371390.

Dunkerton, T. and Crum, F. (1995). Eastward propagating 2 to 15 day equatorial convection and its relation to the tropical intraseasonal oscillation. *J. Geophys. Res.*, 100:25781–25790.

Ebert, E. and Gallus, W. (2009). Toward Better Understanding of the Contiguous Rain Area (CRA) Method for Spatial Forecast Verification. *Wea. and Forecasting*, 24:1401–1415.

Ebert, E. and McBride, J. (2000). Verification of precipitation in weather systems: Determination of systematic errors. *J. Hydrol.*, 239:179–202.

Emanuel, K. (1991). A scheme for representing cumulus convection in large-scale models. *J. Atmos. Sci.*, 48:2313–2335.

Fletcher, R. (1945). The general circulation of the tropical and equatorial atmosphere. *J. Meteor.*, 2:167–174.

Frierson, D., Kim, D., Kang, I., Lee, M., and Lin, J. (2010). Structure of AGCM-Simulated Convectively Coupled Kelvin Waves and Sensitivity to Convective Parameterization. *J. Atmos. Sci.*, 68:26–45.

Fritsch, J. and Chappell, C. (1980). Numerical prediction of convectively driven mesoscale pressure systems. Part I : Cumulus parametrization. *J. Atmos. Sci.*, 37:1722–1733.

Gates, W. L. (1992). Amip: The Atmospheric Model Intercomparison Project. *Bull. Amer. Meteor. Soc.*, 73:1962–1970.

Gill, A. (1980). Some simple solutions for heat-induced tropical circulation. *Q. J. R. Meteorol. Soc.*, 106:447–462.

Gilleland, E., Ahijevych, D., Brown, B., Casati, B., and Ebert, E. (2009). Intercomparison of Spatial Forecast Verication Methods. *Wea. and Forecasting*, 24:1416–1430.

Godshall, F. (1968). Intertropical Convergence Zone and Mean Tropical Cloud Amount. *Mon. Wea. Rev.*, 96:172–175.

Gregory, D. (1995). The representation of moist convection in atmospheric models. In *Seminar on Parametrization of Sub-grid Scale Physical Processes*, Reading, UK. ECMWF.

Gregory, D. (2001). Estimation of entrainment rate in simple models of convective clouds. *Q. J. R. Meteorol. Soc.*, 127:53–72.

Gregory, D. and Rowntree, P. (1990). A mass flux convection scheme with representation of cloud ensemble characteristics and stability dependent closure. *Mon. Wea. Rev.*, 118:1483–1506.

Hagos, S. and Cook, K. (2005). Influence of Surface Processes over Africa on the Atlantic Marine ITCZ and South American Precipitation. *J. Climate*, 18:4993–5010.

Hastenrath, S. (1984). Interannual Variability and Annual Cycle: Mechanisms of Circulation and Climate in the Tropical Atlantic Sector. *Mon. Wea. Rev.*, 112:1097–1107.

Hastenrath, S. (1991). *Climate Dynamics of the Tropics*. Kluwer Academic Publishers, Netherlands.

Hess, P., Battisti, D. S., and Rasch, P. J. (1993). Maintenance of the Intertropical Convergence Zone and the large-scale tropical circulation on a water-covered Earth. *J. Atmos. Sci.*, 50:691713.

Hohenegger, C. and Stevens, B. (2013). Controls on and impacts of the diurnal cycle of deep convective precipitation. *J. Adv. Model. Earth Syst.*, 4:801–815.

Holton, J. R., Wallace, J. M., and Young, J. A. (1971). On the boundary layer dynamics and the ITCZ. *J. Atmos. Sci.*, 28:275–280.

Huffman, G., Adler, R., Bolvin, D., Gu, G., Nelkin, E., Bowman, K., Hong, Y., Stocker, E., and Wolff, D. (2007). The TRMM multi-satellite precipitation analysis: Quasi-global, multi-year, combined-sensor precipitation estimates at fine scale. *J. Hydrol.*, 8:38–55.

Hurrell, J., Hack, J., Shea, D., Caron, J., and Rosinski, J. (2008). A New Sea Surface Temperature and Sea Ice Boundary Dataset for the Community Atmosphere Model. *J. Climate*, 21:51455153.

Insel, N., Poulsen, C., and Ehlers, T. (2009). Inuence of the Andes Mountains on South American moisture transport, convection, and precipitation. *J. Climate*, 35:1477–1492.

Kain, J. S. and Fritsch, J. M. (1990). A one-dimensional entraining/detraining plume model and its application in convective parameterizations. *J. Atmos. Sci.*, 47:2784–2802.

Landu, K., Leung, L., Hagos, S., Vinoj, V., Rauscher, S., T.Ringler, and Taylor, M. (2014). The Dependence of ITCZ Structure on Model Resolution and Dynamical Core in Aquaplanet Simulations. *J. Climate*, 27: 23752385.

Lenters, J. and Cook, K. (1995). Simulation and Diagnosis of the Regional Summertime Precipitation Climatology of South America. *J. Climate*, 8:2988–3005.

Lin, J. (2007). The double-ITCZ problem in IPCC AR4 coupled GCMs: Ocean-atmosphere feedback analysis. *J. Climate*, 20:4497–4525.

Lin, J., Lee, M., Kim, D., Kang, I., and Frierson, D. (2008). The Impacts of Convective Parameterization and Moisture Triggering on AGCM-Simulated Convectively Coupled Equatorial Waves. *J. Climate*, 21:883–909.

Lindzen, R. and Nigam, S. (1987). On the role of sea surface temperature gradients in forcing low-level winds and convergence in the tropics. *J. Atmos. Sci.*, 44:2418–2436.

Lohmann, U. and Roeckner, E. (1996). Design and performance of a new cloud microphysics scheme developed for the ECHAM general circulation model. *Climate Dynamics*, 12:557–572.

Manabe, S., Hahn, D., and Holloway, J. (1974). The Seasonal Variation of the Tropical Circulation as Simulated by a Global Model of the Atmosphere. *J. Atmos. Sci.*, 31:43–83.

Manabe, S., Smagorinsky, J., Holloway, J., and Stone, H. (1970). Simulated climatology of a general circulation model with a hydrologic cycle. *Mon. Wea. Rev.*, 98:(3):175212.

Manabe, S. and Strickler, R. (1964). Thermal equilibrium of the atmosphere with a convective adjustment scheme. *J. Atmos. Sci.*, 21:361–385.

Mechoso, C., Robertson, A., and CoAuthors (1995). The Seasonal Cycle over the Tropical Pacific in Coupled Ocean Atmosphere General Circulation Models. *Mon. Wea. Rev.*, 123:28252838.

Mitchell, T. P. and Wallace, J. M. (1992). The annual cycle in equatorial convection and sea surface temperature. *J. Climate*, 5:1140–1156.

Moebis, B. and Stevens, B. (2012). Factors controlling the position of the Intertropical Convergence Zone on an aquaplanet. *J. Adv. Model. Earth Syst.*, 4:M00A04, doi:10.1029/2012MS000199.

Neelin, J. and Held, I. (1987). Modeling tropical convergence based on the moist static energy budget. *Mon. Wea. Rev.*, 115:3–12.

Nicholson, S. (2013). The West African Sahel: A Review of Recent Studies on the Rainfall Regime and Its Interannual Variability. *ISRN Meteorology*, pages 1–32.

Nordeng, T. (1994). Extended versions of the convection parametrization scheme at ECMWF and their impact upon the mean climate and transient activity of the model in the tropics. *Research Dept Technical Memorandum No. 206, ECMWF, Shinfield Park, Reading RG2 9AX, United Kingdom.*

Okumura, Y. and Xie, S. (2004). Interaction of the Equatorial Cold Tongue and the African Monsoon. *J. Climate*, 17:3589–3602.

Ooyama, K. (1971). A theory on paramaterization of cumulus convection. *J. Meteor. Soc. of Japan*, 49:744–756.

Oueslati, B. and Bellon, G. (2013). Convective Entrainment and Large-Scale Organization of Tropical Precipitation: Sensitivity of the CNRM-CM5 Hierarchy of Models. *J. Climate*, 26:2931–2946.

Patricola, C., Li, M., Xu, Z., Chang, P., Saravanan, R., and Hsieh, J. (2012). An investigation of tropical Atlantic bias in a high-resolution coupled regional climate model. *Climate Dynamics*, 39:2443–2463.

Philander, S., Gu, D., Halpern, D., Lambert, G., Lau, N., Li, T., and Pacanowski, R. (1996). Why the ITCZ Is Mostly North of the Equator. *J. Climate*, 9:2958–2972.

Pike, A. (1971). The intertropical convergence zone studied with an interacting atmosphere and ocean model. *Mon. Wea. Rev.*, 99:469–477.

Pope, V. and Stratton, R. (2002). The processes governing horizontal resolution sensitivity in a climate model. *Climate Dynamics*, 19:(3–4):211236.

Ramage, C. (1974). Structure of an Oceanic Near-Equatorial Trough Deducted from Research Aircraft Traverses. *Mon. Wea. Rev.*, 102:754–759.

Reick, C., Raddatz, T., Brovkin, V., and Gayler, V. (2013). Representation of natural and anthropogenic land cover change in MPI-ESM. *J. Adv. Model. Earth Syst.*, 5:459482.

Richter, I., Mechoso, C., and Roberston, A. (2007). What determines the Position and Intensity of the South Atlantic Anticyclone in Austral Winter?-An AGCM Study. *J. Climate*, 21:214–228.

Richter, I. and Xie, S. (2008). On the origin of equatorial Atlantic biases in coupled general circulation models. *Climate Dynamics*, 31:587–598.

Richter, I., Xie, S., Behera, S., Doi, T., and Masumoto, Y. (2013). Equatorial Atlantic variability and its relation to mean state biases in CMIP5. *Climate Dynamics*, 42:171–188.

Richter, I., Xie, S., Wittenberg, A., and Masumoto, Y. (2012). Tropical Atlantic biases and their relation to surface wind stress and terrestrial precipitation. *Climate Dynamics*, 38:985–1001.

Riehl, H. (1954). *Tropical Meteorology*. McGraw-Hill, New York.

Rodwell, M. J. and Hoskins, B. J. (2001). Subtropical anticyclones and summer monsoons. *J. Climate*, 14:3192–3211.

Sadler, J. (1964). TIROS observations of the summer circulation and weather patterns of the eastern North Pacific. *Proc. Symp. Tropical Meteor.*, pages 553–571.

Schiemann, R., Demory, M., Mizielinski, M., Roberts, M., Shaffrey, L., Strachan, J., and Vidale, P. (2013). The sensitivity of the tropical circulation and Maritime Continent precipitation to climate model resolution. *Climate Dynamics*, 42:2455–2468.

Schneider, T., Bischoff, T., and Haug, G. (2015). Migrations and dynamics of the intertropical convergence zone. *Nature*, 513:45–53.

Seager, R., Naik, N., and Vecchi, G. (2010). Thermodynamic and Dynamic Mechanisms for Large-Scale Changes in the Hydrological Cycle in Response to Global Warming. *J. Climate*, 23:4651–4668.

Semazzi, F. H. M. (1980a). Stationary barotropic flow induced by a mountain over a tropical belt. *Mon. Wea. Rev.*, 108:922–930.

Semazzi, F. H. M. (1980b). Numerical experiments on the orographic dynamic phenomenon over a tropical belt. *Arch. Metoral. Geophys. Bioklimatol.*, 29:55–68.

Semazzi, F. H. M. and Sun, L. (1997). The role of orography in determining the Sahelian climate. *Int. J. Climatol.*, 17:581–596.

Simpson, R. (1947). Synoptic aspects of the intertropical convergence near Central and South America. *Bull. Amer. Meteor. Soc.*, 28:335–346.

Slingo, J. M. (1996). Intraseasonal oscillations in 15 atmospheric general circulation models: Results from an AMIP diagnostic subproject. *Climate Dynamics*, 12:325–357.

Sobel, A. (2007). Simple Models of Ensemble-Averaged Tropical Precipitation and Surface Wind, Given the Sea Surface Temperature. In Schneider, T. and Sobel, A., editors, *The Global Circulation of the Atmosphere*. Princeton University Press, Princeton, New Jersey.

Song, X. and Zhang, G. (2009). Convection Parameterization, Tropical Pacific Double ITCZ, and Upper-Ocean Biases in the NCAR CCSM3. Part I: Climatology and Atmospheric Feedback. *J. Climate*, 14:4299–4315.

Stein, U. and Alpert, P. (1993). Factor Separation in Numerical Simulations. *J. Atmos. Sci.*, 50:2107–2115.

Stevens, B., Bony, M., and Webb, M. (2012). Clouds on-off klimate intercomparison experiment (COOKIE).

Stevens, B., Duan, J., McWilliams, J., Muennich, M., and Neelin, J. (2002). Entrainment, Rayleigh friction, and boundary layer winds over the tropical Pacific. *J. Climate*, 15:30–44.

Stevens, B., Giorgetta, M., Esch, M., Mauritsen, T., Crueger, T., Rast, S., Salzmann, M., Schmidt, H., Bader, J., Block, K., Brokopf, R., Fast, I., Kinne, S., Kornblueh, L., Lohmann, U., Pincus, R., Reichler, T., and Roeckner, E. (2013). Atmospheric component of the MPI-M Earth System Model: ECHAM6. *J. Adv. Model. Earth Syst.*, 5:146–172.

Stockdale, T., Balmaseda, M., and Vidard, A. (2006). Tropical Atlantic SST prediction with coupled ocean-atmosphere GCMs. *J. Climate*, 19:6047–6061.

Sultan, B. and Janicot, S. (2003). The west African monsoon dynamics. Part II: The "pre-onset" and "onset" of the summer monsoon. *J. Climate*, 16:3407–3427.

Sumi, A. (1992). Pattern formation of convective activity over the aqua-planet with globally uniform sea surface temperature. *J. Meteor. Soc. of Japan*, 70:855–876.

Tiedtke, M. (1989). A comprehensive mass flux scheme for cumulus parametrization in large-scale models. *Mon. Wea. Rev.*, 117:1779–1800.

Trenberth, K. E., Dai, A., Rasmussen, R. M., and Parsons, D. B. (2003). The changing character of precipitation. *Bull. Amer. Meteor. Soc.*, 84:12051217.

Virji, H. (1980). A preliminary study of summertime tropospheric circulation patterns over South America estimated from cloud winds. *Mon. Wea. Rev.*, 109:599–610.

Wahl, S., Latif, M., Park, W., and Keenlyside, N. (2011). On the Tropical Atlantic SST warm bias in the Kiel Climate Model. *Climate Dynamics*, 36:891–906.

Waliser, D. and Gautier, C. (1993). A satellite derived climatology of the ITCZ. *J. Climate*, 6:2162–2174.

Walsh, K. (1994). On the Influence of the Andes on the General Circulation of the Southern Hemisphere. *J. Climate*, 7:1019–1025.

Wang, H. and Fu, R. (2006). The Influence of Amazon Rainfall on the Atlantic ITCZ through Convectively Coupled Kelvin Waves. *J. Climate*, 20:1188–1201.

Wernli, H., Paulat, M., Hagen, M., and Frei, C. (2008). SAL-A novel quality measure for the verification of quantitative precipitation forecasts. *Mon. Wea. Rev.*, 136:4470–4487.

Wilcox, E. and Donner, L. (2007). The frequency of extreme rain events in satellite rain-rate estimates and an atmospheric general circulation model. *J. Climate*, 20:53–69.

Xu, H., Wang, Y., and Xie, S. (2004). Effect of the Andes on Eastern Pacific Climate: A Regional Atmospheric Model Study. *J. Climate*, 17:589–602.

Xu, K., Arakawa, A., and Krueger, S. (1992). The macroscopic behavior of cumulus ensembles simulated by a cumulus ensemble model. *J. Atmos. Sci.*, 49:2402–2420.

Yin, L., Fu, R., Shevliakova, E., and Dickson, R. (2012). How well can CMIP5 simulate precipitation and its controlling processes over tropical South America? *Climate Dynamics*, 41:3127–3143.

Yukimoto, S., Yoshimura, H., Hosaka, M., Sakami, T., Tsujino, H., Hirabara, M., Tanaka, T., Deushi, M., Obata, A., Nakano, H., Adachi, Y., Shindo, E., Yabu, S., Ose, T., and Kitoh, A. (2011). Meteorological Research Institute Earth System Model Version 1 (MRI-ESM1): Model Description. *Technical Report of the Meteorological Research Institute*, 64.

Zebiak, S. (1993). Air-sea interaction in the equatorial Atlantic region. *J. Climate*, 6:1567–1586.

Zermeno-Diaz, D. and Zhang, C. (2013). Possible Root Causes of Surface Westerly Biases over the Equatorial Atlantic in Global Climate Models. *J. Climate*, 26:8154–8168.

Zhang, G. and McFarlane, N. (1995). Sensitivity of climate simulations to the parameterization of cumulus convection in the Canadian Climate Centre general circulation model. *Atmos. Ocean*, 33:407–446.

Zhang, G. and Mu, M. (2005). Effects of modifications to the Zhang-McFarlane convection parameterization on the simulation of the tropical precipitation in the National Center for Atmospheric Research Community Climate Model, version 3. *J. Geophys. Res.*, 110.

Zhao, M., Held, I., Lin, S., and Vecchi, G. (2009). Simulations of Global Hurricane Climatology, Interannual Variability, and Response to Global Warming Using a 50-km Resolution GCM. *J. Climate*, 22:6653–6678.

List of Figures

List of Tables

Acknowledgements

I would like to thank my supervisor, Cathy Hohenegger, for her guidance through the course of this work. She has kindly and patiently taught me a lot since my very first plot of an upside down ITCZ. I thank her for sharing her knowledge on the topic and for encouraging me to look at the problem from different perspectives. My gratitude also goes to my co-advisor, Bjorn Stevens, for his guidance, advice, and support during this work. I also thank him for his lectures which have served as a source of knowledge and inspiration for this study. I would like to thank my panel chair, Martin Claussen, for his valuable suggestions and assistance during this work. I thank my examination committee members, Jürgen Bohner and Lars Kaleschke, for taking part in the evaluation of this thesis.

Special thanks to members of the HerZ research group for the interesting meetings and discussions these past years. I especially thank Tobias Becker and Karsten Peters for their useful suggestions for this work. I thank the IMPRS office, Antje Weitz, Cornelia Kampmann, and Wiebke Böhm for their organizational support. Thanks to Angela Grüber for her kind assistance.

The past three and a half years in my office wouldn't be the same without my officemate Dagmar Fläschner. I thank her for her company and friendship and awesome baking skills. I also want to thank Mirjana Sakradzija for her advice and support. Thanks to Dagmar and Mirjana for their help, especially in the very last stages of this dissertation. I also thank Armelle Remedio and Jade Garcia, both of whom I consider as my family here in Hamburg.

Finally, a big thank you to my loved ones. Thank you Mom, Dad, Diane, and Jai for your love and one hundred percent support throughout this endeavor. Thank you Ritthik for your understanding and care, and of course, for the occasional zen koans. Thanks to all of you, I couldn't have done this without your unending love, support, and encouragement.

List of Publications

Siongco, A. C., Hohenegger C., and B. Stevens (2014): The Atlantic ITCZ bias in CMIP5 models. Climate Dynamics, **45**, 1169-1180

Siongco, A. C., Hohenegger C., and B. Stevens (2016): Drivers of summertime precipitation biases over the tropical Atlantic in ECHAM6. (*in preparation*)

Hinweis / Reference

Die gesamten Veröffentlichungen in der Publikationsreihe des MPI-M
„Berichte zur Erdsystemforschung / Reports on Earth System Science“,
ISSN 1614-1199

sind über die Internetseiten des Max-Planck-Instituts für Meteorologie erhältlich:
http://www.mpimet.mpg.de/wissenschaft/publikationen.html

All the publications in the series of the MPI -M
„Berichte zur Erdsystemforschung / Reports on Earth System Science“,
ISSN 1614-1199

are available on the website of the Max Planck Institute for Meteorology:
http://www.mpimet.mpg.de/wissenschaft/publikationen.html

Eidesstattliche Versicherung
Declaration of oath

Hiermit erkläre ich an Eides statt, dass ich die vorliegende Dissertationsschrift selbst verfasst und keine anderen als die angegebenen Quellen und Hilfsmittel benutz habe.

I hereby declare, on oath, that I have written the present dissertation by myself and have not used other than the acknowledged resources and aids.

Hamburg, 27 Januar 2016

[Angela Cheska Siongco]